# University of Alberta

Identification and characterization of a dynactin subunit in *Saccharomyces cerevisiae*

by

Ranran Zhang

A thesis submitted to the Faculty of Graduate Studies and Research
in partial fulfillment of the requirements for the degree of

Master of Science
in
Molecular Biology and Genetics

Department of Biological Sciences

Edmonton, Alberta
Fall 2007

*Your file Votre référence*
*ISBN: 978-0-494-33381-5*
*Our file Notre référence*
*ISBN: 978-0-494-33381-5*

## Abstract

Mitosis is a highly coordinated process in all eukaryotes, and is crucial for maintaining genetic stability. During mitosis of *Saccharomyces cerevisiae*, the cell division site is pre-determined by the bud, so that the mitotic spindle needs to be aligned along the mother-bud axis, and the nucleus has to be inserted into the neck prior to cytokinesis.

Two partially redundant pathways (Kar9 and dynein) are involved in nuclear positioning. These two pathways act in a sequential manner during mitosis, and each of them presumably serves as a back-up mechanism when the other one is disrupted. In this study, the *LDB18* (low dye binding) gene, whose role for nuclear positioning had not been reported before, was identified to be part of the dynein pathway. Further characterization of the gene product supported the hypothesis that Ldb18 is the yeast ortholog of the dynactin (the dynein activator) subunit p24/22 in animals.

Dedication

To my dearest grandparents Deyi Zhang & Rulan Xue,

and wonderful parents Yulin Wang & Aiqin Zhang,

to whom I owe the deepest love and gratitude in the world

## Acknowledgements

I would like to express my sincere appreciation and gratitude to my supervisor, Dr. Neil Adames, for giving me the opportunity to work in his laboratory and providing invaluable guidance through my master's program. Without him, this thesis would not have been possible. I would also like to thank Dr. Andrew Simmonds and Dr. Frank Nargang for their important support and input as members of my supervisory committee. Special thanks to Dr. Andrew Simmonds for his generosity of allowing me to use the microscope in his laboratory to make GFP-tubulin movies for the Ldb18 project.

I am grateful to members of the Adames lab that I had the opportunity to work with over the years. My special thanks to Darren Bugbee and Sean Williams, with whom I shared a lot of discussions and a great amount of fun during my program.

My friends Brian Lee and Darren Horney spent their valuable time proofreading my thesis and correcting my grammatical mistakes. I want to express my genuine appreciation to them. I would also like to thank Dr. Heather McDermid for her helpful suggestions on my thesis writing.

I am thankful to the Department of Biological Science for the training and funding that I received through them. After the years of being a graduate student, I would also like to express my special gratefulness to Mag Haag and Carla Starchuk, for their precious support to my teaching in the department.

Finally, I have to thank my wonderful friends, especially Huirong Chen, Jingru Li, and Joanne Yu, who have supported me throughout this degree. I owe my deepest gratitude to my dearest grandparents and parents, for their unconditional love, which guided me through my difficult times, and will stand by me at every stage of my life in the future.

## Table of Contents


**1. INTRODUCTION** **1**

1.1 The mitotic cycle in *Saccharomyces cerevisiae* 1

1.1.1 Overview of the cell cycle in *S. cerevisiae* 1

1.1.2 The spindle pole and nuclear movements during mitosis 3

1.1.3 The cytoskeleton 7

1.1.3.1 Rearrangement of the actin cytoskeleton 8

1.1.3.2 Septin assembly and regulation 9

1.1.3.3 The microtubule system 10

1.1.4 Mitotic exit and the spindle position checkpoint 12

1.2 The Kar9 and dynein pathways are involved in nuclear positioning 17

1.2.1 The Kar9 pathway 18

1.2.2 The dynein pathway 23

1.3 Composition and structure of dynein/dynactin 30

1.3.1 The structure of cytoplasmic dynein 30

1.3.2 The structure of the dynactin complex 32

1.3.3 Dynein and dynactin mostly function together 38

1.4 Objectives of this study 43

**2. RESULTS** **46**

2.1 Examining nuclear positioning defects in deletion strains 49

2.2 The nuclear positioning defects in *ldb18*Δ 52

2.3 Genetic interactions implicate Ldb18 in the dynein pathway 54

2.4 Sequence analysis supports that Ldb18 may be the yeast ortholog of the dynactin subunit p24/p22 56

2.5 Loss of Ldb18 disrupts microtubule sliding 61

2.6 Ldb18 interacts with Arp1 and Jnm1 63

2.7 Ldb18 localization study 68

**3. CONCLUSIONS and DISCUSSIONS** **69**

3.1 Ldb18 is a component of the dynein pathway 69

3.2 Results support that Ldb18 may be the yeast ortholog of the dynactin p24/p22 subunit 70
3.3 Protein interactions within the dynactin complex 72
3.4 Localization of the dynactin complex 73
3.5 Interactions between dynein and dynactin 75
3.6 Evolution of the dynein and dynactin complex 75
3.7 Future directions 77

**4. MATERIALS and METHODS 78**

4.1 Growth media and conditions 78
4.2 Strains used in this study 78
4.3 PCR protocols to amplify the desired DNA sequence for homologous recombination 80
4.4 Concentration of PCR products 81
4.5 Transformation of *S. cerevisiae* 81
4.6 Genomic DNA extraction 82
4.7 Genomic PCR confirmation of transformants 82
4.8 Synthetic lethality assay 82
4.9 Use DAPI-staining to determine nuclear positioning defects 83
4.10 Time-lapse movies of spindle movements 84
4.11 Western blot 84
4.12 Affinity chromatography 85
4.13 Primers used in this study 86

**5. REFERENCES 99**

**6. APPENDIX** (Using FRET to study protein interactions) **118**

## List of Tables


| | | Page |
|---|---|---|
| Table 1.1 | Sequence identities between *S. cerevisiae* and *Homo sapiens* (human) for the dynein/dynactin subunits and dynein-interacting proteins. | 42 |
| Table 2.1 | A list of the 13 candidates that show genetic interactions with the Kar9 or dynein pathway, and the nuclear positioning defects in their deletion strains. | 47 |
| Table 2.2 | Genetic interactions between Ldb18 and the dynein or Kar9 pathway. | 56 |
| Table 4.1 | Strains used in this study | 91 |
| Table 4.2 | Oligos used in this study. | 93 |
| Table 4.3 | Plasmids used in this study | 98 |
| Table A1 | The excitation/emission wavelengths for all channels | 125 |

## List of Figures


| | | Page |
|---|---|---|
| Figure 1.1 | Major events of the *S. cerevisiae* cell cycle. | 7 |
| Figure 1.2 | The spindle position checkpoint couples spindle positioning with mitotic exit. | 16 |
| Figure 1.3 | The current model for the Kar9 pathway. | 22 |
| Figure 1.4 | The current model for dynein-dependent spindle positioning. | 29 |
| Figure 1.5 | The current model of dynactin ultrastructure. | 37 |
| Figure 1.6 | Genetic interactions between the Kar9 and dynein pathways and objectives of this study. | 45 |
| Figure 2.1 | Confirmation for the correct deletion of each ORF in the deletion strains. | 50 |
| Figure 2.2 | Nuclear positioning defects in *clb4Δ, vid22Δ mon1Δ*, and *fab1Δ* mutant cells. | 51 |
| Figure 2.3 | The nuclear positioning defects in *ldb18*Δ and *fab1*Δ mutant cells. | 52 |
| Figure 2.4 | Nuclear migration defect of the *ldb18*Δ strain compared to the *dyn1*Δ and wild type strains at 30°C or 15°C. | 53 |
| Figure 2.5 | Tetrad analysis of *ldb18*Δ*xarp1*Δ, *ldb18*Δ*xbim1*Δ, *and ldb18*Δ*xkar9*Δ tetratype meiotic products on the original YPAD plates. | 55 |
| Figure 2.6 | Homology analysis of Ldb18 sequence comparing to the p24/p22 orthologs in other eukaryotes | 58 |
| Figure 2.7 | Phylogenetic tree predictions for $p150^{Glued}$ (DCTN1), p50 (dyamitin, or DCTN2), and p24/22 (DCTN3). | 60 |
| Figure 2.8 | Microtubule misalignment in the *ldb18*Δ mutant cells. | 62 |
| Figure 2.9 | Confirmation of TAP and 3HA epitope. | 65 |
| Figure 2.10 | Ldb18 interacts with Arp1 and Jnm1. | 66 |
| Figure 2.11 | Ldb18 does not interact with Dyn3. | 67 |

Figure 2.12 Confirmation of Ldb18-3CFP fusion by genomic PCR. 68

Figure 4.1 The PCR based strategy for making deletion strains. 88

Figure 4.2 Genomic PCR confirmation to determine whether the ORF is still present. 89

Figure 4.3 The PCR-based strategy for tagging the ORF with an epitope. 90

Figure A1 The principle of FRET (fluorescence resonance energy transfer). 128

Figure A2 Spectrum overlap of CFP and YFP leads to "overlap factors". 129

Figure A3 Construction of the strains for FRET analysis. 130

Figure A4 Confirmation of CFP/YFP integration into the genome. 131

Figure A5 An example of images taken under three different channels. 132

Figure A6 An example for measuring the fluorescence intensity. 133

## List of Abbreviations

| | |
|---|---|
| AAA+ | ATPase associated with various cellular activities |
| ABP | actin-binding protein |
| APC | anaphase- promoting complex |
| tumor suppressor APC | adenomatous polyposis coli |
| Cdk | cyclin-dependent kinase |
| cMT | cytoplasmic microtubule |
| CP | capping protein (of actin) |
| DAPI | 4,6-diamidino-2-phenylindole |
| FEAR | Cdc fourteen early anaphase release |
| FRET | fluorescence resonance energy transfer |
| GAP | GTPase-activating protein |
| GEF | guanine nucleotide exchange factor |
| HC | heavy chain (of dynein) |
| HD | Huntington's disease |
| LC | light chain (of dynein) |
| LIC | light intermediate chain (of dynein) |
| MAP | microtubule-associated protein |
| MAP kinase | mitogen-activated protein kinase |
| MEN | mitotic exit network |
| MT | microtubule |
| MTOC | microtubule-organizing center |

| | |
|---|---|
| ORF | open reading frame |
| SPB | spindle pole body |
| TAP | tandem affinity purification |
| +TIP | (microtubule) plus-end tracking protein |

# 1. Introduction

## 1.1 The mitotic cycle in *Saccharomyces cerevisiae*

Mitosis, the asexual cell reproduction process in eukaryotes, generates two genetically identical daughter cells from a single parent cell. In a full mitotic cycle, the cell first duplicates its DNA, and then segregates one copy of each duplicated chromosome to each of the daughter cell. To ensure genetic stability, these processes need to be precisely coordinated, both temporally and spatially. Regulation of the cell cycle is critical for the normal development of multicellular organisms. In humans, loss of cell cycle control can be associated with cancer (reviewed in Soto and Sonnenschein, 2004).

The molecular processes that regulate chromosome replication and cell division are fundamentally similar for all eukaryotic cells. In the late 1980s, it became clear that many of the key actors in the cell cycle perform similar functions in all eukaryotes, from yeast to flies, frogs to humans (reviewed in De Clercq and Inze, 2006; Pines, 1999; King *et al.*, 1996; Peters, 1998; Ohi and Gould, 1999; Sherr and Roberts, 1999; Kaldis, 1999; Nasmyth, 1996; Dunphy, 1994). The ascomycete *Saccharomyces cerevisiae*, commonly referred to as "baker's yeast" or "budding yeast", is a unicellular eukaryote that undergoes a mitotic cell-division cycle in asexual phases. Besides this reproductive similarity to more complex eukaryotes, *S. cerevisiae* has many of the experimentally convenient features of bacteria, such as a short reproduction time (approximately 90 minutes), the ability to form colonies on plates, and a relatively simple and compact genome. Thus, *S. cerevisiae* provides a convenient system for the study of mitosis.

### 1.1.1 Overview of the cell cycle in *S. cerevisiae*

In eukaryotes, the cell cycle is often divided into two general phases: a relatively long period of interphase (I phase) that precedes and makes preparations for mitosis, and a shorter period of actual division (mitosis or M phase). Cell contents are duplicated in interphase and segregated in M phase. Interphase is further subdivided into S phase, during which DNA replication occurs, and G1 and G2 phases, which refer to the two "Gap" phases that precede and follow S phase, respectively. M phase is divided into prophase (nuclear membrane breakdown, DNA condensation and spindle assembly),

metaphase (chromosome alignment at the mid-plate of the cell), anaphase (chromosome segregation) and telophase (decondensation of chromosomes and reformation of the nuclear membrane), followed by cytokinesis (division of the cell cytoplasm).

Mitosis by the budding mode in *S. cerevisiae* differs somewhat from the cell cycle of other eukaryotic cells. For many types of eukaryotic cells, the site of cytokinesis is determined by the orientation of the mitotic spindle. However, the site of cell division in *S. cerevisiae* is pre-determined by the site of bud formation, which occurs early in the cell cycle (G1/S transition). The spindle, therefore, has to be properly aligned along the mother-bud axis, allowing one set of chromosomes to be deposited into the bud before cytokinesis. In addition, as in most fungi, the nuclear membrane does not break down during mitosis in *S. cerevisiae*, so the migration of DNA into the bud occurs via the migration of the nucleus into the mother-bud neck, a process often termed "nuclear migration". The conventional concepts for the different stages of mitosis, therefore, may not always apply to *S. cerevisiae*. However, despite these differences, the fundamental cellular biochemical mechanisms regulating major cell cycle events, such as DNA replication and chromosome segregation in *S. cerevisiae*, do not differ markedly from those in other eukaryotes (reviewed in Nasmyth, 1996; Pringle and Hartwell, 1981; Pringle *et al.*, 1997).

To commit to a full mitotic cycle, *S. cerevisiae* cells have to pass a regulatory point called "Start", which is positioned in late G1 (Pringle and Hartwell, 1981). Before "Start", cells in early G1 could potentially be directed into different developmental directions: to sporulate (diploids), to initiate mating (haploids), or to proceed with the mitotic cycle. However, once a cell passes "Start", it must commit to the mitotic cycle even if the environment provides signals for mating or sporulation. Following "Start", DNA replication, bud emergence, and duplication of the microtubule-organizing center will be initiated almost simultaneously.

In all eukaryotes, the key cell cycle events — such as DNA replication, and chromosomal segregation — are induced by cyclin-dependent kinases (Cdks) (reviewed in Morgan, 1997). Cdks associate with different cyclin subunits, which confer various substrate specificities on the Cdk, and thus trigger different cell cycle events. *S. cerevisiae* has one main Cdk, Cdc28, for governing progression through the cell cycle

(Andrews and Measday, 1998). "Start" is triggered by the association of Cdc28 with G1 cyclins, whereas the onset of M phase and mitotic exit depend on the activation and inactivation, respectively, of Cdc28-cyclin B complexes.

As the cell cycle clock (controlled by Cdk activity) progresses, cells undergo dramatic yet precisely coordinated changes. Besides DNA replication and segregation, an *S. cerevisiae* cell also experiences other cell cycle-regulated events, such as movement of the nucleus, re-organization of cytoskeletal filaments, cell wall synthesis, and re-distribution of organelles.

## 1.1.2 The spindle pole and nuclear movements during mitosis

The spindle pole body (SPB), embedded in the nuclear envelope, is the microtubule-organizing center (MTOC) in the *S. cerevisiae* cell, and nucleates growth of both astral and spindle (kinetochore and interpolar) microtubules (MT). Because the nuclear envelope does not break down during mitosis, the spindle microtubules are often referred to as intranuclear microtubules, and the astral microtubules as cytoplasmic microtubules (cMTs).

The spindle pole and nuclear movements during the cell cycle are illustrated in Fig.1.1A. In G1/S phase, a bud is formed at a pre-determined site on the mother cell. At about the same time, the SPB duplicates itself in a conservative manner, with the new SPB located adjacent to the old SPB in the nuclear envelope. The duplication depends on activation of Cdc28 kinase by G1 cyclins (Winey *et al.*, 1991). The two SPBs are connected by a molecular "bridge", and remain side-by-side until DNA replication is completed. By now, the old SPB is oriented towards the bud site, a position that requires interaction of its cytoplasmic microtubules with the cell cortex and bud neck.

After DNA replication, and typically when the bud is approximately 0.4 times the diameter of the mother cell, the new SPB migrates away to the other side of the nucleus, resulting in the generation of a short nuclear spindle (~1 μm) connecting the two SPBs (Yeh *et al.*, 1995). SPB separation requires B cyclin-Cdk activity (Lim *et al.*, 1996). At the end of S phase or the beginning of G2, formation of the short spindle is already complete. Formation of the bipolar spindle involves the kinesin-related proteins Cin8 and Kip1. At 37 °C, the *cin8Δ* mutant can duplicate SPBs but fails to form a bipolar spindle, and this defect can be suppressed by overexpression of Kip1 (Hoyt *et al.*, 1992).

At lower temperatures, *cin8Δ kip1Δ* double mutants are inviable and fail to form a bipolar spindle, suggesting that Cin8 and Kip1 are redundant for spindle formation (Hoyt *et al.*, 1992).

After formation of the mitotic spindle, Cin8 and Kip1, both of which are plus-end directed MT motors, are also required for maintenance of the spindle prior to the onset of anaphase. During this time, the spindle elongates steadily and achieves a length of approximately 2.5 μm (McAinsh *et al.*, 2003). In a *kip1Δ cin8-ts* double mutant strain, spindles that are already formed collapse when cells are shifted to the nonpermissive temperature. This collapse is partially rescued by deletion of *KAR3*, which encodes a minus-end directed kinesin, suggesting that the integrity of the pre-anaphase spindle is controlled by the balance between forces generated by Cin8/Kip1 (that push the SPBs apart) and those by Kar3 (that pull them together) (Saunders and Hoyt, 1992).

Following SPB separation, the nucleus can move either toward or away from the neck (Yeh *et al.*, 1995). However, once arriving near the neck, the position of the nucleus remains relatively stable, and the short (pre-anaphase) spindle tends to be aligned along the mother-bud axis (Yeh *et al.*, 1995). Nuclear movement toward the mother-bud neck and the pre-anaphase spindle orientation require the activity of the Kar9 pathway, which involves Kar9 (a protein first discovered as being required for karyogamy), the actin cytoskeleton, the actin-based motor Myo2, cytoplasmic microtubules, and several microtubule- or actin- interacting proteins (for a more detailed description refer to section 1.2.1; Pearson and Bloom, 2004).

In metaphase, chromosomes do not undergo congression (chromosome movement toward the mid-plane), and a conventional metaphase plate is absent in *S. cerevisiae*. This is probably because there are only 32 kinetochore MTs and 8 interpolar MTs in the nucleus, which is not enough to generate polar ejection forces (that drive the chromosomes toward the mid-plane of the cell) (O'Toole *et al.*, 1999). However, chromosomes are attached to both poles, and GFP-tagging of chromosomes has revealed a bilobed metaphase configuration analogous to the metaphase plate in animal cells — kinetochores form two lobes that lie on either side of the spindle mid-zone and are separated by roughly half the distance between the SPBs (Goshima and Yanagida, 2000; He *et al.*, 2000). This configuration is a consequence of chromosome oscillation, and

transient stretching of kinetochores by polymerization/depolymerization of MTs prior to sister chromatid separation in anaphase (McAinsh *et al.*, 2003).

The ubiquitin-protein ligase APC/C (anaphase promoting complex/cyclosome) is crucial for entry into anaphase (reviewed in Nasmyth, 2005; Nasmyth, 2002). At the metaphase-to-anaphase transition, the APC is activated by Cdc20, and this activation mediates proteolysis of the anaphase inhibitor Pds1 (securin). Removal of the securin allows the protease Esp1 (separase) to cleave cohesin, thus inducing sister chromatid separation. Subsequently, pulling of chromatids by kinetochore microtubules leads to chromosome segregation in anaphase (Nasmyth, 2005; Nasmyth, 2002).

In animal cells, anaphase is usually divided into two parts: anaphase A, during which sister kinetochores move toward opposite poles of the spindle; and anaphase B, in which spindle elongation results in further separation of the poles and the attached chromosomes. In *S. cerevisiae*, the small size of the metaphase spindle (~2 μm) means that chromosomes at the onset of anaphase are already close to the spindle poles. Elongation of the spindle during anaphase (from ~2 μm to ~8-12 μm) is dramatic and results in significant separation of sister chromatids. Therefore, anaphase B is the primary mechanism responsible for chromosome segregation (Peterson and Ris, 1976). However, anaphase A does occur, as supported by the observation of shortening of the kinetochore microtubules in the nucleus (Peterson and Ris, 1976; Straight *et al.*, 1997).

The force-generating mechanism for chromosome movement during anaphase A (toward the poles) in *S. cerevisiae* is unclear, although it is thought that motor-driven sliding (of kinetochores) along microtubules and MT depolymerization at the plus-end of kinetochore microtubules are both responsible (Maddox *et al.*, 2000). In anaphase B, the spindle experiences an initial rapid elongation (0.54 μm/min and spindle extends to ~6-8 μm), followed by a period of relatively slower elongation (0.21 μm/min and spindle extends to ~8-12 μm) (Yeh *et al.*, 1995; Kahana *et al.*, 1995). The fast elongation results from the sliding of antiparallel MTs, and the slower phase is due to midzone MT polymerization as well as antiparallel MT sliding (Straight *et al.*, 1997, 1998; Maddox *et al.*, 2000). Cin8 and Kip1 are involved in different phases: *cin8*Δ mutants are defective for the fast elongation, whereas in *kip1*Δ mutants, the slow elongation phase is affected (Straight *et al.*, 1998). In addition, the microtubule-associated protein (MAP) Ase1,

which is localized within the spindle midzone during spindle elongation, is required for the slower phase. Loss of Ase1 leads to premature spindle disassembly in mid-anaphase (immediately after fast elongation), and Ase1 overexpression induces premature spindle elongation (Schuyler *et al.*, 2003). It is speculated that Ase1 bundles antiparallel MTs and promotes their polymerization at the midzone as the spindle elongates (Schuyler *et al.*, 2003).

During fast elongation of the spindle, the nucleus inserts into the mother-bud neck (Yeh *et al.*, 1995; Kahana *et al.*, 1995). At this stage, the elongated "sausage-shaped" nucleus oscillates within the neck, parallel to the mother-bud axis, over a range of 1-2 μm (Yeh *et al.*, 1995). This oscillation is presumably due to balance of pulling forces from the mother and the bud, which cooperatively keeps the spindle in the neck (Adames and Cooper, 2000). Both the nuclear positioning (into the neck) and oscillations require the dynein pathway (refer to section 1.2.2, Adames and Cooper, 2000; Bloom, 2001; Hildebrandt and Hoyt, 2000). Following fast elongation, spindle activity pauses briefly, and then elongation resumes at a slower rate until both poles reach the distal ends of the mother and daughter cells. As a result of this slower elongation, the nucleus assumes an "hour-glass" shape (two lobes interconnected by a narrow stem) (Yeh *et al.*, 1995; Kahana *et al.*, 1995).

After proper spindle orientation and elongation brings a complete set of chromosomes to the daughter cell, cells can exit mitosis. Mitotic exit requires destruction of the B-type cyclins by the APC (now activated by Cdh1), and inhibition of Cdk by its inhibitor Sic1 (King *et al.*, 1995; Mendenhall, 1998; Zachariae and Nasmyth, 1999). The spindle is disassembled, and each of the nuclear lobes moves away from the distal site, becoming approximately centered in the mother and bud (Yeh *et al.*, 1995). Subsequently, cytokinesis occurs at the mother-bud neck, yielding two genetically identical progeny. In the next cell cycle, the SPB in the new cell moves toward the site of the incipient bud, and assumes a relatively stable position near the bud site before the emergence of the new bud (Lee *et al.*, 1999).

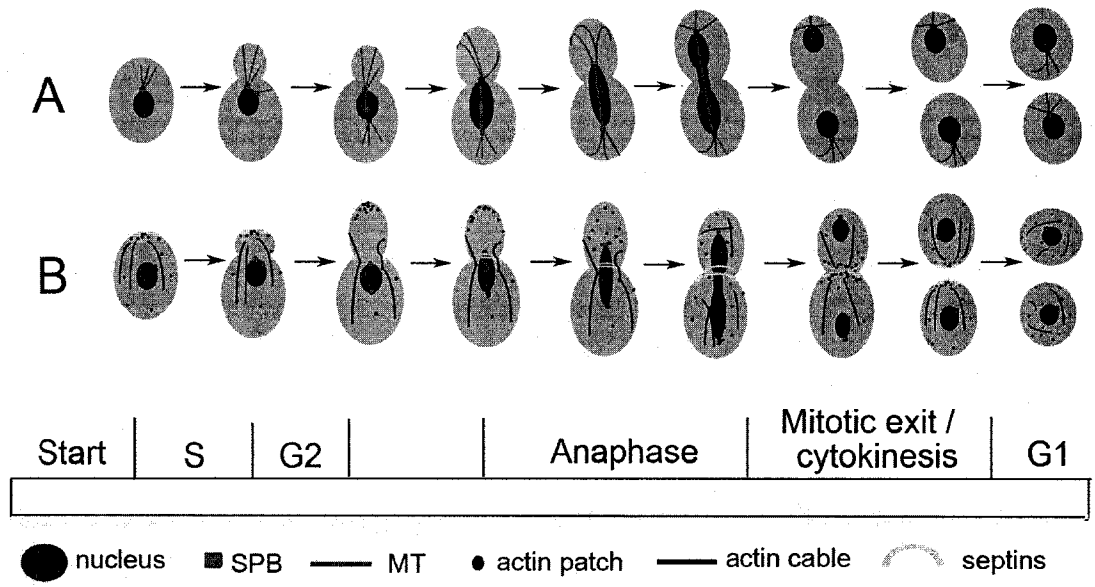


**Figure 1.1. Major events of the *S. cerevisiae* cell cycle.** See text for more details. (A) The spindle pole body (SPB) and microtubule (MT) movements during the mitotic cycle. (B) Rearrangements of the actin cytoskeleton and septins. During late G1, both the septins and actin patches assemble in a ring at the pre-bud site. However, the assembly of the actin and the assembly of the septins are mutually independent (Ayscough *et al.*, 1997).

## 1.1.3 The cytoskeleton

All eukaryotes contain a cytoskeleton consisting of a network of protein polymer filaments. These filaments not only experience remarkable alterations during mitosis, but also contribute to cell cycle regulation in *S. cerevisiae* (Carminati and Stearns, 1999; Schott *et al.*, 2002; Cau and Hall, 2005; Keaton and Lew, 2006). There are three types of cytoskeletal filaments: microfilaments (5-7 nm in diameter, polymers of actin), microtubules (hollow tubes 25 nm in diameter, polymers of tubulin), and intermediate filaments (~10 nm in diameter, polymers of any of a number of related fibrous proteins) (Pringle *et al.*, 1997). Extensive studies have been conducted on both microfilaments and microtubules in *S. cerevisiae* (reviwed in Winsor and Schiebel, 1997).

Only a couple of proteins have been indicated to form intermediate filaments: Fin1 contains putative coiled-coil regions and assembles into a ~10 nm filament between the SPBs in dividing cells, whereas Mdm1 localizes to punctate structures throughout the

cytoplasm, and is required for nuclear and mitochochrial transmission to the bud during mitosis (Fisk and Yaffe, 1997; van Hemert *et al.*, 2002). The functions of these intermediate filaments and the molecular mechanisms of their regulation are poorly understood.

In addition, a group of related proteins (Cdc3, Cdc10, Cdc11, Cdc12 and Shs1) called septins form a set of filaments approximately 10 nm in diameter (Kozubowski *et al.*, 2005). Septins are not related to intermediate filaments, but they experience cell cycle regulated changes, just as microfilaments and MTs do.

#### 1.1.3.1 Rearrangement of the actin cytoskeleton

The major component of microfilaments is actin, which interacts with a large number of actin-binding proteins (ABPs) and other associated proteins. In *S. cerevisiae*, actin is encoded by a single essential gene, *ACT1*, and exists as monomers (G-actin) or polymers (F-actin), but mostly as polymers in the cell (Karpova *et al.*, 1995). By fluorescent phalloidin staining, microfilaments in *S. cerevisiae* can be observed as two types of polymerized structures: cytoplasmic cables, which are bundles of long actin filaments; and cortical patches, which lie beneath the plasma membrane, and are small discs rich in F-actin. Actin filaments have structurally distinct ends: the barbed end (faster growing) and the pointed end (slower growing), and most of new filament assembly takes place at the barbed end. In *S. cerevisiae*, formins (Bni1 and Bnr1) stimulate assembly of actin cables, and loss of formin activity leads to loss of actin cables. Formins are activated when bound to Cdc42, a highly conserved Rho-type small GTPase required for polarized growth (Pruyne *et al.*, 2002).

Rearrangement of the actin cytoskeleton during mitosis is illustrated in Fig.1.1B. The dynamics of the actin cytoskeleton are cell cycle-regulated, and depend on Cdk activity (Ayscough *et al.*, 1997). Regulation of actin distribution is crucial for establishment and maintenance of cell polarity, as well as the controlling of cell surface growth (for example, it directs localized secretion to the new bud).

Before "Start", cortical patches are often evenly distributed at the cell surface and cables are randomly oriented in the cytoplasm. After the cell passes "Start", patches gather at the incipient bud site to form a ring, and cables are oriented toward this area. This process requires Cdc42, which concentrates at the pre-bud site in response to cell

cycle signals in late G1 (Gulli *et al.*, 2000; Ziman *et al.*, 1993). As a visible bud is formed and enlarges, cortical actin patches are concentrated in the bud at areas of cell surface growth. In S phase, as DNA replication occurs, cell wall expansion mostly occurs at the bud tip ("apical" growth). Somewhere in G2 phase, when the bud reaches a critical size, cell wall expansion switches to "isotropic" growth (all over the bud). Subsequently, as the bud continues to grow, chromosome segregation takes place. In late anaphase, the actin patches and cables then become evenly dispersed in both the mother and bud, but only for a very brief period. At the end of the cell cycle, the cortical patches are concentrated in rings on both sides of the neck, and the cables orient toward the neck (Ayscough *et al.*, 1997).

Cytokinesis in *S. cerevisiae* also requires an actomyosin ring, which seems to be a conserved mechanism for eukaryotes (reviewed in Tolliday *et al.*, 2001). At the G1/S transition, the actomyosin proteins assemble at the incipient bud site. During late anaphase, actin filaments are recruited to the actomyosin ring, which is now at the mother-bud neck due to bud growth. A primary septum composed of chitin is desposited to the neck. After that, secondary septum is synthesized at the same site, followed by digestion of the primary septum. At this time, the actomyosin ring constricts, and directs the exocytic machinery to the division site. Septum membrane and cell wall is then generated (Tolliday *et al.*, 2001).

After cytokinesis, the actin cytoskeleton redistributes evenly (Ayscough *et al.*, 1997). At the onset of the next cell cycle, the site of bud formation depends on the cell ploidy and requires upstream regulators of actin such as Cdc42 (Casamayor and Snyder, 2002). Haploid cells form buds adjacent to their previous bud site (axial pattern), whereas for diploid cells, daughter cells initially bud opposite to their previous birth pole and mother cells bud at either pole (bipolar pattern). Bud selection is mediated by a series of BUD proteins, and deletion of BUD genes result in altered bud site selection. Cdc42 is the effector of the bud site selection proteins, and is essential for bud formation, as loss of Cdc42 results in isotopic growth of the mother cell without bud formation (Casamayor and Snyder, 2002).

### 1.1.3.2 Septin assembly and regulation

In *S. cerevisiae*, a family of evolutionarily-conserved proteins called septins (Cdc3, Cdc10, Cdc11, Cdc12 and Shs1) forms a set of filaments (~10 nm) that assemble as a ring (Cid *et al.*, 2001; Gladfelter *et al.*, 2001). Septins belong to a conserved GTP-binding protein family (reviewed in Longtine and Bi, 2003).

The septin ring marks the cytokinetic plane in *S. cerevisiae* (Cid *et al.*, 2001; Gladfelter *et al.*, 2001). In late G1 (after "Start"), the septins assemble at the pre-bud site and directs the actomyosin ring (Tolliday *et al.*, 2001). The cell is polarized so that the bud emerges from inside the septin ring. Following bud emergence, more septin filaments assemble in the neck, and the ring broadens into an hourglass-shaped zone, which remains at the neck. At the end of the cell cycle, the septin "collar" divides into two, one on each side of the neck. After cytokinesis, the mother and daughter cell each inherits a septin ring, which subsequently disassembles after a new ring forms at the bud site for the next cell cycle (Cid *et al.*, 2001; Gladfelter *et al.*, 2001). The dynamics of septin behavior are depicted in Fig.1.1B.

Septin organization is cell cycle regulated. The assembly of the septin ring is dependent on G1 cyclin/Cdc28-mediated cell cycle signals. Cdc42 is also directly involved in guiding the formation of septin rings (Cid *et al.*, 2001; Gladfelter *et al.*, 2002). Transition of the septin ring into the hourglass shape may require several protein kinases such as Cla4, and splitting of the septin hourglass late in the cell cycle depends on the mitotic exit network (as described in section 1.1.4) (Longtine and Bi, 2003). Following cytokinesis, G1 cyclins/Cdc28 may promote the disassembly of the old septin rings through phosphorylation of Cdc3 (Longtine and Bi, 2003).

As well as being cell cycle regulated, septins can help coordinate progression of the cell cycle. Septins are important for a feedback signal called the morphogenesis checkpoint, which monitors bud growth and prevents entry into mitosis if bud growth is insufficient (Gladfelter *et al.*, 2005). In this checkpoint pathway, a critical bud size is necessary for conformational change in the septin ring, which then serves as a scaffold for protein kinases that cause the degradation of the Cdk inhibitor Swe1 (Wee1 ortholog), thus promoting entry into mitosis (Sakchaisri *et al.*, 2004). The scaffold function of septins can also direct localization of other proteins involved in various processes, such

as bud site selection, and cytokinesis. In addition, septins can function as a diffusion barrier for a number of proteins. For example, in late anaphase, septins sequester the mitotic exit activator Lte1 in the bud, thus ensuring that cells do not exit mitosis until the spindle has delivered one SPB into the bud (as described in section 1.1.4) (Castillon *et al.*, 2003).

Septins are found widely in animal cells, and may generally organize cortical domains important for cytokinesis or secretion (Spiliotis and Nelson, 2006).

### 1.1.3.3 The microtubule system

The microtubule system in *S. cerevisiae* consists of MTs, microtubule-associated proteins (MAPs), and the SPBs. Microtubules are composed of polymerized heterodimers of α and β tubulins (1:1 proportion). β tubulin is encoded by a single gene, *TUB2* (Neff *et al.*, 1983), whereas α tubulin is encoded by *TUB1* and *TUB3*, which are nearly identical (90% identity) but with different expression levels (*TUB1* makes most of the protein) (Schatz *et al.*, 1986). Correspondingly, disruption of *TUB2* or *TUB1* results in lethality of the cell, whereas disruption of *TUB3* does not lead to significant phenotypic changes under most conditions (Pringle *et al.*, 1997).

MAPs include motor proteins (kinesins and dynein) that translocate along microtubules, and non-motor proteins that regulate MT dynamics or crosslink MTs, such as Ase1 described above (in section 1.1.2) and Bik1 described later (in section 1.2.2).

As yeast microtubules are sensitive to benzimidazole drugs such as benomyl and nocodazole, treatment with these drugs has been very useful in assessing microtubule functions. Application of high concentrations of nocodazole or benomyl to growing wild-type yeast cells leads to depolymerization of microtubules (Stearns *et al.*, 1990). Interestingly, the sensitivity of yeast cells to benomyl and nocodazole is strongly temperature-dependent: as the growth temperature increases, the sensitivity decreases. This reflects the intrinsic cold sensitivity of the microtubule polymer (Modig *et al.*, 1994).

In yeast, unlike higher organisms, microtubules are not required for vesicular transport or the movement of organelles other than the nucleus. When yeast cells are treated with anti-microtubule drugs, polarized secretion and bud growth are not affected (Jacobs *et al.*, 1988; Huffaker *et al.*, 1988). Nevertheless, the mechanisms for moving the nucleus

during mitosis and karyogamy (nuclear fusion during mating) in *S. cerevisiae* are conserved in metazoans.

During the cell cycle, cytoplasmic and intranuclear microtubules appear to have distinct functions. Intranuclear microtubules are required for nuclear division (spindle assembly and chromosome segregation), whereas cytoplasmic microtubules are needed for nuclear positioning. Early in the cell cycle, cytoplasmic microtubules enter the bud and apparently make contact with the bud cortex (Carminati and Stearns, 1997; Miller and Rose, 1998). Interactions between cortical proteins and the cytoplasmic microtubules are crucial, since the absence of microtubule-cortex interactions results in spindle misorientation and elongation occurring entirely within the mother (Carminati and Stearns, 1997; Miller and Rose, 1998). Experiments with various *tub2* mutants have also revealed the importance of cytoplasmic microtubules for spindle orientation and positioning (Huffaker *et al.*, 1988). At semipermissive temperatures, *tub2-401* mutants have intact spindles but diminished levels of cytoplasmic microtubules. These cells experience normal spindle elongation and chromosome segregation, but these processes occur entirely within the mother, as the nucleus is not inserted into the neck (Sullivan and Huffaker, 1992).

### 1.1.4 Mitotic exit and the spindle position checkpoint

The timing of mitotic exit is critical for the maintenance of genetic stability. In *S. cerevisiae*, exit should only occur after the completion of nuclear division and migration. Mitotic exit is characterized by spindle disassembly and chromosomal decondensation, followed by cytokinesis. Its molecular basis is the inactivation of the mitotic Cdks (mainly B-cyclin/Cdc28), achieved in two ways: proteolysis of Clb cyclins, and direct binding of Sic1 (Cdk inhibitor) to Cdk. The Cdc14 phosphatase plays a crucial role in triggering mitotic exit, contributing to both Clb2 proteolysis and Sic1 accumulation.

For most of the cell cycle, Cdc14 is bound to an inhibitor Net1, which sequesters it in the nucleolus and keeps it inactive (Visintin *et al.*, 1999). Cdc14 experiences two stages of release in anaphase. At the metaphase-to-anaphase transition, Cdc14 is transiently released into the nucleus by a network of proteins named the FEAR (Cdc fourteen early anaphase release) (Stegmeier *et al.*, 2002; Saunders, 2002; reviewed in D'amours and Amon, 2004). The FEAR network includes the Separase Esp1, the kinetochore/spindle

protein Slk19, Spo12 and its homolog Bns1, the polo kinase Cdc5, the Securin Pds1, and the nucleolar protein Fob1, which inhibits Separase. It is noteworthy that the function of Esp1 in the FEAR is independent of its cohesin cleavage activity. The FEAR network promotes Cdc14 release from its inhibitor possibly by promoting its phosphorylation (Stegmeier *et al.*, 2002; Saunders, 2002). However, this transient release of Cdc14 is restricted to the nucleus and cannot trigger mitotic exit. Partially released Cdc14 can act in a feed-forward amplification to activate itself by activating the mitotic exit network (MEN), which in turn triggers the full and sustained release of Cdc14 into the nucleus and the cytoplasm during late anaphase (Lee *et al.*, 2001).

The MEN resembles a Ras-like signaling cascade, and involves the GTPase Tem1, Cdc14 itself, and several protein kinases such as Cdc5 (the yeast homologue of *Drosophila* polo kinase), Cdc15 (a MAP-kinase-like kinase), Dbf2 (Ser/Thr kinase), and Mob1, which forms a heterodimer with Dbf2 and is required for Dbf2 activity (reviewed in Bosl and Li, 2005). The Ras-like GTPase Tem1 functions at the top of the MEN (Shirayama *et al.*, 1994a). All the MEN proteins are required to maintain Cdc14 in its released state: in mutants that lack MEN activity, Cdc14 released during early anaphase returns to the nucleolus later without triggering mitotic exit (Lee *et al.*, 2001).

When Cdc14 is fully released into the cytoplasm, it activates (by dephosphorylation) the APC activator Cdh1, thus triggering proteolysis of mitotic cyclins by the APC. Cdc14 also stabilizes the Cdk inhibitor Sic1 by removing the phosphate group, which would otherwise target Sic1 for proteolysis. Furthermore, Cdc14 induces Sic1 transcription by dephosphorylating and allowing nuclear entry of Swi5, which is the transcriptional activator of Sic1 (Visintin *et al.*, 1998).

When the mitotic spindle is misaligned and spindle elongation occurs entirely in the mother cell, full release of Cdc14 from the nucleolus and mitotic exit are delayed until the spindle has been repositioned properly (Pereira *et al.*, 2000). This surveillance mechanism is called the spindle position checkpoint (Adames *et al.*, 2001; Pereira *et al.*, 2000; Bardin *et al.*, 2000). Fig.1.2 illustrates models for this surveillance mechanism.

Cell cycle checkpoints are highly conserved eukaryotic mechanisms that prevent each step of the cell cycle from occurring unless the previous step has been properly accomplished (Alberts *et al.*, 2002). In response to aberration, checkpoints arrest the cell

cycle to provide time for correction, and induce transcription of genes responsible for correction/repair. Misregulation of the cell cycle due to checkpoint loss can be associated with chromosomal instability and tumorigenesis (Damelin and Bestor, 2007; Malumbres and Barbacid, 2007; Li and Li, 2006; Baker *et al.*, 2005; Kops *et al.*, 2005). In *S. cerevisiae*, when deviation from the coordination of the cell cycle occurs, cell cycle processes are arrested and allowed sufficient time for correcting errors before proceedings of the subsequent events (Pringle *et al.*, 1997).

There are at least two mitotic checkpoints in yeast — the spindle assembly checkpoint and the spindle position checkpoint. When yeast cells are treated with anti-microtubule drugs, the cells proceed through the cell cycle until they reach mitosis, where they arrest with a large bud and an undivided nucleus located randomly in the mother cell. The cells have duplicated their DNA and SPB, but SPB separation, chromosome segregation, and nuclear migration cannot occur (Jacobs *et al.*, 1988). This cell cycle arrest in the absence of microtubules is mediated by a mechanism called the spindle assembly checkpoint, which delays the onset of anaphase until each and every chromosome has established a bipolar orientation. The function of this checkpoint requires multiple protein kinases (including Mps1, Bub1, and BubR1) and checkpoint phosphoproteins (including Mad1).

The existence of the spindle position checkpoint was first suggested by observation of dynein mutants. With misaligned spindles, these cells exhibit significantly prolonged waiting times before mitotic exit, eventually allowing the misaligned spindle to deliver one SPB into the bud (Yeh *et al.*, 1995). This checkpoint is sensitive to spindle positioning, as even transient penetration of one SPB into the bud (without subsequent movement of the nucleus into the neck) will trigger mitotic exit with normal kinetics (Adames *et al.*, 2001).

Research has shed light on how spindle positioning controls mitotic exit. It is thought that the regulation of Tem1 activity by the Bub2-Bfa1 complex (a GTPase activating protein /GAP) and Lte1 (a putative guanine nucleotide exchange factor /GEF) controls mitotic exit (reviewed in reviewed in Lew and Burke, 2003; Fig.1.2A and B). During formation of the mitotic spindle, Tem1 localizes preferentially to the cytoplasmic face of the old SPB, which is destined to move into the bud (Pereira *et al.*, 2000). The Bub2/Bfa1 complex colocalizes with Tem1 on the outer plaque of the SPB, keeping

Tem1 in its inactive form (GDP bound) (Pereira *et al.,* 2000; Geymonat *et al.*, 2002). Lte1 is sequestered at the bud cortex concomitant with bud formation in a process involving Cdc42, and is restricted to the bud by septins (Jensen *et al.*, 2002; Shirayama *et al.,* 1994b; Castillon *et al.*, 2003). When the spindle moves into the neck, bringing Tem1 into contact with Lte1, Tem1 becomes activated (GTP bound), which in turn activates other components of the MEN and triggers the full release of Cdc14. In cases of spindle mispositioning, because Lte1 is not present in the mother cell, Bub2/Bfa1 keeps Tem1 inactive (GDP bound), and Cdc14 is retained in the nucleolus, preventing mitotic exit. Consistent with this model, cells exit mitosis pre-maturely when overexpression of Lte1 causes some of the protein to mislocalize in the mother, or when Lte1 is mislocalized due to septin defects (Bardin *et al.*, 2000; Castillon *et al.*, 2003).

However, Lte1 is only essential for mitotic exit at low temperatures, suggesting alternative mechanisms for the regulation of MEN activity by spindle positioning (Adames *et al.*, 2001). Several lines of evidences point to a role for cytoplasmic MTs in regulating the MEN. For example, *tub2-401* mutants at semi-permissive temperatures have diminished cytoplasmic microtubules, and these cells with mispositioned spindles proceed with mitotic exit to produce binucleate mothers and anucleate daughters (Sullivan and Huffaker, 1992).

One model postulates the spindle position checkpoint monitors contact between the cytoplasmic microtubules and the cortex at the neck (Adames *et al.*, 2001). When an SPB moves into the bud, the cytoplasmic microtubules lose their contact with the neck, allowing the cell to proceed with mitotic exit (Fig.1.2). Experiments with several mutant strains affecting cMTs have revealed that many cells with mispositioned spindles exit mitosis pre-maturely. In these cells, either a SPB transiently inserts into the neck then falls back into the mother, or cytoplasmic microtubules transiently lose interactions with the neck, while both SPBs are still within the mother (Adames *et al.*, 2001). This inappropriate mitotic exit does not require the presence of Lte1. In addition, mitotic exit can occur at normal time upon loss of Bub2/Bfa1 activity in dynein mutants (spindle misaligned and the SPB does not enter the neck). Thus, it is speculated that interactions of cytoplasmic microtubules with the neck provide an inhibitory signal through Bub2/Bfa1 that prevents exit from mitosis (Adames *et al.*, 2001).

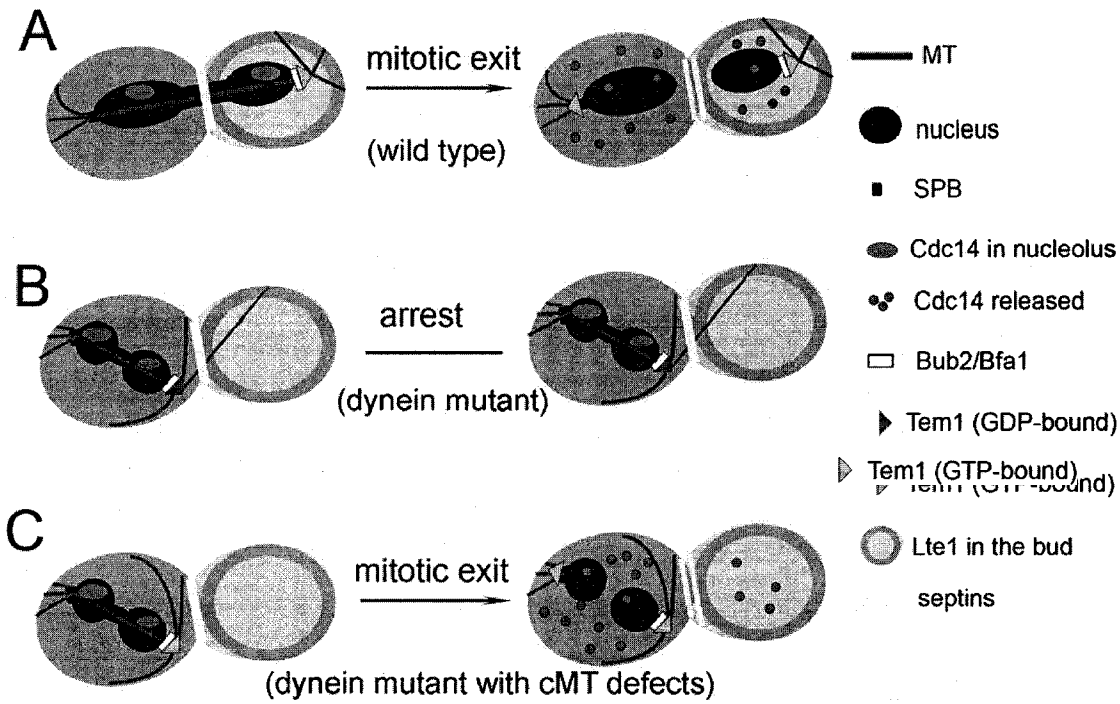


**Figure 1.2. The spindle position checkpoint couples spindle positioning with mitotic exit.** Full release of Cdc14 from the nucleolus into the cytoplasm is a crucial event for mitotic exit, and Cdc14 release requires the mitotic exit network (MEN) proteins. Tem1, which is at the top of the MEN pathway, is localized at the old SPB. (A) During a normal cell cycle, when the spindle is inserted into the neck, Tem1 is activated by Lte1, which is sequestered in the bud. Active Tem1 (GTP bound) activates the MEN and the cell exits from mitosis. (B) When the spindle is mispositioned and cytoplamic MTs extend into the neck, Bub2/Bfa1 (which also localizes at the old SPB) keeps Tem1 inactive (GDP bound). Cdc14 remains in the nucleolus and the cell arrests in late anaphase. Septins at the neck prevent Lte1 from leaking into the mother cell. (C) When the spindle is mispositioned but cytoplamic MTs do not extend into the neck, Cdc14 is released, and leads to pre-mature mitotic exit.

## 1.2 The Kar9 and dynein pathways are involved in nuclear positioning

This study focuses on identifying biomolecular players that are possibly involved in spindle orientation and/or nuclear positioning. Two pathways (the Kar9 pathway and the dynein pathway) are known to participate in spindle orientation and nuclear positioning, but have slightly different roles and function in a sequential manner (reviewed in Pearson and Bloom, 2004; Bloom, 2001). The Kar9 pathway functions before the onset of anaphase and depends on the actin cytoskeleton: it moves the nucleus into the vicinity of the neck, and ensures correct orientation of the short pre-anaphase spindle. The dynein pathway functions after the onset of anaphase, and is actin-independent: it moves the nucleus into the neck during anaphase, at about the time of spindle elongation (Adames and Cooper, 2000).

The Kar9 pathway involves Kar9, the microtubule-interacting protein Bim1, the formin protein Bni1, actin, the actin-based motor Myo2, and the kinesin-related protein Kip3 (reviewed in Huisman and Segal, 2005). This pathway moves the nucleus by capture/shrinkage and sweeping motions of cytoplasmic microtubules at the bud cortex. In mutants of the Kar9 pathway, the nucleus does not move close to the neck and the pre-anaphase spindle is often misaligned (Adames and Cooper, 2000). Misalignment of spindles and failure of capture of cytoplasmic microtubules at the bud cortex can result in spindle elongation entirely in the mother cell (Miller and Rose, 1999; Lee *et al.*, 1999; Miller *et al.*, 1999).

The dynein pathway involves the dynein multisubunit complex, the dynactin multisubunit complex (the dynein regulator), several microtubule plus-end tracking proteins (Pac1, Ndl1, Bik1), the kinesin-related protein Kip2, and the cortical anchor protein Num1 (Bloom, 2001; Li *et al.*, 2005; Lee *et al.*, 2005). During anaphase, this pathway is responsible for the sliding of cytoplamic microtubules along the bud cortex, which pulls the nucleus into the neck (Adames and Cooper, 2000). In dynein heavy chain mutants (*dyn1*Δ), SPB separation and assembly of the bipolar spindle are normal, and the nucleus is correctly positioned close to the neck (Yeh *et al.*, 1995). However, spindle elongation proceeds mainly within the mother cell, and the SPB proximal to the

neck does not efficiently migrate into the bud. Thus, spindle elongation is no longer coupled with nuclear migration into the neck (Li *et al.*, 1993; Eshel *et al.,* 1993).

The Kar9 and dynein pathways are partially redundant, as neither is essential. Double mutations in one pathway do not result in more severe nuclear positioning defects than those observed in single mutants. In mutants of the Kar9 pathway, microtubule capture at the bud cortex is absent, and spindle movement into the neck is delayed (Adames and Cooper, 2000). However, microtubule sliding corrects the nuclear movement defect (Adames and Cooper, 2000; Tirnauer *et al.*, 1999). In dynein/dynactin mutants, spindle movement into the neck is also delayed, but not absent (Yeh *et al.*, 1995; Muhua *et al.*, 1998). The backup mechanism in these mutants is mainly microtubule capture/shrinkage events, which in normal cells are responsible for moving the nucleus close to the neck before anaphase (Adames and Cooper, 2000). In this backup mechanism, the Kar9 pathway proteins probably contribute by maintaining proper spindle and cytoplasmic microtubule orientation, which allows spindle elongation to eventually penetrate the neck as the spindle length exceeds the length of the mother (Miller *et al.*, 1998; Cottingham and Hoyt, 1997; DeZwaan *et al.*, 1997).

However, simultaneous disruption or loss of both the Kar9 and the dynein pathways leads to cell death or slow growth (referred to as synthetic lethality or growth defect) (Tong *et al.*, 2004). Therefore, if loss of a gene product leads to nuclear postioning defects, and mutations in this gene combined with dynein mutations cause synthetic lethality or growth defect, then this gene product may be involved in the Kar9 pathway, and vice versa.

## 1.2.1 The Kar9 pathway

Kar9 was first identified in the mating process of *S. cerevisiae* (Kurihara *et al.*, 1994). In response to the mating pheromone produced by another haploid cell of the opposite mating type, the yeast haploid cell is briefly arrested in G1 phase. Each cell then "shmoos", forming a mating projection toward the pheromone, and the nucleus moves toward the shmoo projection, with cytoplasmic microtubules extending to the shmoo tip. The cell wall between the two mating cells breaks down, and their plasma membranes fuse, allowing the two nuclei to migrate toward each other and fuse (termed karyogamy, Rose 1996; Read *et al.*, 1992). This process results in a diploid zygote. In contrast, in

zygotes of *kar9* mutants, the cytoplasmic microtubules are misoriented, and the nuclei fail to fuse but remain widely separated.

The Kar9 pathway (refer to Fig.1.3) is required for microtubule capture at the bud cortex. Early in the cell cycle, before bud emergence, microtubules are captured at the incipient bud site (Adames and Cooper, 2000). Shrinkage of the captured microtubules is often associated with nuclear movement towards the neck. Cytoplasmic microtubules in the bud also pivot at their minus end at the SPB, with the plus end maintaining contact with the bud cortex. This motion is referred to as microtubule "sweeping", and contributes to spindle rotation until proper alignment along the mother-bud cortex is achieved (Adames and Cooper, 2000).

The Kar9 protein plays key roles for the microtubule capture process. Cells expressing Kar9-YFP at its endogenous level localizes the protein along microtubules and to microtubule plus ends, as well as to spindle poles (Liakopoulos *et al.*, 2003). In metaphase, Kar9 is found only on one spindle pole (the daughter bound) and along the cytoplasmic MTs extending from it. It seems that asymmetric Kar9 distribution directs the cMTs toward the bud site, because upon deletion of *KAR9* or loss of Kar9 asymmetry, alignment of the pre-anaphase spindle becomes random.

How the asymmetry of Kar9 distribution is achieved remains to be elucidated. The polarized actin cytoskeleton is involved (as described next). In addition, Clb4/Cdc28 may regulate Kar9 localization by phosphorylating the protein (Liakopoulos *et al.*, 2003).

The actin cytoskeleton is involved in targeting cMTs (daughter-bound) to the bud cortex. Latrunculin (an actin-depolymerizing drug) treatment of living cells leads to mispositioning and misorientation of the pre-anaphase spindle, suggesting that cytoplasmic microtubules are tethered to the actin cytoskeleton in the bud (Miller *et al.*, 1998). The actin-based type V myosin Myo2 is required for Kar9 asymmetry. In *myo2* mutants (with mutations in the motor domain or in the Kar9-interacting domain), Kar9 localization becomes diffuse throughout the mother and bud, and spindles tend to be misorientated (Beach *et al.*, 2000; Yin *et al.*, 2000; Liakopoulos *et al.*, 2003). Myo2 presumably confines Kar9 in the bud through an actomyosin transport system along polarized actin cables.

As the formin protein Bni1 regulates actin cytoskeleton and cell polarization, it is not

surprising that Bni1 is also involved in the Kar9 pathway (Kohno *et al.*, 1996; Evangelista *et al.*, 1997; Zahner *et al.*, 1996; Fujiwara *et al.*, 1999). Bni1 forms a cap at the incipient bud site in late G1, and remains at the bud tip through the cell cycle (Miller *et al.* 1999). Upon loss of *BNI1*, the mutants show nuclear positioning defects similar to *kar9* mutants, although not as severe. Genetic analysis has placed Bni1 in the Kar9 pathway, as loss of both *BNI1* and *KAR9* does not lead to a more severe phenotype than single *kar9* mutants, whereas loss of *BNI1* and dynein pathway components is synthetically lethal (Lee *et al.*, 1999; Miller *et al.*, 1999).

An actin-interacting protein Bud6 is also involved in the Kar9 pathway. Bud6 interacts with Bni1 in a two-hybrid assay, and associates biochemically with Myo2. Bud6 was initially characterized as required for bud site selection in diploid cells (Amberg *et al.*, 1997). *bud6* mutants have similar but even milder nuclear positioning defects than *bni1* mutants (Miller *et al.* 1999). Bud6 is recruited to the pre-bud site and remains at the bud tip after bud emergence through regulation by Cdc42. It is speculated that Bud6 may serve as the cortical protein that captures cytoplasmic microtubules, because studies show that MT capture/shrinkage occurs almost exclusively at Bud6 sites. However, there must be alternative capture mechanisms, since deletion of *BUD6* does not completely perturb the cortical capture (Segal *et al.*, 2002).

Interestingly, Kar9 is thought to be the functional counterpart of the mammalian tumour suppressor protein adenomatous polyposis coli (APC) (Bloom, 2000). In humans, APC associates with the microtubule plus-end-tracking protein (+TIP) EB1, and can be regulated by Cdk phosphorylation (Nakamura *et al.*, 2001). Kar9 shares sequence similarity with APC within the domain that mediates its binding to EB1.

Does Kar9 in *S. cerevisiae* also bind to +TIP proteins? Bim1, the yeast homologue of the human EB1, interacts with Kar9 in a two-hybrid screen, and the interaction is confirmed by co-immunoprecipitation (Miller *et al.*, 2000). Bim1 has been reported to regulate microtubule dynamics in *S. cerevisiae*: *bim1* mutants contain shorter and less-dynamic cytoplasmic microtubules (Adames and Cooper, 2000; Tirnauer *et al.*, 1999). During mitosis, *bim1* mutant cells are inefficient in moving the nucleus close to the neck, and spindles are misoriented (Adames and Cooper, 2000). In these cells, shorter or less-dynamic microtubules may reduce the probability of a microtubule end being captured at

the bud cortex. The "sweeping" motion is also noticeably reduced, as the spindle is not as motile (Adames and Cooper, 2000).

Loss of Bim1 diminishes Kar9 localization along cytoplasmic microtubules, suggesting that Bim1 mediates interactions between Kar9 and microtubules (Miller *et al.*, 2000). The current model of the Kar9 pathway proposes that Bim1 mediates the Kar9-MT interaction. Because Myo2 confines Kar9 to the bud by linking Kar9 with actin cables (that are polarized towards the bud cortex), the Kar9-Myo2 interaction thus targets cytoplasmic plus end (as well as Kar9) toward the bud cortex(Huisman and Segal, 2005). An observation in support of this model is that a Bim1-Myo2 fusion protein can bypass Kar9 requirement for spindle orientation (Hwang *et al.*, 2003). Once microtubules make contact with the bud cortex, Kar9 (possibly with Bud6) provides a platform for capture at the cortex. Microtubule shrinkage moves the nucleus to the neck, and the "sweeping" motion of microtubules helps align the spindle along the mother-bud axis (Beach *et al.*, 2000; Huisman and Segal, 2005). This model is illustrated in Fig. 1.3.

Genetic analysis has implied that the kinesin-related protein Kip3 (a kinesin-14 family member, minus-end motor) also functions in the Kar9 pathway, although the connection between Kip3 and Kar9 had not been clearly defined until lately (Gupta *et al.*, 2006). Loss of Kip3 function leads to nuclear positioning defects similar to those seen in *kar9* mutants, whereas anaphase B spindle elongation kinetics is not affected (Miller *et al.*, 1998). In these cells, the nucleus is capable of moving towards the neck, but fails to maintain its position there and drifts away (DeZwaan *et al.*, 1997). In addition, *kip3* mutants show very long cytoplasmic microtubules at lower temperatures, so Kip3 may act by destabilizing cytoplasmic microtubules (Cottingham and Hoyt, 1997; Miller *et al.*, 1998).

A very recent study demonstrates how Kip3 functions in the Kar9 pathway. In this study, fluorescent speckle analysis shows that Kip3 moves toward and accumulates on the plus ends of growing microtubules (Gupta *et al.*, 2006). Loss of Kip3 does not affect microtubule capture at the bud cortex, but produces significant reduction in frequency of microtuble catastrophe —switch from growth to shrinkage. So Kip3 affects growth and shrinkage rates of MTs, and loss of Kip3 leads to extra long MTs (Gupta *et al.*, 2006). If these abnormally long MTs are in contact with the bud cortex, the SPB (daughter-bound)

is pushed away from the neck. These observations suggest that the spindles are mispositioned in *kip3* cells because attached microtubules grow inappropriately, pushing pre-anaphase spindles away from their normal position near the bud neck (Gupta *et al.*, 2006).

In summary, the Kar9 pathway confines Kar9 localization asymmetrically into the bud, and provides a platform for MT capture at the bud cortex. Capture/shrinkage of these MTs brings the nucleus up to the neck and aligns the pre-anaphase spindle along the mother-bud axis. Kip3 acts as a regulator of the dynamics of microtubules attached to the bud tip, ensuring that shrinkage of the cMTs pulls the nucleus toward the neck. These two parts (MT capture and the regulation of MT dynamics) are largely independent (Gupta *et al.*, 2006).

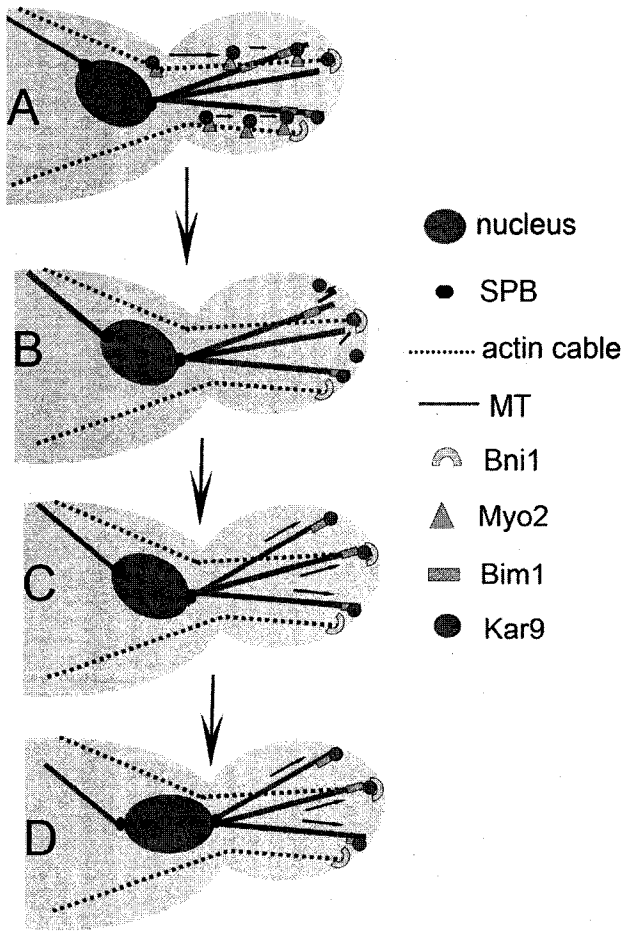


**Figure 1.3. The current model for the Kar9 pathway** (Huisman and Segal, 2005). Asymmetric localization of Kar9 into the bud depends on polarized actin cables and the actin-based motor Myo2. Bim1 mediates interaction of Kar9 with cytoplasmic microtubules, and keeps Kar9 at the plus end. At the microtubule plus ends, in a process dependent on Myo2 and actin cables, Kar9 interacts with the actin formin protein Bni1, which leads to the capture of cytoplasmic microtubules at the bud cortex. Once captured, shrinkage of these microtubules moves the nucleus close to the neck. Cytoplasmic microtubules also "sweep" along the bud cortex (described in the text), which helps align the mitotic spindle along the mother-bud axis.

## 1.2.2 The dynein pathway

Cytoplasmic dynein is a multisubunit, minus end-directed microtubule motor protein. In vertebrates, cytoplasmic dynein contains two heavy chains (HCs), two intermediate chains (ICs), two to four light intermediate chains (LICs), and various numbers of light chains (LCs) (King *et al.*, 2002). The heavy chain contains the motor domain, and the accessory chains mediate the functions performed by the HC. In animal cells, cytoplasmic dynein has been implicated in various subcellular activities, such as vesicle trafficking, retrograde axonal transport, organization and orientation of the mitotic spindle (Holzbaur and Vallee, 1994; Vallee *et al.*, 2004; Hirokawa *et al.*, 1998; Vale, 2003). Dynein-driven movement of organelles along microtubules requires the presence of dynactin (Gill *et al.*, 1991). Studies show that dynactin may promote dynein-based movements by increasing the processivity of the motor (King and Schroer, 2000).

In 1993, two groups identified the gene encoding the heavy chain of cytoplasmic dynein in *S. cerevisiae*: *DYN1/DHC1* (Li *et al.*, 1993; Eshel *et al.*, 1993). DAPI-staining of the *dyn1Δ* mutants showed nuclear positioning defects. At 30°C, 3-14% of the cells are large, budded cells in which two or more nuclei are located in the mother and no nuclei are found in the bud. The fraction of this type of cells increases as the growth temperature decreases (14-38% at 11°C) (Li *et al.*, 1993; Eshel *et al.*, 1993).

In *dyn1* mutants, chromosome segregation is unimpeded, and the speed and length of the fast spindle elongation stage appears normal, although elongation is confined primarily in the mother cell (Yeh *et al.*, 1995). However, oscillation of the nucleus, which occurs in normal cells during nuclear insertion into the neck, is diminished. Anaphase spindles appear to be oriented randomly, and cells with mispositioned spindles arrest before mitotic exit. Nevertheless, over varying lengths of time, the nuclear lobe proximal to the neck eventually moves into the daughter cell. The length of the delay in correcting the spindle position depends on the orientation of the spindle at the time of elongation. If the spindle happens to be orientated along the mother-bud axis, the delay is not noticeable, whereas if the spindle happens to be oriented obliquely to the axis, an obvious delay is observed (Yeh *et al.*, 1995; Adames and Cooper, 2000).

Research later revealed the mechanistic roles of dynein in nuclear positioning. During anaphase, as the spindle elongates, cytoplasmic microtubules associate laterally and slide along the bud cortex, in an actin-independent manner (Adames and Cooper, 2000; Heil-Chapdelaine *et al.*, 2000b). Interactions with the cortex are along the complete length of the microtubules rather than at the end, and the sliding exerts considerable force, pulling the nucleus into the neck. After insertion of the nucleus into the bud, microtubules also slide along the mother cortex, so the nucleus is kept in the neck by a balance of pulling forces from both sides, which may explain its oscillation (Adames and Cooper, 2000).

In dynein mutants, the nucleus moves up to the neck normally, and the pre-anaphase spindle orientation is also normal (Adames and Cooper, 2000). It is during anaphase, when the spindle fails to enter the bud, that it becomes misaligned. In these cells, cytoplasmic microtubules often grow much longer than those in wild type cells. However, even when these long microtubules have the opportunity to interact with the bud cortex, sliding along the bud cortex does not occur (Adames and Cooper, 2000). This suggests a model in which dynein/dynactin is anchored at the cortex, where it binds cytoplasmic microtubules, and walks toward the minus-end (Carminati and Stearns, 1997).

In *S. cerevisiae*, the dynein intermediate chain is Pac11, and Dyn3 is the light intermediate chain (Geiser *et al.*, 1997; Lee *et al.*, 2005). Dyn2, the dynein light chain, was the first LC identified in fungi (Dick *et al.,* 1996; Ho *et al.*, 2002; Tong *et al.*, 2004). For a list of dynein subunits in *S. cerevisiae* and their orthologs in humans, refer to Table 1.1.

For mechanism of the dynein pathway, an off-loading model of dynein at the cell cortex has been proposed (Lee *et al.*, 2005). In this model, the microtubule plus-end tracking proteins (such as Bik1) assist recruitment of dynein to microtubule plus ends. The plus ends are quite dynamic and probe for the bud cortex. Once the plus end interacts with the cortical anchor Num1, dynein is delivered to the cortex. At the cortex, the dynein motor is activated (by its regulator dynactin) and produces force for microtubule sliding. This model is illustrated in Fig. 1.4.

Activity of the dynein motor can be regulated by its accessory proteins, and different subunits may mediate the interaction between the motor and diverse cellular components

(refer to section 1.3.1). Dyn1-3GFP localizes at the distal plus ends of cytoplasmic microtubules and in stationary dots at the mother or bud cortex (Lee *et al.*, 2003; Sheeman *et al.*, 2003). Before late anaphase, Dyn1 localization at the mother cortex is predominant, whereas in cells with a long spindle, localization to the bud cortex is more common. The localization of Pac11(IC) is virtually identical to Dyn1, whereas Dyn3 (LIC) appears to be fairly motile and often colocalizes with Dyn1 at the plus ends of cytoplasmic microtubules but not at the cell cortex (Lee *et al.*, 2003; Lee *et al.*, 2005). Pac11 and Dyn3 localization are dependent on Dyn1. Conversely, Dyn1 localization at the microtubule plus ends requires Pac11, while its localization at the cell cortex is supported by Dyn3, suggesting that Pac11 (IC) is necessary for Dyn1 (HC) stability along microtubules, whereas Dyn3 (LIC) may mediate interaction between Dyn1 and proteins at the cortex (Lee *et al.*, 2005).

Dynactin also regulates dynein activity. Several dynactin components are known in *S. cerevisiae*: Arp1, the actin-related protein; Jnm1, the ortholog of p50/dynamitin (DCTN2) from vertebrates; and Nip100, the ortholog of $p150^{Glued}$ (DCTN1) (McMillan and Tatchell, 1994; Clark and Meyer, 1994; Geiser *et al.*, 1997; Kahana *et al.*, 1998). For a list of these subunits and their orthologs in human, refer to Table 1.1. Loss of function of any of these dynactin components leads to *dyn1*-like nuclear positioning defects, and microtubule sliding along the bud cortex is absent in these mutants (Adames and Cooper, 2000). Loss of dynactin leads to dynein accumulation at the plus ends of microtubules during anaphase, and the cortical localization is diminished (Lee *et al.*, 2005). This accumulation of Dyn1 is also observed in *dyn3* mutants, or when the Dyn1 protein itself is mutated (for example, in the motor domain) (Lee *et al.*, 2005). Thus, dynactin activity is required for the off-loading of dynein to the cortex, where the motor protein functions to pull microtubules. It can be speculated that Dyn3, as the dynein accessory subunit, may help link the dynein complex to dynactin.

Dynactin localization studies, however, have not been very successful (possibly due to low protein abundance) — none of these proteins have been localized directly at endogenous levels. In the off-loading model, when and how dynactin is recruited to the plus end (or cell cortex) remains unknown. In addition, the mechanism for activation of dynein by dynactin is not clearly understood, although it has been demonstrated that

dynactin can increase the processivity of dynein *in vitro* (King and Schroer, 2000).

In cultured mammalian cells and filamentous fungi (*Aspergillus* and *Neurospora*), dynein and dynactin are found as small punctae at microtubule plus ends (Valetti *et al.*, 1999; Vaughan *et al.*, 1999; Morris *et al.*, 2003; Ozeki *et al.*, 2003; Brandon *et al.*, 2004; Liang *et al.*, 2004). These plus ends are often tethered to either chromosome kinetochores or to the cell cortex, in order to organize and orient the mitotic spindle (for a detailed description of this process, refer to section 1.3.3). In either case, dynein/dynactin recruitment to microtubule plus ends requires LIS1 (Lissencephaly 1), NudE/Nudel (nuclear distribution), and DISC1 (Disrupted-In-Schizophrenia-1) (Dujardin and Vallee, 2002). Notably, all these proteins are mutated in different neuronal diseases in human (Reiner *et al.*, 1993; Pilz *et al.*, 1998). Studies have been done in order to find the counterparts for dynein/dynactin recruitment in *S. cerevisiae*. As expected, Pac1 (a homologue of LIS1) and Ndl1 (the yeast orthologue of NUDE), are both required for Dyn1 localization at microtubule plus ends in *S. cerevisiae* (Lee *et al.*, 2003; Li *et al.*, 2005).

So how is dynein recruited to the plus ends? Besides the above-mentioned Pac1 and Ndl1, the microtubule-associated protein Bik1 (an ortholog of the mammalian microtubule plus-end tracking protein CLIP170), and Kip2 (a kinesin-related protein), have also been implicated in this process. In any of these four mutants, Dyn1 localization at the plus ends is significantly reduced (Lee *et al.*, 2003). Pac1 and Ndl1 proteins are found to colocalize at the plus-ends, while Bik1 and Kip2 are located along cytoplasmic microtubules (Tong *et al.*, 2004; Lee *et al.*, 2003; Li *et al.*, 2005; Carvalho *et al.*, 2004; Sheeman *et al.*, 2003). Because Ndl1 and Pac1 co-localize and interact biochemically, while Bik1 biochemically interacts with Kip2 and co-migrates with Kip2 along microtubles, it is suggested that Ndl1/Pac1 and Bik1/Kip2 are in two pathways that are largely independent for recruiting dynein to the plus ends. However, inactivation of either pathway leads to an almost complete absence of dynein localization at the plus end, so the two pathways are not redundant but may function cooperatively (Li *et al.*, 2005).

How these two pathways connect with each other is unknown. In the Pac1/Ndl1 pathway, Ndl1 may act upstream of Pac1, as Pac1 overexpression suppresses an *ndl1* mutation, but not vice versa (Li *et al.*, 2005). It is speculated that Ndl1 stabilizes or

activates Pac1 at the plus end. In the Bik1/Kip2 pathway, both proteins may stabilize MTs, since mutations in *BIK1* destabilize the cytoplasmic microtubules, and *kip2* mutants also have very short or absent cytoplasmic microtubules (in contrast to *kip3* mutants). One possible role for Kip2 is as a transporter that moves dynein from the SPB back toward the plus ends of the microtubules, during which Bik1 is needed as the MAP (Carvalho *et al.*, 2004). In addition, Kip2 may stabilize microtubules by targeting Bik1 to the plus end. In the absence of Bik1, Pac1/Ndl1 localization at the plus ends are reduced, suggesting that Bik1 may mediate the interaction between MT and Pac1/Ndl1. Alternatively, Bik1 affects the interaction (between MT and Pac1/Ndl1) by acting as the MT stabilizer.

Interestingly, it has been suggested that Bik1 may also be involved in the Kar9 pathway, and contributs to the asymmetric localization of Kar9 by promoting Kar9 phosphorylation (Moore *et al.*, 2006). This mechanism is not fully elucidated. Nevertheless, it seems that the MAPs play multiple roles during mitosis, by regulating MT dynamics or mediating the interaction between MT and other proteins.

Following recruitment to MT plus ends, dynein needs to be offloaded to the cell cortex, where it can be anchored and activated, and move toward the minus-end (the SPB). So what proteins at the cortex may anchor or activate the dynein motor? The cortical protein Num1 appears to be a cortical anchor for dynein (Kormanec *et al.*, 1991; Farkasovsky and Kuntzel, 1995; Geiser *et al.*, 1997; Schwartz *et al.*, 1997). Num1 is localized at the cortex, and this localization is not dependent on microtubules, dynein, or dynactin (Heil-Chapdelaine *et al.*, 2000a). Loss of Num1 leads to absence of the MT sliding motion along the cortex (Heil-Chapdelaine *et al.*, 2000a). What is more, Num1 contains a domain capable of directly binding to membrane lipids, which might help anchor Num1 (and dynein) to the plasma membrane (Farkasovsky and Kuntzel, 1995).

In cells lacking Num1, dynein accumulates at the plus ends of microtubules during anaphase, and the cortical localization is diminished. This is in sharp contrast to what is observed in *bik1*, *ndl1*, *pac1* or *kip2* mutants, in which Dyn1 localization at the plus ends is significantly reduced (Lee *et al.*, 2003). Therefore, Num1 is proposed to be required for the delivery of dynein to the cortex. Considering that this accumulation (of dynein) at the microtubule plus ends is also observed in dynactin mutants, it is tempting to speculate

that dynactin actually mediates the interaction between dynein and the cortical protein Num1.

In summary of the dynein pathway for nuclear positioning: dynein is recruited to the microtubule plus ends (by Pac1/Ndl1 and Kip2/Bik1), then delivered to the cortex, where it becomes activated and drives the microtubule sliding behavior, generating the force to pull the nucleus into the neck. Both dynein off-loading and activation may require dynactin and the cortical protein Num1. This model is illustrated in Fig. 1.4.

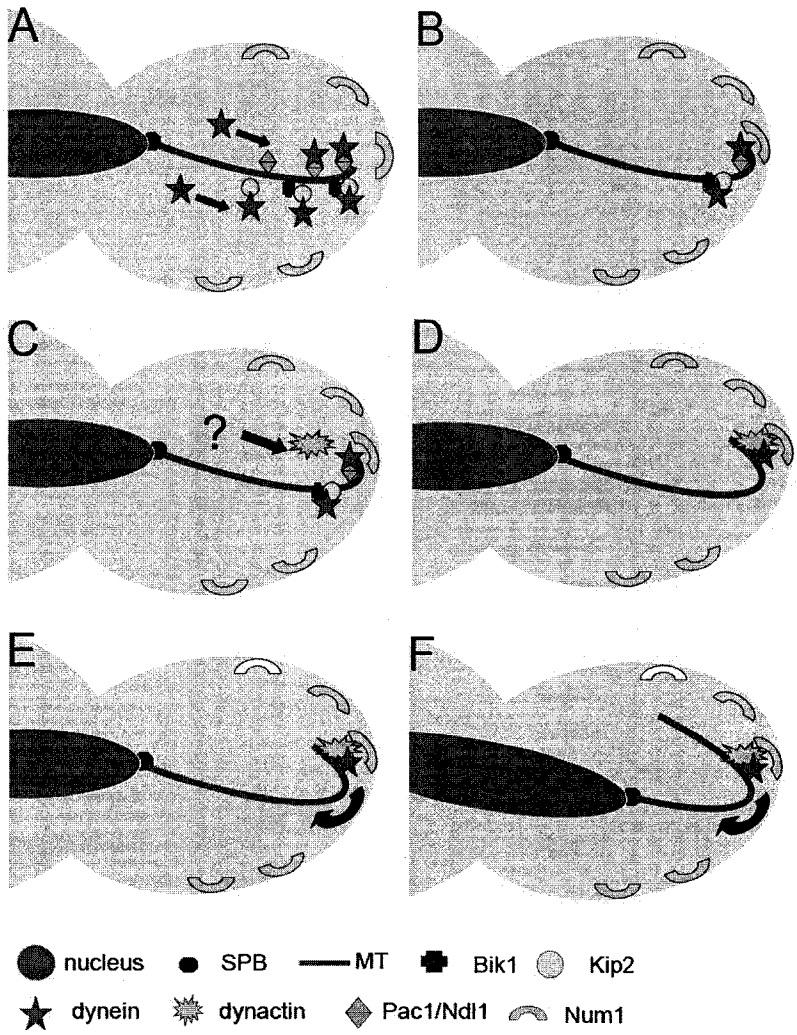


**Figure 1.4 The current model for dynein-dependent spindle positioning** (Sheeman *et al.*, 2003; Lee *et al.*, 2003; Li *et al.*, 2005). (A/ B) Dynein is delivered to the microtubule plus ends cooperatively by Pac1 (which interacts with Ndl1), and Bik1 (which is presumably targeted to the plus end by Kip2). (C/D) At the cell cortex, dynein is offloaded, which requires both the cortical anchor Num1 and the dynactin activity. The detail of how dynactin is delivered is not fully understood. (E/F) Once dynein is offloaded to the cortex and becomes anchored, its motor activity is activated. The motor then moves towards the minus end of the cytoplasmic microtubule, producing the force for microtubule sliding, which in turn pulls the nucleus into the neck.

## 1.3 Composition and structure of dynein/dynactin

### 1.3.1 The structure of cytoplasmic dynein

In the early 1960s, axonemal dynein was identified as the major force-producing ATPase of cilia and flagella (Gibbons and Rowe, 1965). Two decades later, cytoplasmic dynein was first isolated from rat brain tissue (Paschal and Vallee, 1987). This group found that a microtubule-associated protein, MAP 1C, is a microtubule-activated ATPase that produces force along microtubules in a retrograde direction (Bloom *et al.,* 1984). They found that the MAP 1C protein is related to the axonemal form of dynein by sequence analysis, and therefore, referred to this protein as cytoplasmic dynein. In higher organisms, cytoplasmic dynein is involved in multiple cellular processes, such as retrograde axonal transport, transportation of intracellular organelles, organization and orientation of the mitotic spindle, and chromosome separation during mitosis (Holzbaur and Vallee, 1994; Vallee *et al.*, 2004; Hirokawa *et al.*, 1998; Vale, 2003).

The structure of dynein is important for its motor function, as it has to interact with diverse cellular components during various cellular activities. However, despite our knowledge of its functions, the ultrastructure of the dynein complex remains to be elucidated, as all forms of dynein are very large proteins and attempts to crystallize even the heavy chain alone have failed thus far. In electron microscope studies, cytoplasmic dynein is observed to have two globular "heads" with a slender extension called the "stalk". Dynein "walks" along MTs by way of repeated cycles of detachment and reattachment (Johnson and Wall, 1983; Goodenough and Heuser, 1985; Vallee *et al.*, 1998). Each of the two "heads" actually consists of the C-terminal region of one heavy chain, which possesses an active ATPase site and generates force for movement. Besides the two heavy chains (HC, each ~500-530 kDa), cytoplasmic dynein (1.2 MDa) also contains multiple intermediate chains (IC, ~70-74 kDa each), light intermediate chains (LIC, ~53-59 kDa), and light chains (IC, ~8-22 kDa) (Hughes *et al.*, 1995; King *et al.*, 1996a; King *et al.*, 1996b).

Analysis of the dynein heavy chain sequence has revealed the presence of multiple highly conserved P-loop elements (GXXGXGKT/S, also called the Walker A motif, a feature of the AAA+ protein superfamily: *A*TPase *a*ssociated with various cellular

*a*ctivites) involved in phosphate binding and ATPase hydrolysis (Ogawa, 1991; Mikami *et al.*, 1993; Walker *et al.,* 1982). The first P-loop is functionally essential for ATP binding and hydrolysis, but further evidence suggests that the other P-loop elements are also important, and may contribute to ATP binding (Kon *et al.*, 2004; Silvanovich *et al.*, 2003; Gibbons *et al.*, 1987).

The "stalk" has a microtubule-binding motif, and is spatially isolated from the ATPase domain at the tip of a projecting coiled-coil (mapped to a site of 340 amino acid residues downstream from the fourth P-loop element) (Gee *et al.*, 1997). The N-terminus of the heavy chain makes a "stem" that contains a cargo-binding domain (Oiwa and Sakakibara, 2005). The stem can also mediate self-dimerization of the HC, and can interact with intermediate chains, which in turn bind dynactin (Sakato and King, 2003; King, 2000).

Many organisms have only one isoform for cytoplasmic dynein heavy chain, yet, dynein-driven movement is found in a wide variety of cellular activities. This functional diversity is achieved in multiple ways: via the association of the HC with various accessory proteins or dynactin (both of which can target dynein for different sites and regulate its activity), or through post-translational modifications (such as phosphorylation) (Barton and Goldstein, 1996; Karki and Holzbaur, 1999).

Isoform diversity has been described for the intermediate chains, which tend to have a conserved C-terminal region and a divergent N-terminus. This suggests a common function for the C-terminus (such as heavy chain binding), and more specific roles for the N-terminus (such as directing the complex to an organelle surface or microtubules, or for interaction with dynactin) (King and Witman, 1990; King *et al.*, 1991; Karki and Holzbaur, 1995). The intermediate chains can regulate dynein activity, as separation of intermediate chains from the remainder of the dynein complex leads to enhancement of ATP hydrolysis (Kini and Collins, 2001). In addition, removal of different isoforms of intermediate chains (from brain or testes) leads to the elimination of the difference in ATPase activities of dynein (Kini and Collins, 2001).

Direct phosphorylation of the heavy chain can also regulate dynein-based motility (Dillman and Pfister, 1994). In an *in vivo* experiment, labeling of cytoplasmic dynein in rat nerves shows that the HC derived from the total cellular pool and that from vesicles moving in the anterograde direction (where dynein is presumably inactive) have different

extents of phosphorylation (Dillman and Pfister, 1994). Dynein phosphorylation may be regulated by dynactin, as its ATPase activity is dramatically reduced when produced in dynactin mutants (as compared to those isolated from wild-type), and can be restored by treatment with phosphatase (Kumar *et al.*, 2000). Radiolabeling experiments show that it is the light chains that are dephosphorylated upon phosphatase treatment, suggesting that dynactin regulates phosphorylation of the dynein light chains (Kumar *et al.*, 2000). So phosphorylation of different subunits can directly or indirectly modulate the motor activity of dynein.

## 1.3.2 The structure of the dynactin complex

The existence of dynactin as a dynein regulator was first suggested by experiments that used an assay developed from chick embryo fibroblasts (Schroer *et al.*, 1989). Cytoplasmic dynein present in the cytosol caused the retrograde movement of purified organelles on microtubules. However, purified cytoplasmic dynein itself was not enough to support such movement, indicating that the cytosol contains additional factors required for organelle motility (Schroer *et al.*, 1989).

Several other research groups observed that cytoplasmic dynein co-purifies with additional poplypeptides (Collins and Vallee, 1989; Steuer *et al.*, 1990; Holzbaur *et al.*, 1991). One of these co-purified polypeptides is approximately 150 kDa in size, and homologous to the product of the *Drosophila* gene *Glued.* In flies, *Glued* is expressed in all cells, and its null mutation is lethal during development (Harte and Kankel, 1982). The first identified allele of *Glued* causes aberrant development of the compound eye and optic lobe, a dominant phenotype in heterozygous flies, suggesting the importance of this protein during neuronal development (Plough and Ives, 1935).

*In vitro* studies reveal that the 150 kDa polypeptide and other polypeptides co-purified with dynein are indeed the factors required for dynein-mediated vesicular transport along microtubules (Gill *et al.*, 1991; Schroer and Sheetz, 1991). The 150 kDa polypeptide is one component of a heteromeric microtubule-associated complex that consists of at least seven distinct poplypeptides (Paschal *et al.*, 1993). The complex is referred to as "dynactin" (*dyn*ein *act*ivator), with each subunit named after its molecular mass — for example, $p150^{Glued}$.

As dynein interacts with various cellular components, and often these interactions are mediated by dynactin, the structure of dynactin has to accommodate its ability to interact with diverse partners. Extensive studies have been conducted on the dynactin complex, and its ultrastructure has been revealed (illustrated in Fig.1.5, reviewed in Schroer, 2004).

Dynactin is a 1200 kDa complex. Under the electron microscope, the dynactin molecule appears to be asymmetric and consists of a rod (~10× 40nm) with a projecting arm (25-50 nm) (Schafer *et al.*, 1994a). The arm terminates with two globular heads that point upward. The current view of dynactin organization postulates that each of the globular heads binds microtubules. Dynein (presumably the IC) binds to dynactin along or near the base of the arm. The rod may bind to the membrane of organelles.

The arm projecting from the rod contains p150$^{Glued}$ (DCTN1), p50 (dynamitin or DCTN2), and p24/p22 (DCTN3). A stable "side-arm" complex of these three proteins can be isolated from the "rod" (Eckley *et al.* 1999).

p150$^{Glued}$, a highly conserved polypeptide, is the largest dynactin subunit. Although usually encoded by a single gene, p150$^{Glued}$ is often expressed as a doublet of 150 and 135 kDa, resulting from alternative splicing (Tokito and Holzbaur, 1996). In humans, the p150$^{Glued}$ primary transcript has been reported to generate 32 exons (Tokito and Holzbaur, 1998). Alternative splicing generates functionally distinct isoforms of the polypeptide.

The p150$^{Glued}$ polypeptide is highly α–helical, and possesses extended regions of heptad repeat sequences that form coiled-coiled motifs. The α–helical coiled-coils mediate protein-protein interactions within the complex, and possibly facilitate its self-dimerization. The N-terminus of the polypeptide forms the globular heads of the dynactin arm, and contains a conserved motif (CAP-Gly) that binds microtubules (Li *et al.*, 2002; Waterman-Storer *et al.*, 1995; Vaughan *et al.*, 2002). Interestingly, this domain is also capable of binding microtubule-binding proteins, such as EB1 and CLIP-170, in mammalian cells (Berrueta *et al.*, 1999; Askham *et al.*, 2002; Bu and Su, 2003; Ligon *et al.*, 2003). The C-terminal region contains a conserved actin-binding motif that may be involved in binding to the rod, which consists largely of Arp1, an actin-related protein (Waterman-Storer *et al.*, 1995). In *Drosophila* mutants that lack the C-terminus of p150$^{Glued}$, the protein is not incorporated into dynactin (McGrail *et al.*, 1995). In

addition, interactions exist between p150$^{Glued}$ and the dynein intermediate chain at multiple sites in the central region of p150$^{Glued}$ (King *et al.*, 2003; Vaughan *et al.*, 2002). In *S. cerevisiae*, Nip100 is the p150$^{Glued}$ ortholog (Kahana *et al.*, 1998).

The p50 subunit, referred to as dynamitin or DCTN2, contains three coiled-coil regions that mediate protein-protein interactions (McMillan and Tatchell, 1994, Echeverri *et al.*, 1996). One molecule of dynactin has four subunits of dynamitin (Eckley *et al.*, 1999). The N-terminal region of dynamitin is highly conserved and may bind a variety of proteins, including cortical, kinetochore and organelle-associated proteins (Starr *et al.*, 1998; Yue *et al.*, 2000; Jin *et al.*, 2001; Hoogenraad *et al.*, 2001). In *S. cerevisiae*, the dynamitin ortholog is Jnm1 (*j*ust for *n*uclear *m*igration) (McMillan and Tatchell, 1994).

The p24/22 (DCTN3) polypeptide, one of dynactin's smallest subunits (the molecular weight turns out to be approximately 21 kDa upon closer investigation), is also predicted to adopt α-helical structures (Karki *et al.* 1998, Pfister *et al.* 1998). p24/22 can be isolated from dynactin in a 1:2 complex with dynamitin; thus, it is believed to bind to dynamitin directly (Karki *et al.* 1998). In this thesis, I identified a possible p24/p22 ortholog in *S. cerevisiae* for the first time, and this protein was found to be involved in nuclear positioning during mitosis.

The projecting arm of the dynactin structure endows the complex with a large surface area relative to its mass, exposing multiple sites for interaction with various partners, such as dynein, microtubules, and proteins on the cargo membrane (Schroer, 2004). It is also noteworthy that these proteins are highly α-helical, and contain multiple coiled-coil structures. These structures are capable of mediating protein-protein interactions that can stabilize the complex. Furthermore, because specific amino acids are not required for the formation of these α-helical and coiled-coil structures, the proteins are able to accommodate considerable sequence variation. Correspondingly, between yeast and animals, sequence identity of these proteins is relatively low. Secondary structures of these proteins, however, appear to be largely conserved (Schroer, 2004).

Of all the subunits of the dynactin complex, the 45 kDa polypeptide is the most abundant. It is a novel form of actin described as centractin (because of its prominent localization to the centrosome) or actin-RPV (Lees-Miller *et al.*, 1992; Clark and Meyer, 1992). This centractin/actin-RPV is less conserved than conventional forms of actin, but

shares many of the binding sites for actin-binding proteins such as myosin and spectrin (Schroer, 1994; Mullins *et al.*, 1996; Holleran *et al.*, 1996). For this reason, it is referred to as *a*ctin-*r*elated *p*rotein, Arp1. Arp1 possesses the ATP-hydrolyzing and polymerization capabilities of conventional actin, and assembles as a polymer similar to conventional actin, which comprises the rod structure of the dynactin complex (Schafer *et al.*, 1994a; Bingham and Schroer, 1999). Despite its similarity to conventional actin, Arp1 does not copolymerize with actin, and only exists in the dynactin complex *in vivo* (Holleran *et al.*, 1996; Paschal *et al.*, 1993). The size of the rod (37 nm filament) resembles that of a short actin filament, and contains eight to thirteen Arp1 monomers. The rod can interact with proteins on the cargo membrane, as interactions between Arp1 and the Golgi-associated βIII spectrin isoform from rat brain cytosol have been observed using co-purification and co-immunoprecipitation assays (Holleran *et al.*, 2001). Arp1 in *S. cerevisiae* is also involved in nuclear positioning (Clark and Meyer, 1994; Geiser *et al.*, 1997).

The conventional actin filament has two ends — a fast growing end, referred to as the barbed end, and a slower-growing pointed end. Capping protein (CP), a heterodimer, binds to the barbed end of actin filaments, and stabilizes the filament (Karpova *et al.*, 1995; Sizonenk *et al.*, 1996). Correspondingly, the barbed end of the Arp1 rod terminates with the conventional actin-capping protein CapZ (Paschal *et al.*, 1993; Schafer *et al.*, 1994a,b). CapZ is not only found as a subunit of dynactin, but also in a free form in the cytosol and in association with the conventional actin cytoskeleton (Shafer *et al.*, 1994b).

Biochemical analysis of bovine brain cytosol revealed another actin-related protein, Arp11, at the other end (pointed end) of the Arp1 rod. Arp11 is less related to conventional actin than Arp1, and is also found only in dynactin. Arp11 does not form a filament itself; instead, it serves as a cap to prevent further polymerization at this minus end of the Arp1 filament (Eckley *et al.* 1999).

The remaining three subunits of the dynactin complex— p62, p27, and p25— are predicted to localize at the pointed end of Arp1 rod, yet their functions remain largely unknown. p62 is homologous to the nuclear migration protein Ropy-2 from *Neurospora* (Garces *et al.*, 1999; Vierula and Mais, 1997). Affinity chromatography experiments

demonstrate that p62 binds directly to Arp1 (Karki *et al.*, 2000). In addition, p62 contains a RING domain, which is often involved in protein-protein interactions, hinting at a possible role in interacting with cargo membranes. No p62, p27, and p25 have been discovered in *S. cerevisiae* yet.

In summary, in the dynactin complex, $p150^{Glued}$ (DCTN1), dynamitin (DCTN2), and p22/p24 (DCTN3) form an arm structure, which projects from a rod structure mainly made of Arp1 filament. The $p150^{Glued}$ protein contains a microtubule-binding motif at the N-terminus, and can interact with dynein (presumably the intermediate chain) at the central region. Arp1 may interact with proteins on the cargo membrane. Thus, the structure of dynactin provides great advantages to link dynein, microtubules, and cargos together, and facilitates dynein-driven movements in various cellular activities.

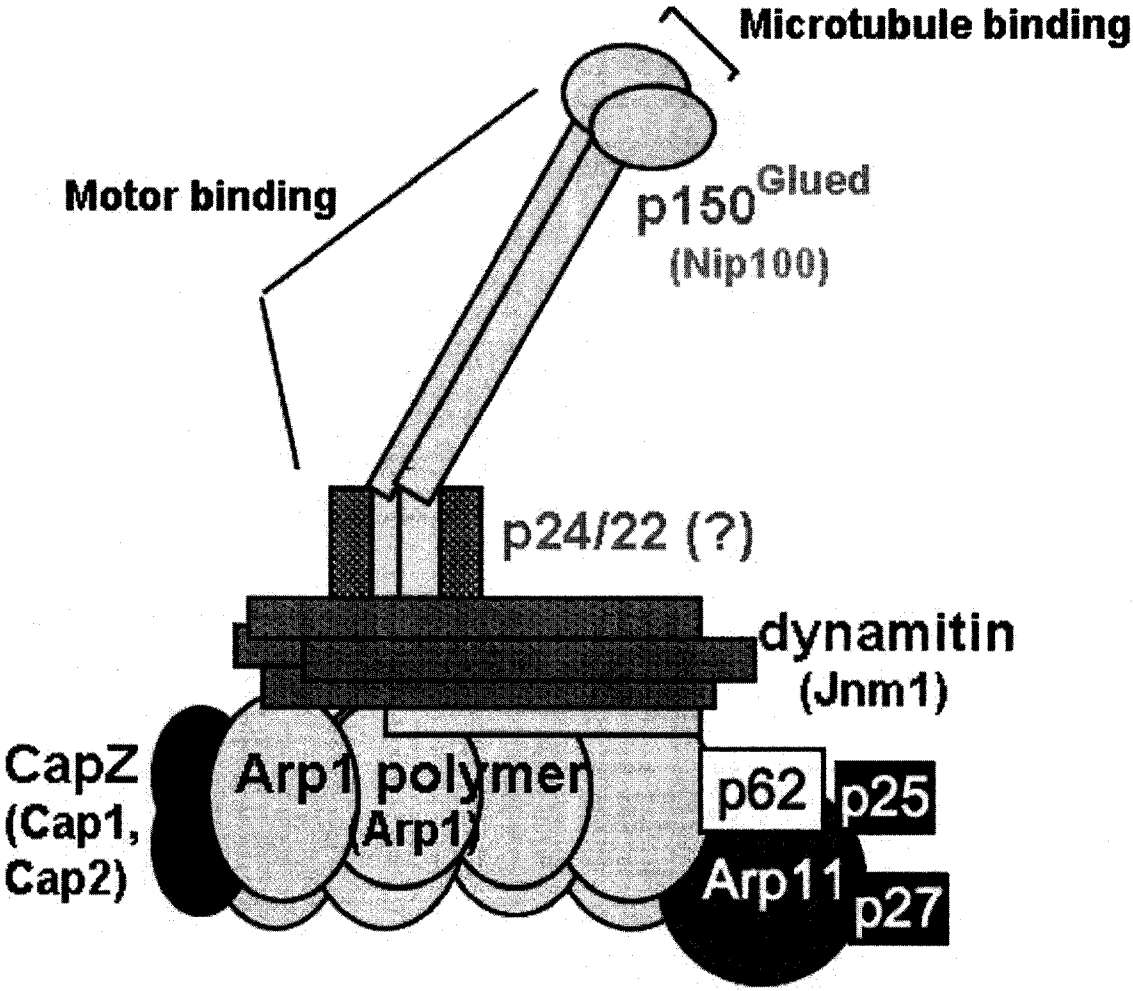


**Figure 1.5. The current model of dynactin ultrastructure** (based on the figure in Schroer, 2004). Counterparts of the subunits from *S. cerevisiae* are indicated in brackets. In this model, the dynactin complex resembles a rod with a projecting arm (Schafer *et al.*, 1994a). The Arp1 polymer forms a filament: one end is capped by capping proteins, and the other end by Arp11. Three uncharacterized proteins, p62, p27, and p25, are also predicted to be at the pointed end. The arm is composed of $p150^{Glued}$, dynamitin (p50), and p24/p22, and has one or two globular heads. The globular head is the N-terminal region of $p150^{Glued}$, and contains the microtubule-binding domain. Dynamitin (p50) and p24/p22 link the arm to the rod. It is predicted that dynein may bind to dynactin along or near the base of the arm, and the rod can interact with cargos.

## 1.3.3 Dynein and dynactin mostly function together

Dynein and dynactin are difficult to co-purify, and large proportions of each of the two complexes do not appear to be tightly associated, suggesting that they interact weakly (Karki and Holzbaur, 1999). When alone, each complex sediments at 20S on sucrose density gradients. However, in preparations containing both complexes, no obvious shift toward a higher S-value is observed. Cytoplasmic dynein does not co-immunoprecipitate with dynactin from bovine brain extracts (Paschal *et al.*, 1993). In the original purification of dynactin from chick brain extracts, dynein was separated from the whole dynactin complex by ion-exchange chromatography (Bingham *et al.*, 1988).

Dynactin can function in non-motile cellular processes, independent of dynein (Suzuki *et al.*, 2004; Quintyne and Schroer, 2002). Cytoplasmic dynein is also involved in intraflagellar transport, by wich protein complexes are transported between the flagellar membrane and the outer doublet tubule of flagella or cilia (reviewed in Rosenbaum and Witman, 2002; Pazour and Rosenbaum, 2002). This intraflagellar transport function of dynein seems to be independent of dynactin.

Nevertheless, genetic interactions suggest that dynein and dynactin are mostly, if not all, interdependent for their cytoplasmic functions. Direct binding between the two complexes has been confirmed both *in vitro* and *in vivo* (Karki and Holzbaur, 1995; Vaughan and Vallee, 1995). Purified vertebrate cytoplamic dynein is capable of binding to microtubules and moving towards the minus end, but purified dynein can only support the transport of purified vesicles to the minus ends of microtubules in the presence of dynactin (Paschal and Vallee, 1987; Bingham *et al.*, 1988). In many other subcellular activities, such as retrograde axonal transport, organization (and orientation) of the mitotic spindle, chromosome capture, and nuclear migration, dynein activity depends on the presence of dynactin as well. In *Drosophila*, Dhc64C (cytoplasmic dynein heavy chain) mutations can act as dominant suppressors or enhancers of the *Glued* phenotype – developmental defects in the compound eye and in the neurons of the optic lobe (McGrail *et al.*, 1995; Gepner *et al.*, 1996). In filamentous fungi and yeast, disruption of dynactin results in nuclear migration defects similar to those seen with disruption of dynein (Kahana *et al.*, 1998; Xiang *et al.*, 1994; Plamann *et al.*, 1994).

In higher organisms, multiple subcellular functions of dynein/dynactin have been widely studied. Immunolocalization studies show both dynein and dynactin associate with vesicle structures, and various receptors for dynein/dynactin are found on Golgi membranes, late endosomes, and lysosomes (Schroer, 2004). Overexpression of the dynactin subunit dynamitin disrupts dynein/dynactin function and blocks transport of pre-Golgi carrier structures from the endoplasmic reticulum to the Golgi, as well as interfering with Golgi distribution throughout the cytoplasm (Presley *et al.*, 1997; Holleran *et al.*, 1996; Burkhardt *et al.*, 1997). In the nervous system, dynein/dynactin mediates axonal transport in motor neurons, and a single base-pair change resulting in a one amino-acid substitution in the p150$^{Glued}$ (DCTN1) protein is linked to human motor neuron disease (Puls *et al.*, 2003). During karyogamy (nuclear fusion in zygotes), dynein accumulates around and binds to the egg pronucleus on sperm aster microtubules. Here, it interacts with dynactin, which in turn interacts with the nuclear pore complex and drives the movement of the pronuclei (Payne *et al.*, 2003). In addition, dynein/dynactin can drive movements of lipid and protein assemblies that are not enclosed by a membrane, such as RNA-protein particles in oocytes, or pathogenic inclusions (Kloc *et al.*, 2002; Guignot *et al.*, 2004; Kuhle *et al.*, 2004; Dohner *et al.*, 2002; McDonald *et al.*, 2002; reviewed in Schroer, 2004).

Dynein/dynactin function is essential for mitosis in higher organisms, and null mutants are lethal for embryonic development (Harada *et al.*, 1998). The mitotic function of dynein was initially suggested by immunolocalization of dynein to kinetochores, spindle poles, and spindle fibers during mitosis (Steuer *et al.*, 1990; Pfarr *et al.*, 1990). Research to date has revealed that the function of dynein during mitosis is rather dynamic, as it generates forces at multiple sites at various stages of the cell cycle, and often acts cooperatively with other microtubule motor proteins, such as kinesins (Gadde and Heald, 2004). In these various processes, dynein may not only act as a motor (that walks along the microtubules), but may also modify microtubule dynamics (by destabilizing microtubules) (Sharp and Rogers, 2004; Gadde and Heald, 2004). The balancing of oppositely-directed forces (by minus end and plus end motors) appears to be a key element of spindle dynamics during mitosis (Gadde and Heald, 2004).

During mitosis, dynein/dynactin is first recruited to the outer nuclear membrane. Dynein-powered movement of the nuclear surface results in twisting and stretching of the nuclear envelope, which facilitates its breakdown (Salina *et al.*, 2002; Beaudouin *et al.*, 2002). Subsequently, dynein is involved in formation of the mitotic spindle. Microjection of antibodies raised against the motor domain of dynein into mammalian PtK1 cells causes the separating centrosomes to collapse, suggesting a role for dynein in stabilizing the preanaphase spindle (Vaisberg *et al.*, 1993). Disruption of the dynein–dynactin complex by overexpression of the dynamitin subunit of dynactin also disrupts the spindles of dividing cells, suggesting dynamitin is important for maintaining dynactin structure (Echeverri *et al.*, 1996).

Dynein can also direct spindle polarity. In *Xenopus* or Hela cell extracts, blockage of dynein leads to splayed poles and abnormally long spindles, independent of the presence or absence of centrosomes. This suggests a role for dynein in cross-linking MTs and orienting them in the same polarity (Heald *et al.*, 1997; Merde *et al.*, 1996). Indeed, research shows that dynein can drive microtubule bundles to move inward from the cell periphery and incorporate into the spindle, a process in which association of dynein/dynactin with NuMA (a protein required for spindle assembly) is required (Tulu *et al.*, 2003; Rusan *et al.*, 2002; Merdes *et al.*, 1996). In addition, dynein at the cortex also orients astral microtubules, thus orienting the spindle (Gadde and Heald, 2004).

Besides spindle organization, dynein/dynactin may also be involved in the initial capture of microtubules by kinetochores (Inoue and Salmon, 1995). During anaphase A, dynein is seen to localize to kinetochores in *Drosophila* embryos, and inhibition of dynein disrupts kinetochore and chromosome movement toward the poles (Sharp *et al.*, 2000). In a two-hybrid screen, interaction between the dynactin subunit dynamitin and ZW10 (a kinetochore component) is observed, and mutations in ZW10 abolish dynein localization to the kinetochores in *Drosophila* (Starr *et al.*, 1998). In this process, dynein/dynactin presumably acts with other motor proteins (such as kinesins) in a cooperative manner to ensure chromosome movements toward the spindle poles (Gadde and Heald, 2004). Subsequently, during anaphase B, a fraction of dynein contributes to spindle elongation by localizing to the cell cortex and pulling on astral microtubules

(Gonczy, 2002; Sharp *et al.*, 2000). This is observed in both flies and the fungus *Ustilago maydis* (Fink *et al.*, 2006).

At the end of the cell cycle, dynein/dynactin can also participate in cytokinesis. Dynein and dynactin has been localized to the developing cleavage furrow during telophase (Karki *et al*, 1998; Campbell *et al.*, 1998; Tai *et al.*, 1998). Later, dynactin is found on the midbody, the remnant of the cleavage furrow that contains tightly packed microtubules surrounded by plasma membrane (Karki *et al.*, 1998). As interactions between the midzone microtubules and the contractile ring play a key role in cytokineisis, it can be speculated that dynein/dynactin is involved in these interactions (Wheatley and Wang, 1996; Giansanti *et al.*, 1998). Cytokinesis also involves kinesin-related proteins, which, once again, may act cooperatively with dynein (Williams *et al.*, 1995; Raich *et al.*, 1998).

In the cellular functions described above, dynein is localized at multiple sites inside the cell, which leads to the question of how dynein can become associated with so many different cellular components. Interestingly, dynamitin is important for dynein localization at the kinetochores, whereas association of dynein with cargo membranes may be mediated by Arp1 protein, which contains a conserved motif for spectrin binding (Lippincott-Schwartz, 1998; Starr *et al.*, 1998). In support of this, interactions between dynactin and spectrin have been detected (Holleran *et al.*, 1996). In neurons, an antibody to p150$^{Glued}$ blocks dynein association with vesicles as well as transport of vesicles along microtubules in extruded suid axoplasm (Waterman-Storer *et al.*, 1997). Based on these observations, it is tempting to speculate that dynactin serves as an adaptor between dynein and different cellular components, and that dynactin itself can be differentially localized via specific interactions mediated by different subunits.

More intriguingly, microtubule-binding sites are not only found in the dynein HC, but also on the p150$^{Glued}$ subunit of dynactin, suggesting that dynactin may also enhance the association of dynein with microtubules (Waterman-Storer *et al.*, 1995). In a very recent study, replacement of p150$^{Glued}$ with a mutant form ΔN-p150 that lacks the microtubule-binding motif in *Drosophila* results in the generation of multipolar spindles and free microtubule-organizing centers, but has no effect on the rate or processivity of cargo

transport (Kim *et al.*, 2007). Therefore, the microtubule-binding role of dynactin differs with cellular activities, and is especially important during mitosis.

**Table 1.1 Sequence identities between *S. cerevisiae* and *Homo sapiens* (human) for the dynein/dynactin subunits and dynein-interacting proteins.** Yeast protein sequences were retrieved from SGD (Sacharomyces Genome Database) and human protein sequences from NCBI database. Sequences were analyzed using BLAST (Tatusova and Madden, 1999) except Jnm1, Ldb18 and Nip100. For the dynactin subunits Jnm1, Ldb18, and Nip100, sequences were aligned by Jalview based on secondary structure conservation, and percentage of identical residues were calculated (Cuff and Barton, 1999).

| Protein in *S. cerevisiae* | Protein in *Homo sapien* | Protein sequence identity |
|---|---|---|
| Dyn1 (dynein heavy chain) | Cytoplasmic heavy chain isoform 1 (Accession No: AAT74625) | 36% |
| Dyn1 (dynein heavy chain) | Cytoplasmic heavy chain isoform 2 (Accession No: XP_942900) | 24% |
| Pac11 (dynein intermediate chain) | Cytoplasmic dynein intermediate chain 1 (Accession No: O14576) | 23% |
| Pac11 (dynein intermediate chain) | Cytoplasmic dynein intermediate chain 2 (Accession No: Q13409) | No significant similarity |
| Dyn 3 (dynein light intermediate chain) | Cytoplasmic dynein light intermediate chain (Acesssion No: NP_057225) | No significant similarity |
| Dyn 2 (dynein light cahin) | dynein light chain 1 (Accession No: P63167) | 49% |
| Arp1 (dynactin subunit) | Dynactin subunit Centractin (Acesssion No: NP_005727) | 51% |
| Jnm1 (dynactin subunit) | Dynactin subunit Dynamitin (DCTN2) (Accession No: NP_006391) | 8.9% |
| Nip100 (dynactin subunit) | Dynactin subunit subunit p150$^{Glued}$ (DCTN1) (Accession No: NP_004073) | 5.6% |
| Ldb18 (dynactin subunit) | Dynactin subunit p22 (DCTN3) (Accesssion No: NP_009165) | 10% |
| Pac 1 (dynein offloading protein) | Dynein offloading protein LIS1 (Accession No: AAL34973) | 29% |
| Ndl1 (dynein offloading protein) | Dynein offloading protein nudEA and B (Accession No: NP_001020750 and NP_110435) | No significant similarity |
| Bik1 (MAP) | CLIP170 (+TIP) | 35% |

## 1.4 Objectives of this study

Many of the main players (such as cyclin-dependent kinases, the anaphase-promoting complex) that regulate the cell cycle perform similar functions in all eukaryotes, and the mechanisms have been conserved during evolution (De Clercq and Inze, 2006; Pines, 1999; King *et al.*, 1996; Peters, 1998; Ohi and Gould, 1999; Sherr and Roberts, 1999; Kaldis, 1999; Nasmyth, 1996; Dunphy, 1994). Research on cell cycle regulation using the genetically tractable model organism *S. cerevisiae* can therefore contribute to our understanding of mitosis in animals.

In specific regards to dynein/dynactin, it is involved in various cellular activities, such as mitosis and axonal transport in higher organisms. Up-regulation of dynein light chain 1 (DLC1) has recently been found to promote tumorigenesis (den Hollander and Kumar, 2006). Additionally, The tumor suppressor protein p53 is known to be transported to the nucleus along microtubular tracks by cytoplasmic dynein (Galigniana *et al.*, 2004). Studies have also identified potential links between dynein/dynactin and Huntington's disease (HD), a neuromuscular disease called limb-girdle muscular dystrophy type 2B, and Alzheimer's disease (Puls *et al.*, 2003; Li *et al.*, 1998; Engelender *et al.*, 1997; Tokito and Holzbaur, 1998; Kopec and Chambers, 1997). In addition, cytoplasmic dynein may mediate the infection and spread of viral pathogens, as the viral caspid transport of herpes simplex virus 1 (Sodeik *et al.*, 1997).

Intriguingly, despite the lack of identity in primary sequence of dynein/dynactin subunits between *S. cerevisiae* and animals, the secondary structures and organization of both complexes has been highly conserved during evolution. Also, yeast has only one isoform of most components, and loss of dynein or dynactin is not lethal (in contrast to animals). Hence, studies on the dynein and dynactin subunits and interactions among them using *S. cerevisiae* can provide insights into the structure and function of their counterparts in animals. Considering that no homologues of the animal dynactin subunits p62, p27, p25 and p24 have been reported in *S. cerevisiae*, and only one dynein light chain (Dyn2) has been found in this eukaryote, research in this area can be exciting and productive. Analysis of novel mutants exhibiting *dyn1*-like phenotypes can lead to the discovery of new dynein or dynactin subunits in yeast.

The Kar9 and dynein pathways are partially redundant for nuclear positioning during mitosis in *S. cerevisiae*, but disruption of both results in cell death. Synthetic lethality screens are, therefore, a powerful tool for identifying new proteins in the dynein or Kar9 pathway. There are a number of genes identified in previous genetic screens whose null mutations show synthetic lethality or growth defects with deletion of either dynein or Kar9 pathway components (Tong *et al.*, 2004). However, there have been few reports characterizing possible roles for these genes in mitotic spindle orientation or nuclear positioning (Fig.1.6 and Table 2.1). Therefore, I decided to further examine these candidates, hoping to find their possible involvements in either the Kar9 or the dynein pathway.

I examined deletion strains that showed synthetic lethality with mutation in the Kar9 or dynein pathway. Deletion of *BOI2, CLB4, CPR6, FAB1, HCM1, MON1, SMI1, VAM7, VID22, VPS29, or VPS35* shows synthetic lethality or growth defects in combination with dynein mutations, whereas deletion of *NBP2* and *YLL049W (LDB18)* show synthetic lethality with disruption of the Kar9 pathway (Fig. 1.6). I started by observing the positioning of the nuclei in these mutants to determine if the single mutants had *kar9-* or *dyn1-* like nuclear positioning defects.

*vid22Δ, fab1Δ, mon1Δ,* and *clb4Δ* mutants exhibited nuclear positioning defects of varying degrees. These candidates are to be further characterized in other studies. Most notably, the *yll049wΔ* (*ldb18*Δ), strain demonstrated nuclear positioning defects that are strikingly similar in type and severity to dynein pathway mutants. *YLL049W* encodes a 21-kDa polypeptide, and further characterization of this polypeptide supported the hypothesis that it may be the yeast ortholog of the dynactin subunit p24/p22 in animals.

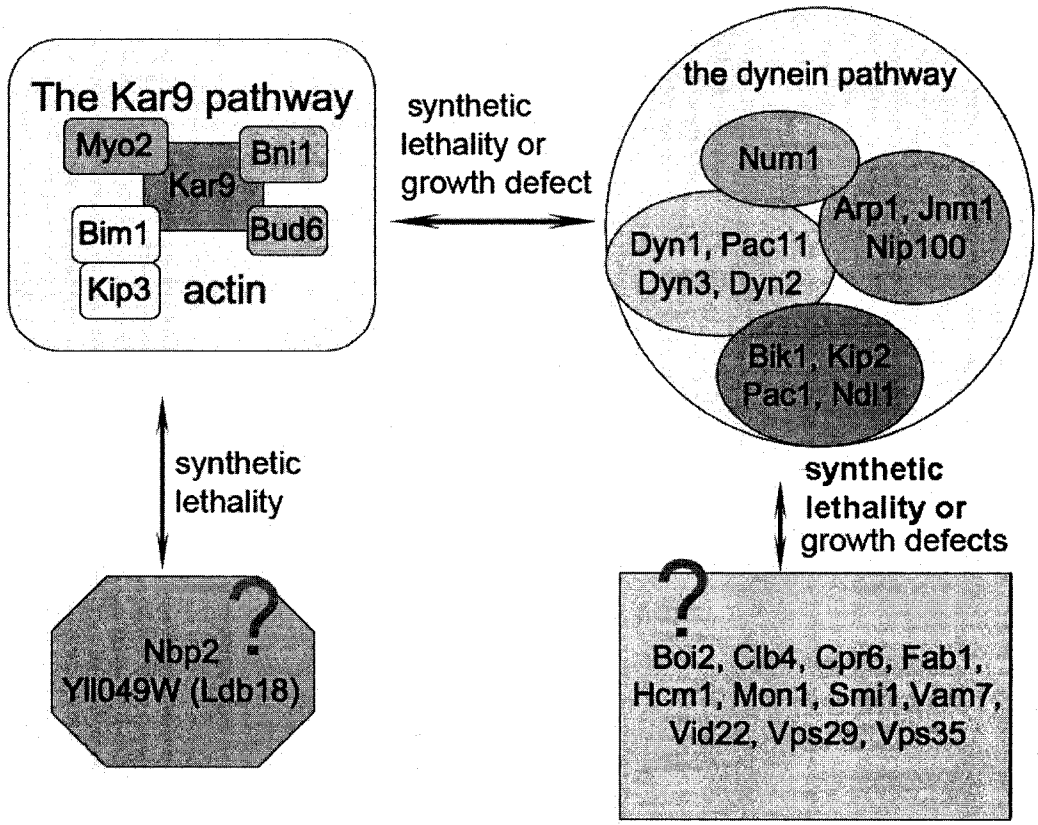


**Figure 1.6 Genetic interactions between the Kar9 and dynein pathways and objectives of this study.** The two pathways are partially redundant but disruption of both leads to synthetic lethality. Elements of the dynein pathway have been grouped together in a way that shows the interactions among them; those contained in the same ellipse form stable complexes (such as dynein or dynactin) or act cooperatively in one particular aspect (Bik1/Kip2 and Pac1/Ndl1 deliver dynein to the plus end). Sites of ellipse overlap indicate a transient/occasional interaction between complexes. In the representation of the Kar9 pathway, overlap between rectangles indicates experimentally observed interaction between pathway components. The gene products whose genetic interactions with the Kar9 or dynein pathway were assessed in this study are shown in the lower, question mark-labelled boxes.

# 2. Results

As described previously, the Kar9 and dynein pathways are both involved in nuclear positioning in *S. cerevisiae* (Pearson and Bloom, 2004; Bloom, 2001). The dynein pathway includes components of the dynein complex (Dyn1, Dyn2, Dyn3, Pac11), the dynactin complex (Jnm1, Nip100, Arp1), and several dynein-interacting proteins (Num1, Ndl1, Pac1, Bik1/Kip2). The Kar9 pathway includes Kar9 itself, several proteins that interact with Kar9 (Bim1, Bni1, Myo2), the bud-tip protein Bud6, and the kinesin-related protein Kip3. The two pathways are largely separate but partially redundant. Disruption of two components from the same pathway does not lead to a more severe defect than disruption of only one component, whereas simultaneous mutations in both pathways lead to synthetic lethality.

Mutants of either pathway demonstrate nuclear positioning defects during mitosis, although slightly different from each other. Nuclear mass staining of a *dyn1*Δ mutant (or any other component of the dynein pathway) by DAPI shows a portion of cells (approximately 12% at 15°C) with two nuclear masses within the mother cell and none in the bud, which is rarely observed in wild type strains (Fig.2.2 and Fig.2.3). For *kar9*Δ mutants, DAPI staining at 15°C show only ~5% cells with two nuclear masses entirely in the mother (Figure 2.2). However, a portion of G2/M cells (~30%) in the *kar9*Δ mutant had their single nucleus far away from the neck (along the mother-bud axis, distance between the nucleus and the neck is more than 1/3 of the mother cell length), in contrast to wild type or *dyn1*Δ cells, in which the nucleus is in vicinity to the neck after formation of the short spindle (distance between the nucleus and the neck is usually less than 1/3 of the mother cell length).

By observing the position of the nucleus in various mutants, we can determine if the mutants are defective in the Kar9- or dynein- regulated processes of nuclear positioning.

None of the 13 gene products (listed in Table 2.1) have known roles in nuclear positioning during mitosis of *S. cerevisiae*. Deletion of any of these genes, when combined with deletion of a component of either the dynein or Kar9 pathways, however, leads to synthetic lethality or growth defects, suggesting that these gene products could be involved in nuclear positioning.

**Table 2.1 A list of the 13 candidates that show genetic interactions with the Kar9 or dynein pathway, and the nuclear positioning defects in their deletion strains.** The deletion strains were purchased from Open Biosystems (Huntsville, AL). Correct deletion of each ORF was confirmed by genomic PCR (Fig.2.1). Each of the mutant strains was then grown in YPAD liquid medium at 15 °C until $OD_{600}$ of the cell culture reached 1.0-1.4. Cells were fixed with ethanol and stained with DAPI , then observed under microscope (refer to Fig. 2.2).

| Gene name | Identified function | Synthetic lethality or growth defect (Tong *et al.*, 2004) | Nuclear positioning phenotype of the deletion strain (observed in this study) |
|---|---|---|---|
| *NBP2* | protein involved in the HOG (high osmolarity glycerol) pathway | synthetic lethal with *KAR9* deletion | None;<br>Similar growth rate to the parental strain |
| *LDB18 (YLL049W)* | Unknown function | synthetic lethal with *KAR9* deletion | Similar to *dyn1Δ*, two nuclear masses in the mother cell and none in the bud;<br>Similar growth rate to the parental strain |
| *BOI2* | protein implicated in polar growth | synthetic growth defect with *ARP1* deletion | None;<br>Similar growth rate to the parental strain |
| *CLB4* | B-type cyclin involved in cell cycle progression; activates Cdc28p to promote the G2/M transition | synthetic growth defect with *ARP1* deletion | Similar to but milder than *dyn1Δ*;<br>Similar growth rate to the parental strain |
| *CPR6* | peptidyl-prolyl cis-trans isomerase (cyclophilin) | synthetic lethal with *NIP100* or *JNM1* deletion | None;<br>Similar growth rate to the parental strain |
| *FAB1* | vacuolar membrane kinase involved in vacuolar sorting and homeostasis | synthetic lethal with *NUM1* or *PAC1* deletion | A single nuclear maass in the bud and none in the mother;<br>Similar growth rate to the parental strain |

| | | | |
|---|---|---|---|
| *HCM1* | forkhead transcription factor involved in cell cycle specific transcription of SPC110, encoding a spindle pole body (SPB) calmodulin binding protein | synthetic growth defect with *ARP1* deletion | Cells stretch very long and narrow (not similar to either *dyn1Δ* or *kar9Δ* mutants);<br>Very slow growth (doubling time was about 2 times of the doubling time for the parental strain) |
| *MON1* | protein required for fusion of cvt-vesicles and autophagosomes with the vacuole | synthetic growth defect with *ARP1* deletion | Similar to but milder than *kar9Δ*;<br>Similar growth rate to the parental strain |
| *SMI1* | protein involved in the regulation of cell wall synthesis | synthetic growth defect with *ARP1* deletion | None;<br>Similar growth rate to the parental strain |
| *VAM7* | involved in vacuolar morphogenesis | synthetic growth defect with *NBP2* deletion | None;<br>Similar growth rate to the parental strain |
| *VID22* | involved in FBPase transport from the cytosol to Vid (vacuole import and degradation) vesicles | synthetic growth defect with *ARP1* deletion | *dyn1Δ*-like phenotype, but much milder;<br>Very slow growth (doubling time was about 3 times of the doubling time for the parental strain) |
| *VPS29* | endosomal protein that is a subunit of the membrane-associated retromer complex essential for endosome-to-Golgi retrograde transport | synthetic growth defect with *ARP1* deletion | None;<br>Similar growth rate to the parental strain |
| *VPS35* | subunit of the membrane-associated retromer complex essential for endosome-to-Golgi retrograde transport | synthetic lethal with *JNM1* deletion | None;<br>Similar growth rate to the parental strain |

## 2.1 Examining nuclear positioning defects in deletion strains

For all the 13 deletion strains (purchased from Open Biosystems, Huntsville, AL), a particular ORF was replaced by the *KanMX4* module in a parental haploid (*MATα*) yeast strain. I confirmed correct deletion of the ORF by genomic PCR (Fig. 2.1). All of the deletion strains were viable. Most of them (except *hcm1*Δ and *vid22*Δ) showed growth rates similar to the wild-type parental strain (BY4742) in YPAD liquid medium. The doubling time of *hcm1*Δ was approximately 2 times of the doubling time for the parental strain, and *vid22*Δ had a doubling time approximately 3 times of the parental strain (at 15 °C).

DAPI-staining of the mutant cells grown at 15°C revealed that several of them demonstrated nuclear positioning defects (Table 2.1, Fig.2.2, and for *ldb18*Δ, refer to Fig 2.4). The *ldb18*Δ and *vid22*Δ mutants showed *dyn1*Δ-like nuclear positioning defects to different extents. The severity of the *ldb18*Δ defect was similar to the *dyn1*Δ mutant, whereas the severity of the *vid22*Δ defects was much milder. The *mon1*Δ mutants showed less severe *kar9*Δ-like phenotypes. The *fab1*Δ mutant had approximately 3% (as compared to less than 0.5% in the wild type strain) of the cells containing a single nuclear mass in the bud but not in the mother (Fig. 2.2 and Fig. 2.3). The nuclear positioning defects observed *clb4*Δ mutant were somewhat different to those of *dyn1*Δ or *kar9*Δ mutants, but almost similar to the *fab1*Δ mutant. I also found that the *mon1*Δ cells tended to stretch very long and narrow, suggesting a cell morphogenesis defect, which was not observed in *dyn1*Δ or *kar9*Δ cells.

The *ldb18*Δ mutant was the only strain that demonstrated nuclear positioning defects similar (in type and severity) to the *dyn1*Δ mutant (Fig. 2.4). No previous report had elaborated the role of this gene product, except that the deletion strain was reported to exhibit a low dye (alcian blue staining) binding (LDB) phenotype (Corbacho *et al.*, 2005). I therefore decided to study *LDB18* more closely.

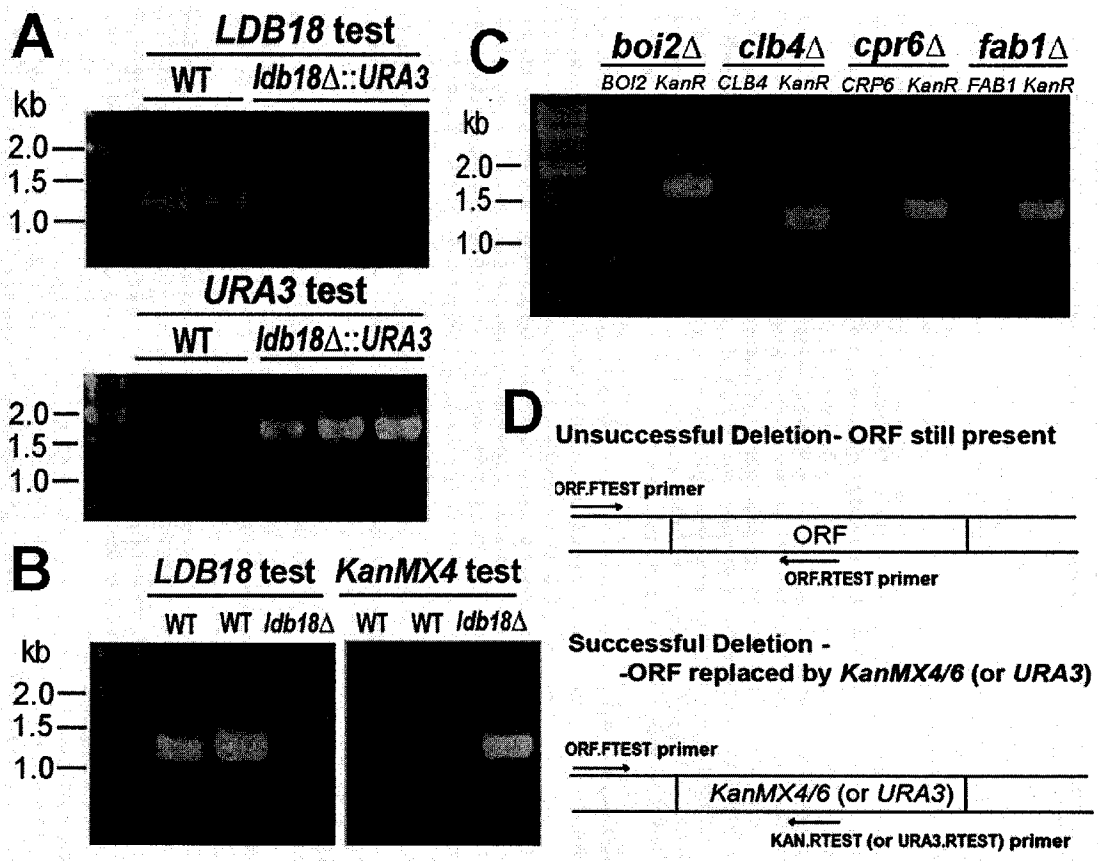


**Figure 2.1. Confirmation of correct deletion of each ORF in the deletion strains.** (A) Replacement of *LDB18* with *URA3*. LDB18.FTEST and LDB18.RTEST primers were used to test whether the *LDB18* open reading frame was still present. LDB18.FTEST and URA3.RTEST were used to test whether the *URA3* module was inserted at the right place. The first two lanes were wild type strains used as controls (Lane 1, BY4742; Lane 2, Y2295), and the other three lanes were all *MATa* deletion strains. (B) Replacement of *LDB18* open reading frame with *KanMX4*. The first two lanes were wild type strains, used as controls (Lane 1, BY4742; Lane 2, Y2295), and the third lane was a *MATα* deletion strain. (C) Replacement of the *BOI2*, *CLB4*, *CPR6*, *FAB1* ORF with *KanMX4*. For each deletion strain, the first lane was a genomic PCR testing if the ORF was still present, and the second lane tested if the *KanMX4* module was interted at the correct place. (D) An illustration of the genomic PCR stragegy.

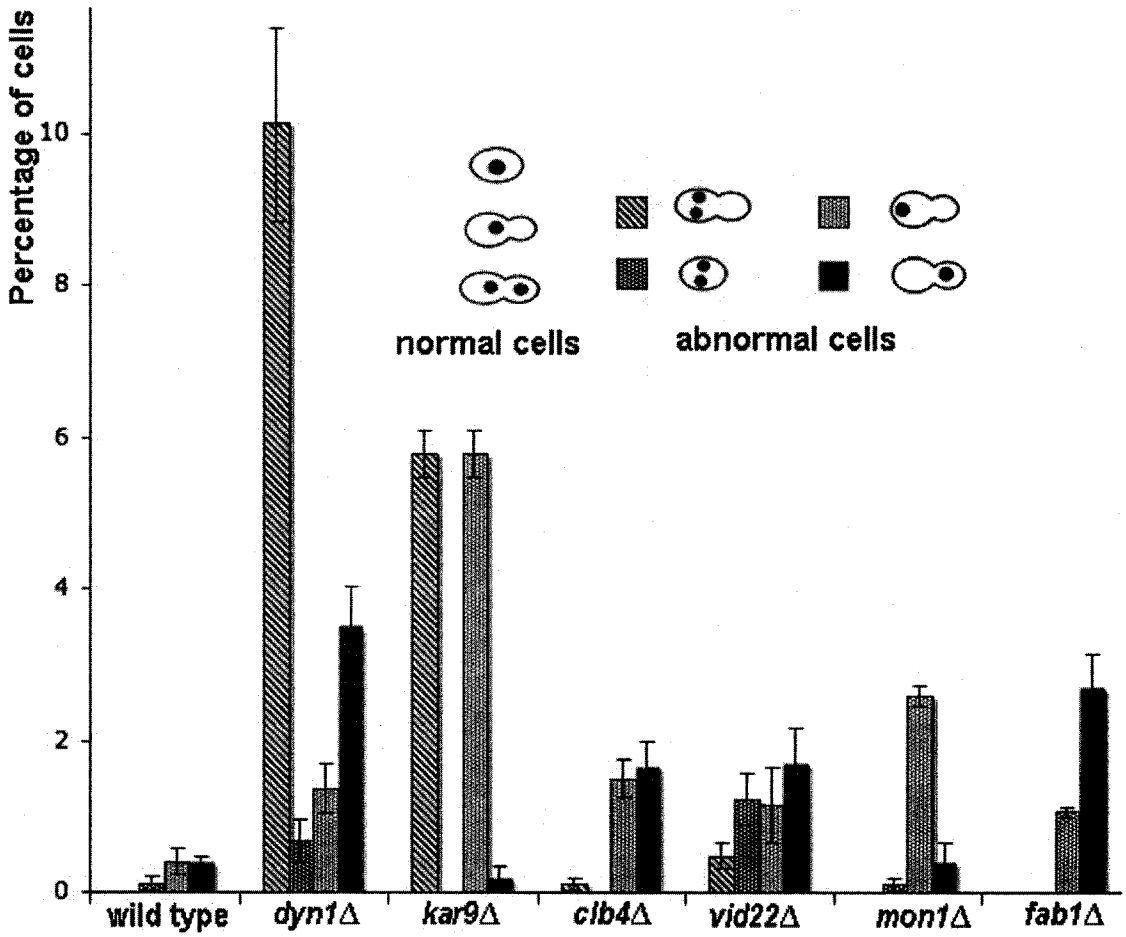


**Figure 2.2. Nuclear positioning defects in *clb4Δ*, *vid22Δ*, *mon1Δ*, and *fab1Δ* mutant cells** (as compared to wild type, *dyn1Δ*, and *kar9Δ* mutants). For each strain, a single colony was inoculated into 5 mL YPAD liquid medium and grown overnight at 30°C. The overnight culture was diluted into 5mL fresh YPAD liquid to give an $OD_{600}$ 0.07, and grown at 15 °C until $OD_{600}$ reached 1.0-1.4. 0.5 mL culture was fixed by 70% ethanol and stained with 100 μL DAPI (1μg/mL). The stained cells were observed under the microscope with a filter for DAPI. For each strain, at least 300 cells were visualized and percentage of each type of cells (different morphologies based on the postions of the nuclei, shown above the figure) were calculated. Experiments were done in triplicates (n=3) and the average percentage and standard deviations were calculated. Percentage of normal cells (which are majority of the cells) are not shown in this figure, in order to have a better comparison of the abnormal cells.

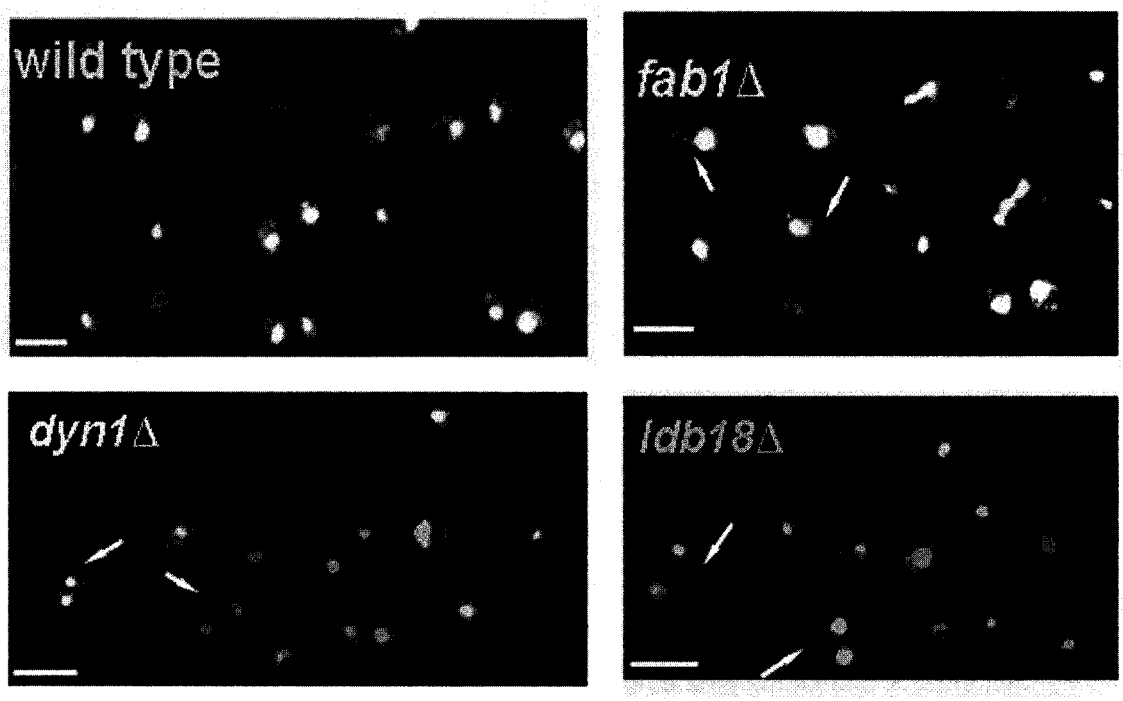


**Figure 2.3. The nuclear positioning defects in *ldb18*Δ and *fab1*Δ mutant cells** (as compared to wild type and *dyn1*Δ cells). Cells were visualized after DAPI-staining. Scale bars represent 6 μm. For detailed procedure of cell growth and DAPI-staining, refer to the legend for Fig. 2.2.

## 2.2 The nuclear positioning defects in *ldb18*Δ

The *ldb18*Δ mutant showed an increased percentage of binucleate cells (two nuclear masses in the mother and none in the bud) comparing to wild type strain, which is a typical nuclear positioning defect seen in dynein mutants. The severity of this defect is also very similar to that observed in *dyn1*Δ mutants (Fig. 2.4.). In addition, the nuclear positioning defects of the *ldb18*Δ mutant are also temperature dependent, as *ldb18*Δ strains grown at a lower temperature (15 °C) showed a higher percentage of binucleate cells than strains grown at the optimal temperature (30 °C) (Fig.2.4). The temperature dependence of the nuclear positioning deficiency is similar to known dynein or dynactin mutants (Li *et al.*, 1993; Kahana *et al.*, 1998).

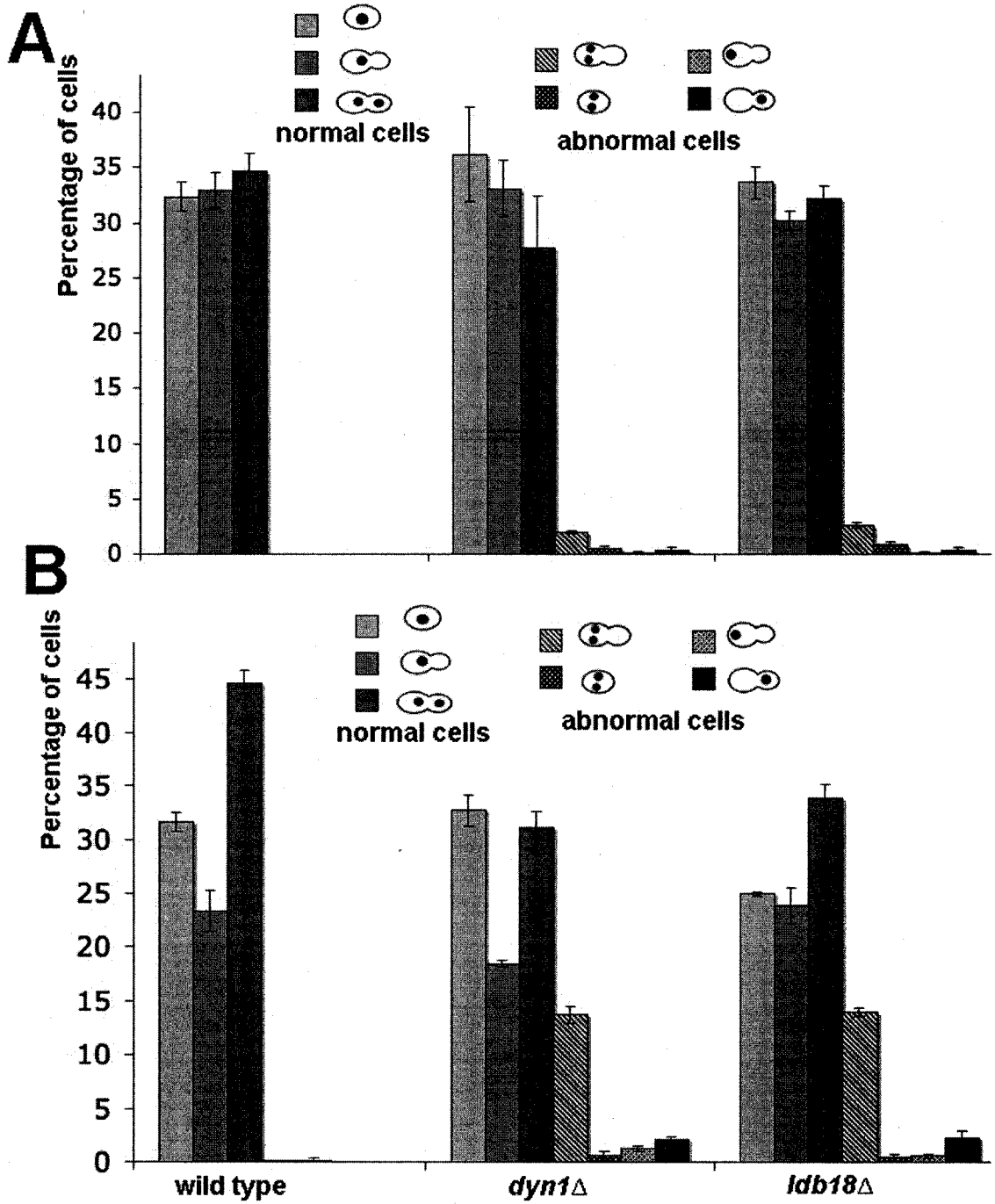


**Figure 2.4. Nuclear positioning defects of *ldb18*Δ compared to *dyn1*Δ and wild type strains at (A) 30°C or (B) 15°C.** Cell growth and DAPI-staining methods were as described in the legend for Fig. .2. Experiments were performed in triplicate (n=3). At least 300 cells were visualized each time for each strain. The average percentage of each type of cells (including normal cells) over the total cell numbers and standard errors were calculated.

## 2.3 Genetic interactions implicate Ldb18 in the dynein pathway

The nuclear positioning defects of the *ldb18Δ* mutant suggested that Ldb18 participates in the dynein pathway. Previous genetic screens showed that deletion of both *LDB18* and *KAR9* (or *BIM1,* or *BNI1*) were synthetically lethal (Tong *et al.*, 2004; Pan *et al.*, 2004). Because these were all large-scaled screens, and errors may have occurred, I proceeded to confirm the genetic interactions between Ldb18 and the Kar9 pathway. In addition, if Ldb18 were indeed involved in the dynein pathway, simultaneous deletion of *LDB18* and any other dynein pathway component should not cause cell death or slow growth.

All the deletion strains that we purchased (from Open Biosystems) were of α mating type, with a specific ORF replaced with *KanMX4.* To make crosses, a *MATa ldb18Δ* strain with a different selectable marker (*URA3*) was constructed. Deletion of the *LDB18* open reading frame with *URA3* replacement in a wild-type haploid *MATa* yeast strain was performed using a PCR-based strategy (refer to Fig. 4.1 in Materials and Methods). Correct deletion of *LDB18* was confirmed by genomic PCR (Fig. 2.1 A).

The *ldb18Δ* strain was then mated with deletion strains of the Kar9 and dynein pathway components. The resulting diploids were selected for both the *KanMX4* and the *URA3* markers (on SD-Ura+G418 plates), then sporulated. Tetrad analysis of the tetratype meiotic products showed that *ldb18Δ* mutation was synthetically lethal with *bim1Δ*, and demonstrated a synthetic growth defect with *kar9Δ and bni1Δ* (Fig.2.5 B and C, and Table 2.2). In contrast, *ldb18Δ* combined with deletion of any other component from the dynein pathway did not show any growth defect (Fig. 2.5 A and Table 2.2).

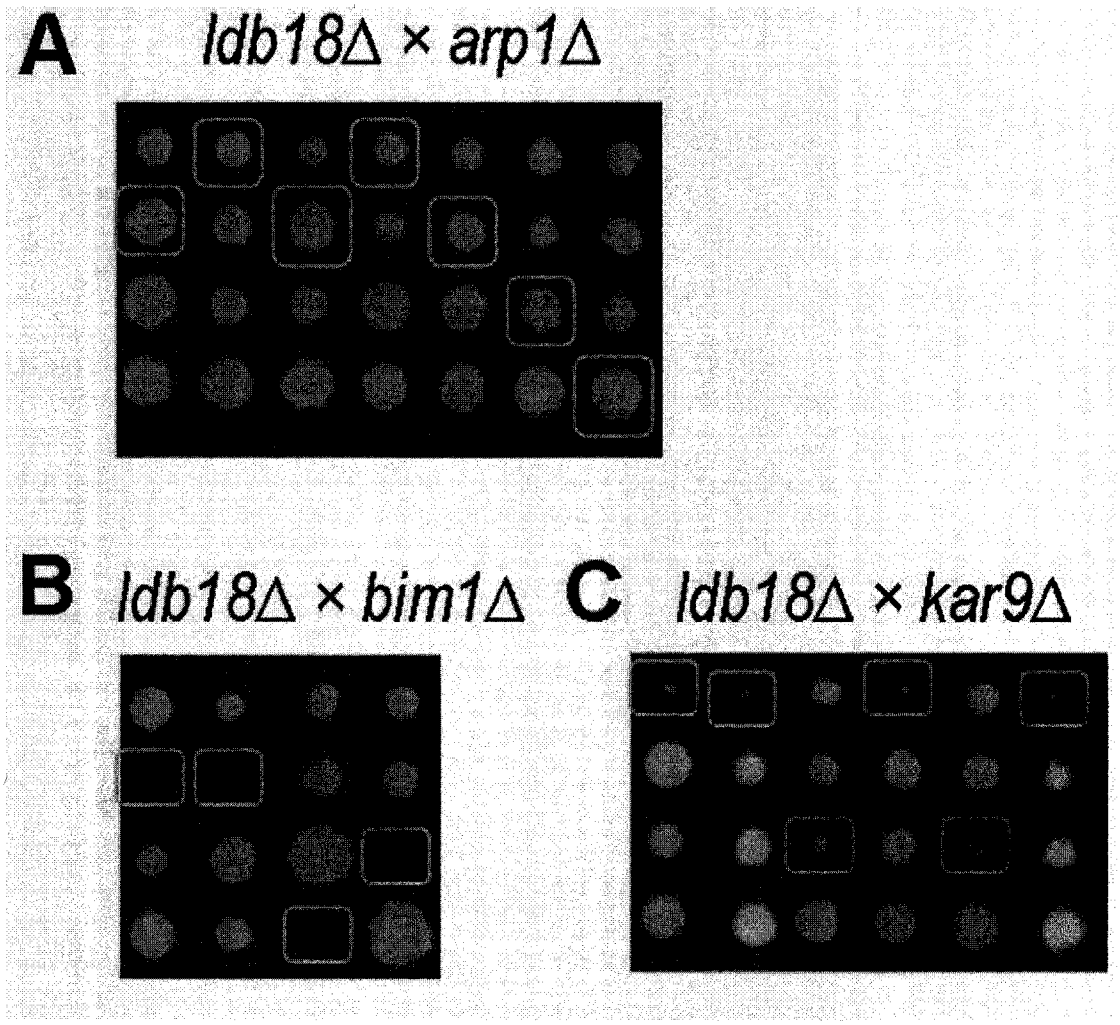


**Figure 2.5. Tetrad analysis of (A) *ldb18Δ× arp1Δ*, (B) *ldb18Δ× bim1Δ, and* (C) *ldb18Δ× kar9Δ* tetratype meiotic products on the original YPAD plates.** Only tetratype spores are shown in this figure, Parental Ditype (PD) and Non-parental Ditype (NPD) are not included. A rectangle indicates the double deletion progeny with both *KanMX4* and *URA3* markers (ability to grow on both YPAD+G418 and URA drop-out plates). Single deletion strains (*MATa ldb18Δ::URA3 and MATα xxxΔ::KanMX4*) were mated overnight on YPAD plates, diploids were selected on SC-ura+G418 plates, then sporulated in sporulation medium for at least 3 days. The ascus cell wall was digested with zymolyase. For each tetrad, four spores were separated under dissecting microscope with micromanipulator using a glass needle. The four spores from one ascus were placed on a YPAD plate in a row and grown for 2-3 days. All the colonies were replica-plated onto SC-ura plates and YPAD+G418 plates to determine their genotypes. To test their mating type, the colonies were also replica-plated onto YPAD plates with Y2081 (*MATα*) or Y2082 (*MATa*).

**Table 2.2. Genetic interactions between Ldb18 and the dynein or Kar9 pathway.** Single deletion strains (*MATa ldb18Δ::URA3* and *MATα xxxΔ::KanMX4)* were mated, and diploids were selected and sporulated. For each diploid, meisois would produce one ascus. The ascus cell wall was digested with zymolyase. For each tetrad, the four spores were separated under dissecting microscope with an micromanipulator. The four spores from one ascus were placed on a YPAD plate in a row and grown for 2-3 days. The progeny grown on YPAD plates were then replica-plated onto YPAD+G418 and SC-ura plates to determine genotypes (for example, if one spore grew on both YPAD+G418 plates and SC-ura plateas, then the genotype of the spore would be *ldb18Δ::URA3; xxxΔ::KanMX4*). The mating type was also tested, as described in Fig. 2.5.

| *ldb18Δ* crossed to: | Number of spores assayed | Number of full tetrads assayed | Number of (*ldb18Δ::URA3; xxxΔ::KanMX4*) spores growing | Number of (*ldb18Δ::URA3; xxxΔ::KanMX4*) spores not growing | Expected number of (*ldb18Δ; xxxΔ*) spores | Synthetic growth defect/ lethality |
|---|---|---|---|---|---|---|
| *dyn1Δ* | 37 | 2 | 11 | 0 | 9 | No |
| *dyn2Δ* | 51 | 11 | 12 | 0 | 13 | No |
| *dyn3Δ* | 71 | 9 | 23 | 0 | 18 | No |
| *pac11Δ* | 95 | 17 | 24 | 0 | 23 | No |
| *pac1Δ* | 130 | 20 | 30 | 0 | 32 | No |
| *num1Δ* | 117 | 21 | 32 | 0 | 29 | No |
| *nip100Δ* | 116 | 18 | 29 | 0 | 29 | No |
| *jnm1Δ* | 50 | 5 | 15 | 0 | 12 | No |
| *arp1Δ* | 57 | 9 | 15 | 0 | 16 | No |
| *bik1Δ* | 57 | 14 | 9 | 0 | 14 | No |
| *bim1Δ* | 48 | 12 | 0 | 16 | 12 | Synth. Lethal |
| *kar9Δ* | 74 | 14 | 14 | 2 | 18 | Synth. Growth |
| *bni1Δ* | 73 | 18 | 18 | 3 | 18 | Synth. Growth |

## 2.4 Sequence analysis supports that Ldb18 may be the yeast ortholog of the dynactin subunit p24/p22

Sequence analysis of the Ldb18 protein predicts α–helical structures with a coiled-coil domain at the N-terminus (Fig. 2.6). When compared to the p24/p22 (DCTN3) subunit of dynactin from other eukaryotes, Ldb18 showed homology and similarities in protein structures (Fig. 2.6). A phylogenetic tree was also made based on their sequence conservation (Fig. 2.7). A well-conserved Ldb18 ortholog was found in a related yeast species, *Saccharomyces paradoxus.*

**Figure 2.6. Homology analysis of Ldb18 protein sequence comparing to the p24/p22 orthologs in other eukaryotes.** Sequences of p24/p22 protein (or hypothetical proteins for some organisms) from several eukaryotes were retreived from the NCBI database by BLAST search, and aligned using BOXSHADE program (3.2 version) (Marchler-Bauer and Bryant, 2004). Residues conserved in at least half of the species (7 species) are shown in black and similar residues are shown in grey. All protein sequences were then aligned using Jalview and coiled-coil regions were predicted for each individual protein, and the black boxes in the picture show where there is 80-90% possibility of forming coiled-coil structures (Clamp *et al.*, 2004; Lupas *et al.*, 1991). With sequences aligned with Jalview, the JNet Sccondary Strucuture Prediction program was also used, and the average of all predicted protein structures is shown below the aligned sequences in the picture. There is a well-conserved coiled-coil domain at the N-terminus of the p24/p22 protein from all species (indicated as "...CCCCCCC..." below the sequence) (Cuff and Barton, 1999).
*Hsap, homo sapiens* (human), Accession NP_009165;
*Cfam, canis familiaris* (dog), Accession XP_531981;
*Btau, Bos Taurus* (cow), Accession: NP_001069128;
*Mmus, Mus musculus* (mouse), Accession NP_058586;
**Ggal, Gallus gallus* (chicken), Accession NP_001026616;
*Xlae, Xenopus laevis* (African clawed frog), Accession: AAH68862;
*Drer, Danio rerio* (zebrafish), Accession NP_001002220;
**Spur, Strongylocentrotus purpuratus* (sea urchin), Accession XP_782749;
**Tcas, Tribolium castaneum* (red flour beetle), Accession XP_970242;
**Dmel, Drosophila melanogaster* (fruit fly), Accession CAL26841;
*Agam, Anopheles gambiae* (mosquito), Accession NP_984330;
**Sjap, Schistosoma japonicum* (bilharzia), Accession AAW26236;
**Scer, Saccharomyces cerevisiae* (budding yeast);
*Spar, *Saccharomyces paradoxus* (member of the *Saccharomyces sensu stricto* group).
The * before the name of an organism suggests that the protein in this organism presented here is hypothetical p24/p22 (DCTN3) protein, but its function has not been described in detail.

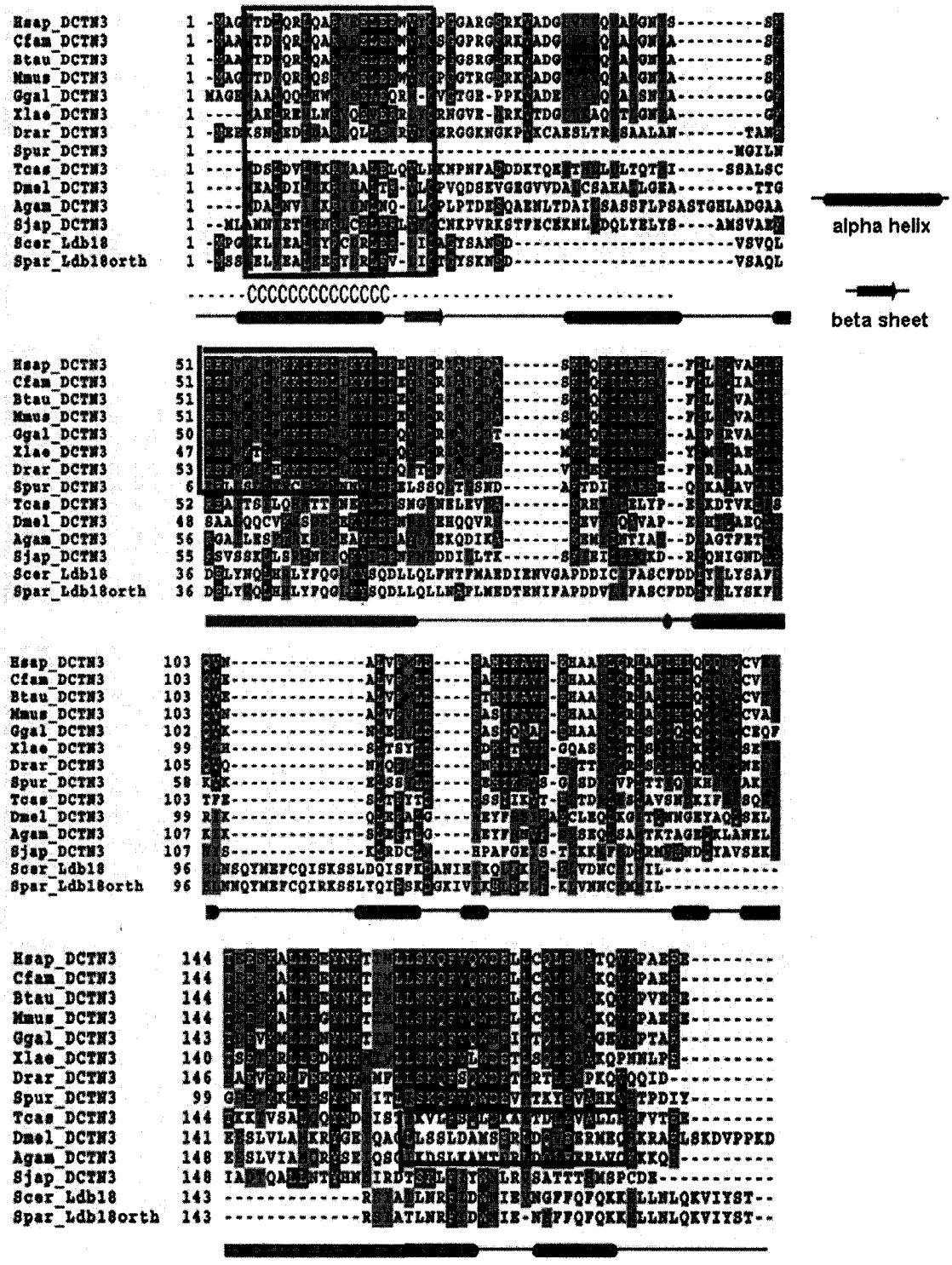

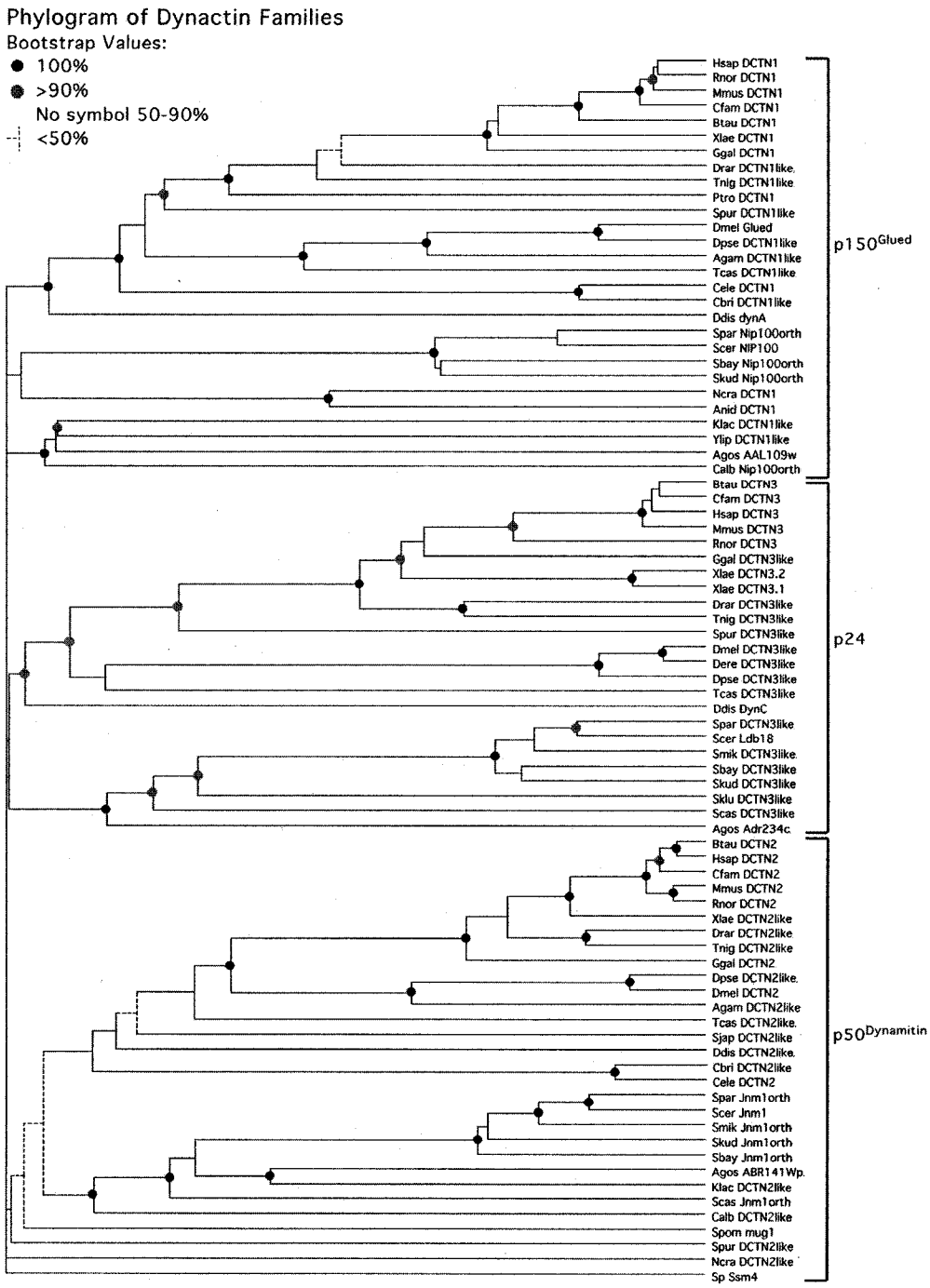


**Figure 2.7. Phylogenetic tree predictions for p150$^{Glued}$ (DCTN1), p50 (dyamitin, or DCTN2), and p24/22 (DCTN3).** Protein sequences were aligned by topological algorithms (unrooted) using TreeTop (Phylogenetic Tree prediction, Chumakov and Yushmanov, 1988; Yushmanov and Chumakov,1988; Brodsky *et al.*, 1992, 1995) . The distance between two organisms reflects the topological deviation of the protein considered. The bootstrap value reflects the possibility of the tree alignment (the alignments were resampled 100 times, which means 100 trees were generated, and the bootstrap value is the percentage of the tree being aligned in this particular way).

## 2.5 Loss of Ldb18 disrupts microtubule sliding

As described in the introduction, disruption of the dynein or dynactin complex disturbs microtubule-sliding behavior along the cortex during anaphase, and nucleus oscillation is mostly diminished. However, in these mutants, the nucleus does move close to the neck before anaphase, and the orientation of the pre-anaphase spindle is not affected. If Ldb18 were indeed a dynactin subunit in *S. cerevisiae*, loss of Ldb18 should show a similar phenotype (i.e. affects microtubule sliding).

Live GFP-tublin movies of a *ldb18*Δ strain showed abolishment of the microtubule sliding along the cortex, comparing to the wild type strain. With wild type cells, the mitotic spindle is correctly aligned the mother-bud axis prior to anaphase. During anaphase, as spindle elongation occurs, the spindle penetrates into the bud and translocates into the neck. Microtubule sliding along the bud cortex concurrent with spindle entry into the bud was often observed during anaphase, although the exact proportion of these cells need to be further quantified. In contrast, in *ldb18*Δ cells, cytoplasmic microtubules can grow very long and become curved inside the cell thus contact with the cortex, yet no sliding behavior was ever observed in these cells (approximately 300 cells observed) (Fig. 2.8). Prior to anaphase, when the bud is small (approximately 0.4 times of the mother) and the spindle is relatively short, alignment of the spindle along the mother-bud axis appeared to be normal.

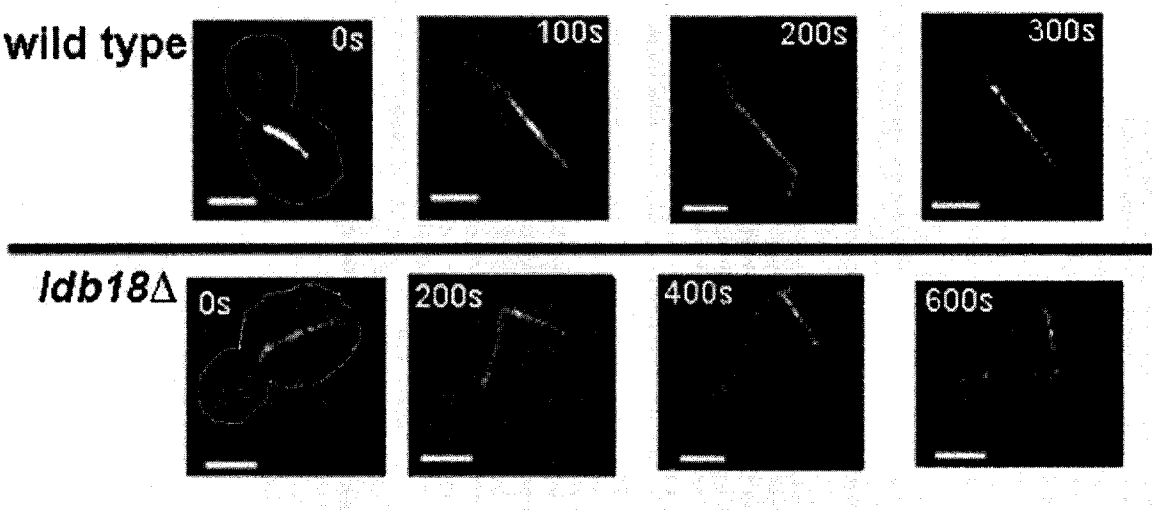


**Figure 2.8. Microtubule misalignment in the *ldb18*Δ mutant cells.** Expression of GFP-tubulin fusion protein was induced in both strains (wild type and *ldb18*Δ) in methionine-drop out medium for 2-3 hrs. An agarase pad slide was made for each strain, and the cells were observed under the microscope with a GFP filter. The exposure time was set at 0.2 seconds. From left to right, the images were taken in the order of time, tracing the microtubule movements in a single cell. Scale bar respesents 2 μm.

## 2.6 Ldb18 interacts with Arp1 and Jnm1

The observations described above suggested that Ldb18 is a dynactin subunit in *S. cerevisiae*. In addition, previous report showed that Ldb18 interacts with Jnm1 in a two-hybrid assay (Ito *et al.*, 2001). So I next proceeded to examine biochemical interactions between Ldb18 and the other dynactin subunits (Arp1, Nip100, and Jnm1) using double tagged strains (*LDB18-3HA*, and *NIP100/ARP1* with *TAP*). Dr. Kelly Tatchell (Louisiana State University Medical Center, Shreveport LA) provided rabbit anti-Jnm1, so I did not need to tag Jnm1. As the interaction between dynein and dynactin is fairly weak and was not well preserved in standard co-purification essays, I also constructed the *LDB18-3HA DYN3-TAP* strain as one of my negative controls.

The TAP epitope in *ARP1-TAP*, *DYN3-TAP*, and *NIP100-TAP* (purchased from Open Biosystems) strains was confirmed by both genomic PCR and western blot (Fig. 2.9 B and C). By integration of a PCR product into the genome, the endogenous copy of *LDB18* was tagged with *3HA* in the TAP strains. Another negative control, an isogenic single-tagged *LDB18-3HA* strain was also constructed, without any TAP-epitoped proteins. The HA epitope was confirmed by genomic PCR and western blot (Fig. 2.9 A and C).

To test if the epitope tagging affected the stability of the dynactin complex and caused nuclear postioning defects, I also performed DAPI-staining on the epitope-tagged strains. *LDB18-3HA* single-tagged strain did not show observable nuclear positioning defects, suggesting the 3HA epitope did not affect Ldb18 function. *DYN3-TAP* single-tagged and *LDB18-3HA DYN3-TAP* double-tagged strains also showed normal nuclear postioning phenotypes, indicating Dyn3-TAP was fully functional.

Both *ARP1-TAP* single-tagged and *LDB18-3HA ARP1-TAP* double-tagged strains showed a slight defect (at 15 °C, approximately 2.5% cells had 2 nuclear masses in the mother and none in the bud), suggesting that the TAP epitope affected Arp1 function. However, the nuclear positioning defects were much milder than those caused by loss of Arp1 (approximately 12% same type of cells at 15 °C), suggesting that Arp1 was at least partially functional in *ARP1-TAP* or *ARP1-TAP LDB18-3HA* strains.

Both the *NIP100-TAP* and *LDB18-3HA NIP100-TAP* strains showed approximately 10% binucleate large-budded cells, suggesting the TAP eptitope may have significantly disrupted Nip100 structure and its interactions with other dynactin subunits, causing the observed nuclear postioning defects.

I used human IgG sepharose Fast Flow (Amersham) to bind the protein A domain of the TAP epitope. Cell lysates of the *LDB18-3HA* single-tagged strain and *LDB18-3HA ARP1-TAP* double-tagged strain were applied to the IgG sepharose column. Arp1-TAP specifically bound to the IgG column and was eluted from the sepharose. Both Ldb18-3HA and Jnm1 were found in the eluate, indicating that Ldb18-3HA and Jnm1 bound to the IgG column, together with Arp1-TAP (Fig. 2.10 A). In contrast, when extracts from the *LDB18-3HA* single-tagged strain were applied to the column, no specific binding was detected, and neither Ldb18-3HA nor Jnm1 was detected in the eluate (Fig.2.10 B). These results suggested that Arp1, Ldb18 and Jnm1 interact with each other.

Using the double-tagged strain *LDB18-3HA NIP100-TAP*, Nip100-TAP did not bind to the column efficiently (Fig.2.11 A and B). Considering that the TAP epitope affected Nip100 function in this strain, these results are not completely conclusive.

The same protein affinity-binding method was used to study the *LDB18-3HA DYN3-TAP* double-tagged strain. Dyn3-TAP bound to the IgG column and was eluted specifically. However, Ldb18-3HA was not detected in the eluate (Fig. 2.11 C). These results implied that although dynein and dynactin function together, Ldb18 does not directly bind the dynein LIC, suggesting interactions between dynein and dynactin may not be mediated by these two subunits (Ldb18 and LIC), or the interactions are too weak/transient to be detected by the method described in this study.

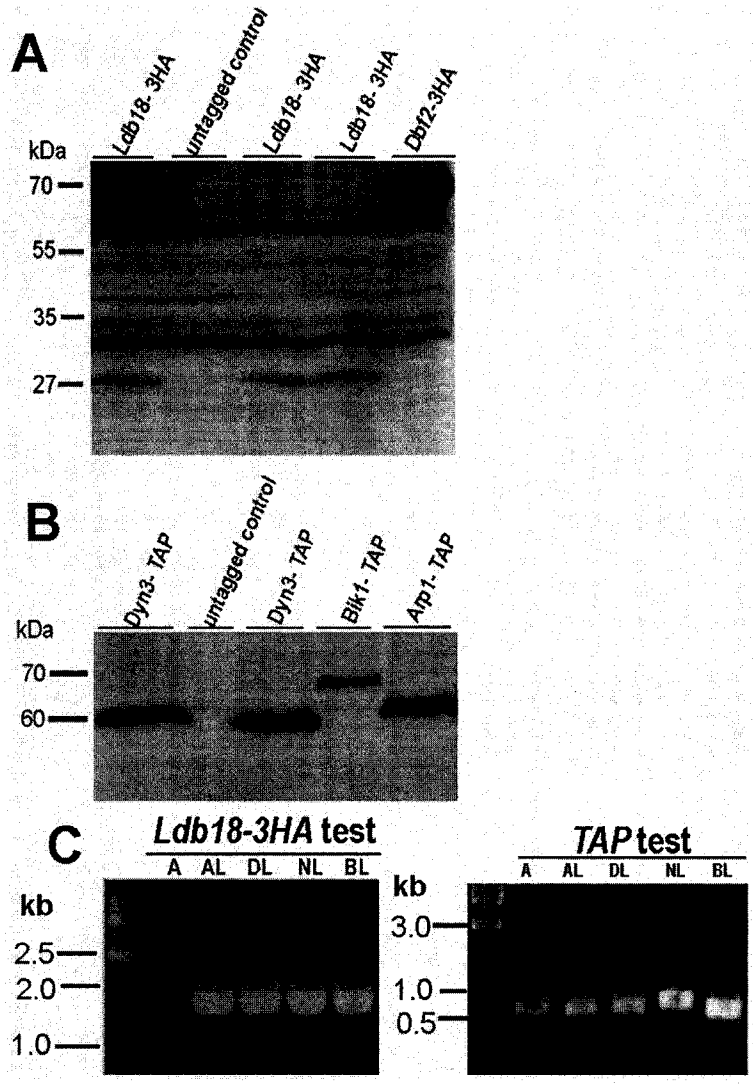


**Figure 2.9. Confirmation of TAP and 3HA epitope** by (A) anti-HA western blot, (B) anti-TAP western blot, (C) genomic PCR test of *LDB18-3HA*, and (D) genmic PCR test of *TAP*. For western blot, cells were grown to $OD_{600}$ 1.0-1.2 in YPAD medium at 30°C. 3 mL culture was harvested, washed, re-suspended in 100μL 0.1M NaOH, and incubated at room temperature for 5 minutes. The alkali was washed away and cells were re-suspended in 50μL 1×SDS sample buffer, boiled at 100 °C for 5 minutes, and loaded to a 15% mini SDS-PAGE gel. After electrophoresis, proteins on the gel were transferred to a PVDF membrane. Primary goat anti-HA (Bethyl) was used in 1:2500 dilution, and rabbit Peroxidase-anti-Peroxidase (Sigma) in 1:4000 diluiton was used to probe TAP epitope. Donkey anti-Goat secondary (Bethyl) and Goat anti-Rabbit (Sigma) were used in 1:10000 dilution. ECL plus kit was used for detection and film was exposed for 30 seconds. For PCR, forward primers prime within the ORFs, and reverse primers prime within the epitope tag (3HA or TAP) sequence. A, *ARP1-TAP* single tagged; AL: *ARP1-TAP LDB18-3HA* double tagged; DL: *DYN3-TAP LDB18-3HA* double tagged; NL: *NIP100-TAP LDB18-3HA* double tagged; BL: *BIK1-TAP LDB18-3HA* double tagged strain.

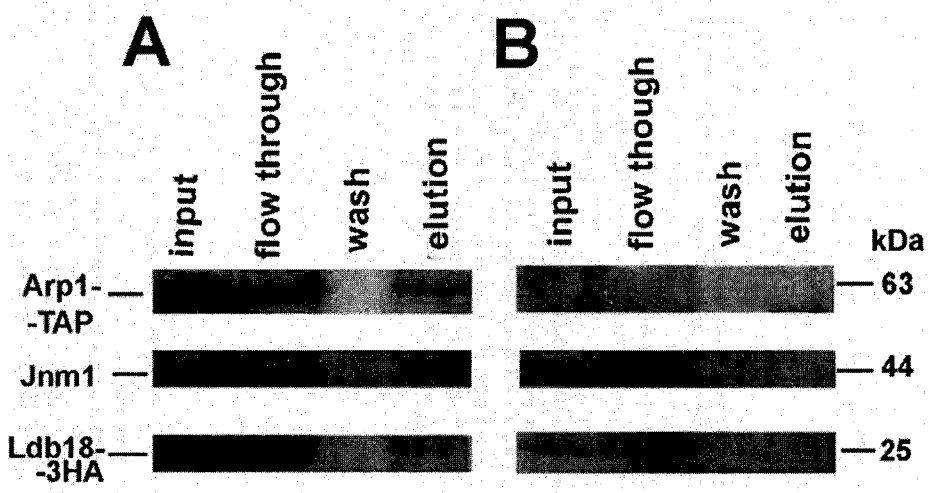


**Figure 2.10. Ldb18 interacts with Arp1 and Jnm1.** (A) *LDB18-3HA ARP1-TAP* double-tagged strain. (B) *LDB18-3HA* single-tagged strain. Both strains were grown to $OD_{600}$ 1.0-1.2 in YPAD liquid at 30°C. 100mL culture was harvested, washed by sterile distilled water, re-suspended in 200 μL NP-40 lysis buffer and bead-beaten for 10 rounds. The raw lysate was diluted to 2 mL with NP-40 lysis buffer and cleared up by centrifugation. Half of the clear lysate was applied to 500 μL IgG speharose Fast Flow (Amersham) packed in column. Binding, washing and eluting conditions were as described in the manufacturer's instruction book. The flow through, last patch of wash, and eluate were collected. Input (the other half of the clear lysate), flow through, and the wash were concentrated by aceton precipitation. The eluate was concentrated by TCA precipitation. 1:2500 goat anti-HA, 1:5000 rabbit PAP, and 1:5000 rabbit anti-Jnm1 was used. Secondary antibodies were all used in 1:10000 dilutions. Before a different detection, the membrane was stripped in stripping buffer at room temperature for 30 minutes, then re-blocked and re-probed with the next antibody.

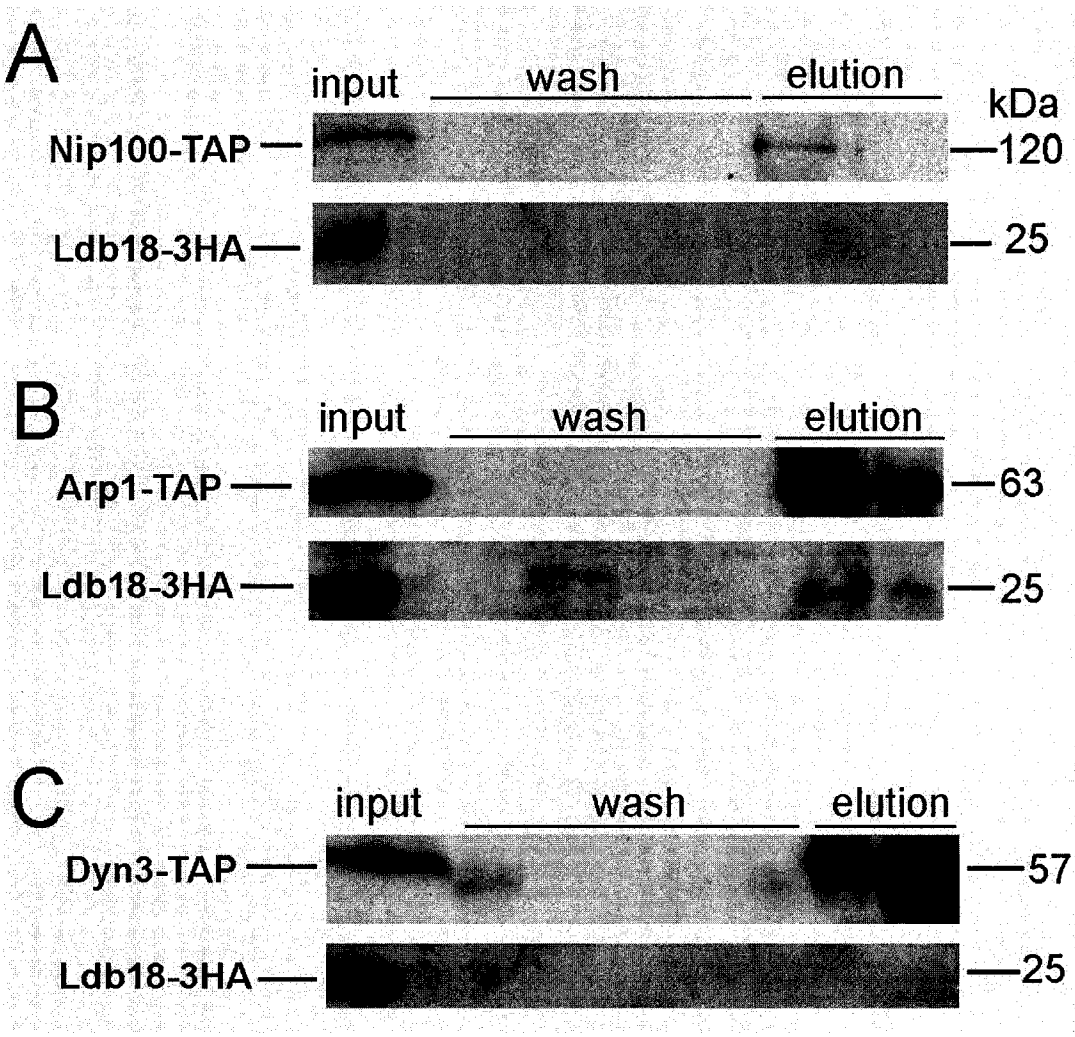


**Figure 2.11. Ldb18 does not interact with Dyn3.** (A) Double tagged *NIP100-TAP LDB18-3HA* strain. (B) Double tagged *ARP1-TAP LDB18-3HA* strain. (C) DYN3-TAP *LDB18-3HA* double-tagged strain. All strains were grown to $OD_{600}$ 1.0-1.2 in YPAD liquid at 30°C. 100 mL culture was harvested, washed, and re-suspended in 200 μL NP-40 lysis buffer, and bead-beaten for 10 rounds. The procedures for affinity binding, gel electropheresis, and western blots were as described in Figure 2.10.

## 2.7 Ldb18 localization study

Correct tagging of *LDB18* with *GFP* and three tandem *CFP*s was confirmed by genomic PCR (Fig. 2.12). However, I was not able to detect any fluorescence signals. This may be explained by the low abundance of the Ldb18 protein. Fig. 2.9 shows Ldb18p abundance compared to Dbf2p, which has an abundance of 3500 molecules /cell (Ghaemmaghami *et al.*, 2003).

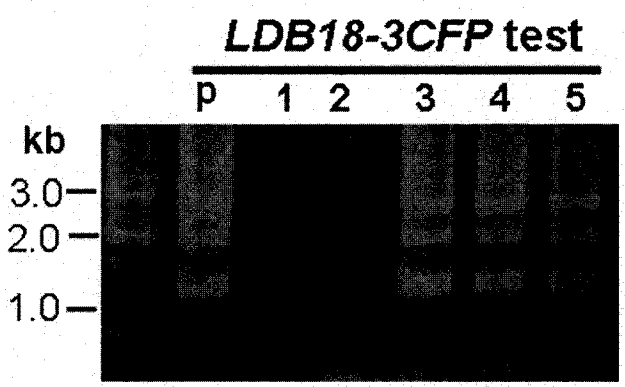


**Figure 2.12. Confirmation of *LDB18-3CFP* fusion** by genomic PCR. A plasmid containing the truncated *LDB18* sequence followed by three *CFP* sequences in tandem (p1523-LDB18) was linearized, then transformed into the parental strain (described in Materials and Methods). The forward primer primes in the middle of the *LDB18* ORF, and the reverse primer primes in the middle of the *CFP* sequence. P: positive control, using the plasmid p1523-LDB18 DNA as template. 1: negative control, using the genomic DNA of the parent strain (BY4742) as the template. 2,3,4,5: transformants selected on URA drop-out media.

# 3. Conclusions and Discussions

Results in this study indicated that *LDB18* psossibly encodes the yeast ortholog of the vertebrate dynactin subunit p24/p22. Ldb18 resembles p24/p22 at the primary sequence level, especially structurally. Strains lacking the Ldb18 protein demonstrated nuclear positioning defects similar to other mutants of the dynein pathway. *ldb18Δ* mutants also display genetic interactions typical of dynein and dynactin mutants. Ldb18 interacts biochemically with the dynactin subunits Jnm1 and Arp1, but not the dynein light intermediate chain Dyn3.

## 3.1 Ldb18 is a component of the dynein pathway

Mutants of the dynein pathway and of the Kar9 pathway have slightly different phenotypes. Disruption of the dynein pathway leads to large-budded cells with two DNA masses in the mother and none in the bud. Since the dynein pathway functions after the onset of anaphase, movement of the nucleus up close to the neck and orientation of the pre-anaphase spindle are not affected in dynein mutants. The Kar9 pathway, however, functions before anaphase. In mutants of the Kar9 pathway, the nucleus does not move close to the neck, or moves to the neck but cannot maintain its position there, and the pre-anaphase spindle tends to be misaligned. Like dynein mutants, the Kar9 pathway mutants show large-budded cells with two nuclear regions completely in the mother (less severe than in dynein mutants, Fig. 2.2). However, unique to the Kar9 pathway mutants, there are a portion of G2/M cells that fail to move the nucleus close to the neck before spindle elongation.

In DAPI-staining assays, loss of Ldb18 resulted in a phenotype typical of the dynein pathway mutants. Loss of Ldb18 did not have significant effects on nuclear movement up to the neck before spindle elongation, the phenotype uniquely seen in the Kar9 pathway mutants. In time-lapse movies of GFP-tubulin in *ldb18Δ* mutants, the orientation of the pre-anaphase spindle also seemed to be normal. Collectively, these results suggest that Ldb18 is a component of the dynein pathway involved in nuclear positioning during mitosis of *S. cerevisiae*.

In GFP-tubulin movies of dynein pathway mutants, the cytoplasmic microtubules fail to slide along the bud cortex, even when they are actually in contact with the cortex. In addition, in these mutants, cytoplasmic microtubules often grow longer than those in wild type cells, a phenomenon whose mechanism remains unknown (Adames and Cooper, 2000). This was also observed in GFP-tubulin movies of *ldb18Δ* mutants, which, once again, suggesting Ldb18 is a dynein pathway component.

Why do the MTs grow longer in dynein/dynactin mutants? It can be speculated that activation of dynein (or dynein associates with a MT-regulator after the activation) change the MT dynamics: before dynein is activated, MT is more stable and the catastrophe rate is lower (so it keeps growing); but once dynein is activated, with regulation of dynein or the associated proteins (maybe from the cortex, or dynactin), the catastrophe rate becomes higher. It is also possible that the cytoplasmic microtubules simply continue to grow during anaphase, until the cell sends the signals for mitotic exit. Alternatively, there are MT stabilizers (such as Bik1 and Kip1) at the MT plus ends, and during offloading of dynein, these stabilizers may be redistributed or off-loaded as well. Delay of the dynein offloading thus delays redistribution/offloading of these stabilizers, resulting in longer MTs. However, these speculations need further investigation.

In this study, genetic interaction assays also were consistent with Ldb18 being part of the dynein pathway. Simultaneous deletion of both *LDB18* and *BIM1* resulted in cell death, and loss of both Ldb18 and Kar9 (or Bni1) led to very slow growth of the progenies. This was slightly different from previous studies, as Tong *et al.* (2004) and Pan *et al.* (2004) reported synthetic lethality of *ldb18Δ* and *kar9Δ* (or *bni1Δ*, or *bim1Δ*). The differences may be due to the strain backgrounds, or the large-scaled genetic screens may have missed the slow growth of *ldb18Δ kar9Δ* and *ldb18Δ bni1Δ* progenies. In contrast, simultaneous loss of Ldb18 and any other dynein pathway component (such as Arp1, Dyn1, Jnm1) did not result in observable growth defects.

## 3.2 Results support that Ldb18 may be the yeast ortholog of the dynactin p24/p22 subunit

Ldb18 is a very small protein (approximately 21 kDa) of 179 amino acids. The primary sequence for the protein resembles the dynactin subunit p24/p22 from other

eukaryotes, and secondary structure analysis predicted Ldb18 to consist largely of helices with one coiled-coil domain. The size and secondary structure predictions for this protein are strikingly similar to the dynactin subunit p24/p22 (DCTN3) from higher organisms.

Affinity binding of Arp1-TAP from cell extracts to an IgG column also retained the dynactin subunits Jnm1 (dynamitin) and Ldb18. Whether Ldb18 was retained together with the Nip100-TAP ($p150^{Glued}$) to the IgG column remains unclear. No strong interaction was detected between Ldb18 and the dynein complex subunit Dyn3, as Ldb18 was not retained by affinity binding of Dyn3-TAP to the IgG column.

The interaction between Ldb18 and Arp1 does not seem to be very strong, as shown by the faint detection of Ldb18-3HA eluted from the IgG column (Fig 2.10 and 2.11). This might be partially due to the extremely low abundance of the Ldb18 protein. In addition, the *LDB18-3HA ARP1-TAP* double-tagged strain showed a slight nuclear positioning defect (~2.5% binucleate large-budded cells at 15 °C), suggesting that the stability of the dynactin complex may be slightly affected by the TAP epitope of Arp1, so dynactin is not fully functional in this strain.

Previous reports showed Arp1 to be the most abundant protein in the dynactin complex, whereas dynamitin was identified as the second most prevalent. It is predicted that each dynactin complex might have 8-13 Arp1 subunits and two $p150^{Glued}$ subunits (Schafer *et al.*, 1994a). Consistently, in this study, Arp1 and Jnm1 seemed to have relatively higher level of protein abundance, comparing to Ldb18 and Nip100 (Fig. 2.11).

If all the subunits of dynactin form a stable complex, one would expect that the whole dynactin complex will be retained by the IgG column with either Nip100-TAP or Arp1-TAP from cell extracts. However, TAP-tagging of Nip100 seemed to affect the stability of the dynactin complex (~10% binucleate large-budded cells at 15 °C), so further experiments without disruption of dynactin struture need to be performed to test the interaction between Nip100 and Ldb18. Anti-Nip100 antibody would be a great help.

Despite the uncertainty mentioned above, the interaction between Arp1 and Ldb18, seemed to be specific and reliable. The co-binding of Ldb18 and Arp1 was detected in repeated experiments. Furthermore, the same interaction was not seen between Ldb18 and Dyn3, or in a controlled assay done on strains lacking the TAP epitope. Nevertheless, more experiments need to be done to fully understand the interaction

between Ldb18 and the other dynactin subunits, including Jnm1, Arp1, and Nip100. The interaction between Ldb18 and Arp1 also has to be confirmed by reciprocal assays, such as detection of Arp1-TAP after the affinity binding of Ldb18-3HA to HA antibodies, using the same strain *ARP1-TAP LDB18-3HA.*

It would be interesting to test if dynactin binds to Pac11 (IC), since it has been shown that a recombinant p150$^{Glued}$ from rat brain cytosol binds the dynein intermediate chain *in vitro* (Karki and Holzbaur, 1995). However, previous reports showed no direct interaction between Pac11(IC) and Nip100 (ortholog of p150$^{Glued}$) (Kahana *et al.*, 1998). Based on the ultrastructure of dynactin (described in section 1.3.2), it can be predicted that Ldb18 should not bind Pac11 directly. However, this needs to be confirmed by further experiments.

## 3.3 Protein interactions within the dynactin complex

For mammalian cells, all subunits of the dynactin complex co-sediment at 20S in sucrose density gradients, including p22/24, dynamitin, p150$^{Glued}$, Arp1, CapZ, Arp11, p62, p27, and p25 (Karki *et al.*, 1998). In addition, a more stable complex of p150$^{Glued}$, dynamitin, and p24/22, which comprises the arm projecting from the rod of Arp1 polymer (Fig.1.5), can be isolated from dynactin (Eckley *et al.* 1999).

Dynamitin seems to play important roles in stabilizing interactions between the subunits in order to form a functional dynactin complex. Echeverri *et al.* (1996) found that excess dynamitin in mammalian cells disrupted the association of the p150$^{Glued}$ sidearm with the remainder of the dynactin complex, and this led to the arrest of the cells in a prometaphase-like stage. With excess dynamitin, p24/p22 is not found exclusively at 20S in sucrose density gradients anymore. Dynein and dynactin localization to kinetochores and membranous organelles is also diminished by excessive dynamitin (Burkardt *et al.*, 1997; Presley *et al.*, 1997).

Despite the lack of similarities in primary sequence of all subunits in the dynactin complex, the organization and structure of these subunits appear to be largely conserved from species to species. In *S. cerevisiae*, biochemical assays show that Nip100 (p150$^{Glued}$), Jnm1 (dynamitin), and Arp1 form a complex, and this co-sedimented complex does not include dynein (Kahana *et al.*, 1998).

It has been shown that affinity precipitation of Nip100 retains both Jnm1 and Arp1, and interaction between Nip100 and Arp1 is greatly diminished (but not completely absent) upon the loss of Jnm1 protein, suggesting that the interaction between Nip100 ($p150^{Glued}$) and Arp1 may be indirect, and mediated partially by Jnm1 (Kahana *et al.*, 1998). Additionally, in mammalian cells, a $p150^{Glued}$ affinity column retains both p24/p22 and Arp1(Waterman-Storer *et al.*, 1995; Karki *et al.*, 1998). Therefore, it can be speculated that the interaction between the projecting arm $p150^{Glued}$ (Nip100) and the Arp1 rod is mediated by both p24/22 (Ldb18) and dynamitin (Jnm1), in a cooperative manner.

If my prediction above were indeed correct, a direct interaction is expected to exist between Nip100 and Ldb18, and between Nip100 and Jnm1. However, the TAP epitope tagging to Nip100 seemed to affect dynactin structure and caused nuclear postioning defects, so whether Nip100 interacts Ldb18 still needs to be further tested. As deletion of *JNM1* diminishes but does not fully abolish the interaction between Nip100 and Arp1, it would be interesting to test whether deletion of *LDB18* has a similar effect on Nip100 and Arp1 interaction.

## 3.4 Localization of the dynactin complex

In mammalian cells, dynactin localization has been observed on centrosomes or the nuclear envelope, as well as being associated with vesicle structures (reviewed by Schroer, 2004). Localization of the complex in *S. cerevisiae* is poorly understood, one reason being the low protein abundance of the subunits. So far, localization studies have only appeared in two reports, but one of them overexpressed the protein on a plasmid (Nip100), and the other one immunostained β-galactosidase in a *JNM1::lacZ* strain (McMillan and Tatchell, 1994; Kahana *et al.*, 1998).

Immuno-staining with anti-β-galactosidase of a strain containing an integrated *JNM1::lacZ* fusion gene (integrated onto the *JNM1* locus in the gonome, and transcribed from the endogenous *JNM1* promoter) has localized Jnm1: β-galactosidase to the SPB and along cytoplasmic microtubules (McMillan and Tatchell, 1994). The localization seems to be cell cycle regulated. In cells with an unduplicated SPB or short spindle, the Jnm1: β-galactosidase fusion protein is often associated with an SPB. In cells at later

stages of the cell cycle (with longer spindles), it is often seen along cytoplasmic microtubules. The localization is asymmetric, as the spot is mostly found in the bud or at the SPB nearest the bud (McMillan and Tatchell, 1994). In a different study, Nip100-GFP constitutively expressed from a multicopy 2μ plasmid was found to co-localize with both SPBs in dividing cells (Kahana *et al.*, 1998).

The localization pattern shown in these two studies raises questions asking where and how dynactin interacts with dynein, as dynein is mostly found at the plus end of cytoplasmic microtubules and on the bud cortex. The off-loading model proposes that dynactin is required for dynein delivery to the cortex and dynein activation at the cortex. If this were correct, then dynactin should mainly be found along cytoplasmic microtubules and at the cell cortex, similar to dynein.

Nevertheless, it needs to be noted that early studies on dynein using similar constructs (for example, lacZ fusion) showed similar localization pattern of dynein, as compared to the dynactin localization studies described above. Also, dynein accumulates at the MT plus ends upon loss of dynactin, presumably due to failure of delivery to the cell cortex (Sheeman *et al.*, 2003; Lee *et al.*, 2003). Therefore, it can be speculated dynein and dynactin may actually co-localize throughout the cell cycle, making it convenient for these two complexes to function together. The SPB localization seen in the Nip100-GFP study is probably due to overexpression of the protein. The Jnm1:lacZ localization revealed by immunostaining may be due to disruption of the dynactin complex by binding of the antibody, as dynamitin is crucial for stabilizing interactions between the subunits and holding the whole complex together.

Localization of Ldb18 (*LDB18-GFP* and *LDB18-3CFP*) in this study was unsuccessful, due to the extremely low abundance of this protein. Overexpression of Ldb18 on a plasmid or under an inducible promoter may allow us to locate it, but could produce artifactual accumulation of cellular structures that does not occur in normal cells. Nevertheless, it can still be tested if dynein accumulates at the cytoplasmic MT plus ends in *ldb18Δ* mutants.

## 3.5 Interactions between dynein and dynactin

In *S. cerevisiae*, the disruption of either dynein or dynactin produces similar phenotypes in terms of microtubule sliding along the cortex, leading to non-distinguishable nuclear positioning defects. Also, simultaneous mutations in both dynein and dynactin do not result in a more severe phenotype than that observed for single mutants of dynein or dynactin alone. So, dynein and dynactin is part of the same nuclear positioning control pathway. However, Nip100 does not show biochemical interactions with Pac11, the intermediate chain (Kahana *et al.*, 1998). Immuno-precipitation of Arp1 or Jnm1 does not bring down Pac11 either. And, in this study, interaction between Dyn3 and Ldb18 was not detected, although it remains to be determined whether Ldb18 ineracts with Pac11. These results support the speculation of transient or indirect interactions between the two complexes. The transient/indirect interactions, however, must be crucial for the microtubule-sliding process, as loss of either completely prevents microtubule sliding (along the cortex) and results in extra long cytoplasmic microtubules.

## 3.6 Evolution of the dynein and dynactin complex

The primary protein sequence identity between dynein/dynactin subunits from *S. cerevisiae* and those from other eukaryotes is very low . Nip100 only has 13.7% overall sequence similarity to p150$^{Glued}$ (DCTN1) from rat. Primary sequence analysis of Jnm1 did not reveal any homology to p50 (dynamitin or DCTN2) either (refer to Table 1.1).

However, the secondary structures of most subunits are highly conserved. Nip100 N-terminal and C-terminal regions are predicted to form coiled-coil structures, similar to p150$^{Glued}$ (Kahana *et al.*, 1998). Jnm1 is predicted to contain three distinct coiled-coil structures, similar to dynamitin. Ldb18 is largely composed of α–helices with a coiled-coil structure, similar to p24/p22 (Fig. 2.6).

It should be noted that Nip100 (p150$^{Glued}$), Jnm1 (dynamitin), and Ldb18 (p24/p22) are highly α-helical. As specific amino acids are not required to form α-helical and coiled-coil structures, the proteins are able to accommodate considerable sequence variation among species, thus decreasing the evolutionary pressure for primary sequence conservation (Schroer, 2004). In addition, α-helical and coiled-coil structures are often

capable of mediating protein-protein interactions, providing possible links among multiple subunits, as well as with dynein or cargos.

Some subunits of dynactin identified in animals are yet to be found in *S. cerevisiae*, such as p62, p27, and p25. The 20S complex of dynactin seems to be conserved throughout metazoan evolution. It has been described in chicken, bovine brain, and *Drosophila* extracts (Gill *et al.*, 1991; Paschal *et al.*, 1993; McGrail *et al.*, 1995; Waterman-Storer and Holzbaur, 1996). Reports so far suggest that the interactions between the main subunits ($p150^{Glued}$, dynamitin, Arp1, and p24/p22) are similar in all species.

The dynein/dynactin complex is involved in multiple processes in animal cells, organelle transport being one of its major roles. In *S. cerevisiae*, dynactin seems to be involved only in nuclear positioning. In other words, the nucleus is the only organelle that requires dynein for movement. This makes evolutionary sense, considering the cell size of *S. cerevisiae*. In a cell as small as 5-10 μm, vesicles might be able to flow around in the cytoplasm and reach their destinations, without requiring a motor-driving system that consumes extra energy.

During mitosis of animal cells, dynein/dynactin has multiple functions. Besides mitotic spindle orientation, it is also involved in spindle organization and chromsome movements. In the budding yeast, absence of dynein function in the process of chromosome movement may be due to the small size of the metaphase spindle — prior to elongation (when spindle extends to ~8-12 μm), the spindle is only around 2 μm. Because the spindle is so small, chromosomes are close both to the mid-plate and to the poles. In metaphase, maintainance of chromosomes at the mid-plane may not be as crucial, consistent with the observation that a conventional mid-plate is absent in *S. cerevisiae*, and the chromosomes can oscillate in the nucleus. In anaphase A, MT polymerization/depolymerization and kinesins may already be enough for chromosome movements toward the poles. Considering the budding mode of mitosis in this organism, it seems more important to align the spindle along the cell polarity, as the bud site is pre-determined early in the cell cycle.

## 3.7 Future directions

In *S. cerevisiae*, although the terminal phenotypes resulting from disruption of the dynein pathway during mitosis are well defined, many questions remain about the details of this process of nuclear positioning. What is the real function of dynactin? Does it activate the motor activity of dynein, or does it mediate the interaction between dynein and other cellular components, such as the cortex and microtubules? How is dynein delivered to the plus end and the cortex? How and when is dynactin delivered to its site of function? And why do cytoplasmic microtubules grow much longer in dynein/dynactin mutants than in normal cells?

The interactions among the dynactin subunits in *S. cerevisiae* also need to be further elucidated. More biochemical assays need to be done to find the interactions between Arp1, Jnm1, Nip100, and Ldb18. These protein interactions can shed some light on organization and ultrastructure of the whole complex, and provide insights into how dynactin interacts with dynein or the other cellular components (such as the cortex) in animal cells. Detailed localization studies on the dynactin subunits and their co-localization with either dynein or microtubules will indicate how dynein-driven movements are coordinated during the cell cycle.

The behaviors of the dynactin subunits in *S. cerevisiae* are largely analogous to their vertebrate and insect counterparts, in terms of their organization, and their interactions with dynein, or microtubules. *S. cerevisiae* thus provides a genetically tractable eukaryotic system to study this crucial motor system in eukaryotes. In animals, loss of dynein/dynactin is lethal due to disruption of mitosis, and overexpression of dynein subunit has been implicated in carcinogenesis (den Hollander and Kumar, 2006). A single mutation in the dynactin subunit can have severe consequence, such as motor neuron disease (Puls *et al.*, 2003). Therefore, studies on dynactin from *S. cerevisiae* can be very helpful, and will provide insight on how the complex assembles and interacts with other cellular components in animals.

# 4. Materials and Methods

## 4.1 Growth media and conditions

If not specified, to grow a cell culture, a single colony was inoculated into 5mL of YPAD liquid medium, grown overnight at 30 °C with agitation (250rpm), then diluted into fresh YPAD (or synthetic media) to an $OD_{600}$ 0.1-0.2. The diluted culture was then grown until the specified $OD_{600}$ was reached.

YPAD: 2% peptone (Merck, Darmstadt, Germany), 1% yeast extract (Difco, Sparks, MD), 2% glucose, 0.004% adenine (Q-Biogene, Montreal QC), with or without 2% agar (Invitrogen, Carlsbad CA)

Synthetic complete (SC) media: 0.67% Yeast Nitrogen Base with Ammonium Sulfate but without Amino Acids (Difco), 2% glucose, 0.082% complete amino acids mix (CSM, Q-Biogene), with or without 2% agar (Difco).

Synthetic drop-out media: 0.67% Yeast Nitrogen Base with Ammonium Sulfate but no Amino Acids (Difco), 2% glucose, 0.054% CSM-Ade-His-Leu-Lys-Trp-Ura drop out mix (Q-Biogene). Drop one of the following: 0.004% Adenine, 0.002% Histidine, 0.01% Leucine, 0.005% Lysine, 0.005% Tryptophan, 0.002% Uracil (all amino acids from Q-Biogene). 2% agar (Difco) added for plates.

Synthetic drop-out media with G418: 0.17% Yeast Nitrogen Base without Ammonium Sulfate (Q-Biogene), 0.1% monosodium glutamate (Sigma-Aldrich, St. Louis MO), 2% glucose, 0.054% CSM-Ade-His-Leu-Lys-Trp-Ura drop out mix (Q-Biogene), drop one of the following: 0.004% Adenine, 0.002% Histidine, 0.01% Leucine, 0.005% Lysine, 0.005% Tryptophan, 0.002% Uracil. 2% agar (Difco) added for plates. 200 mg/L G418 (Q-Biogene) is added when the autoclaved media is cooled below 60°C.

Sporulation media: 1% potassium acetate, and 2% agar (Difco).

## 4.2 Strains used in this study

A complete list of all the strains used for this study is shown in Table 4.1.
All primers used are described in Section 4.12 and listed in Table 4.2. Plasmids used are listed in Table 4.3. Below are description of how specific types of yeast strains were constructed.

General Strategy for constructing a deletion strain or epitope-tagging a protein: All deletion strains and epitope-tagged strains were constructed by PCR-based strategies, as shown by Fig. 4.1 and Fig. 4.3 (Wach *et al.*, 1994 and Winzeler *et al.*, 1999).

For deletion strains of a particular open reading frame (ORF), using plasmid DNA as the template, a *URA3/KanMX4/KanMX6* PCR cassette was amplified using primer

ORF.F1 and ORF.R1. The PCR protocol is described in Section 4.3. The amplified DNA was concentrated (Section 4.4), transformed (Section 4.5), and integrated into chromosomes of competent host cells by homologous recombination. Transformants were selected on synthetic medium lacking uracil (SC-ura) or YPAD medium with G418 (YPAD+G418), depending on the selectable marker (Section 4.2). Genomic DNA was extracted (Section 4.6) from several individual transformants. As shown by Fig. 4.2, correct deletion of the ORF was confirmed by genomic PCR (Section 4.7). The ORF.FTEST and ORF.RTEST primers test if the ORF is still present, whereas the ORF.FTEST and URA3.RTEST/ KAN.RTEST primers test if the ORF is replaced by *URA3* or *KanMX4/6*.

To tag a particular ORF-encoded protein with an epitope tag, a Longtine plasmid for the epitope was used as the template (Longtine *et al.*, 1998). A PCR cassette for the epitope was amplified using primer ORF.F2 and ORF.R1. DNA concentration, transformation, and genomic PCR confirmation were as described above.

Deletion Strains with *KanMX4* marker: All deletion strains with the wild type allele replaced by *KanMX4* are from Open Biosystems (parental strain BY4742, *MATα*) (Winzeler *et al.*, 1999). Correct deletion of each ORF was confirmed by genomic PCR.

Construction of the *ldb18Δ::URA3* strain: A *URA3* PCR cassette was amplified with primer LDB18.F1 and LDB18.R1, using plasmid p4439 DNA as the template. The amplified DNA was transformed into competent Y2295 (*MATa*) cells. Transformants were selected on SC-ura plates. Correct deletion of the *LDB18* ORF by *URA3* replacement was confirmed by genomic PCR, using primer LDB18.FTEST and LDB18.RTEST (or URA3.RTEST) (Fig.2.2 in Results).

Construction of the *ldb18Δ::KanMX6 GFP-TUB1* strain: A *KanMX6* PCR cassette was amplified using the same primers (LDB.F1 and LDB18.R1), and pFA6a-kanMX6 plasmid DNA as the template (Longtine *et al.*, 1998). The amplified DNA was transformed into competent *GFP-TUB1* strain (Table 4.1). Deletion of the *LDB18* ORF was confirmed by genomic PCR, using primer LDB18.FTEST with LDB18.RTEST or KAN.RTEST.

Construction of the *LDB18-3HA* single-tagged strain: Sequence encoding three tandem copies of the HA epitope followed by *KanMX6* marker was amplified using pFA6a-3HA-kanMX6 plasmid DNA as the template (Longtine *et al.*, 1998). The LDB18.F2 and LDB18.R1 primers were used. The amplified DNA was transformed into competent BY4742 cells. Stable transformants were confirmed by genomic PCR using primer LDB18.TAGTEST and KAN.RTEST. Correct tagging of 3HA epitope was also confirmed by western blots (Fig. 2.7 in Results).

Tandem Affinity Purification (TAP) strains: TAP tag consists of a calmodulin binding peptide, a TEV cleavage site and two IgG binding domains of *Staphylococcus aureus* protein A, as well as a *HIS3* selectable marker. All TAP strains (*ARP1-TAP*, *NIP100-TAP*, and *DYN3-TAP*) were purchased from Open Biosystems (Ghaemmaghami *et al.*, 2003). Each ORF is tagged with the TAP epitope at the C-terminus and expressed from

its natural chromosomal location. The parental strain is BY4741(*MATa*). Correct TAP tagging was confirmed by genomic PCR, using the F2CHK reverse primer and a forward primer containing sequence homologous to sequence on the ORF (ARP1.TAGTEST, NIP100.TAGTEST and DYN3.TAGTEST). The tagging of TAP epitope was also confirmed by western blots (Fig. 2.7).

Construction of double epitope-tagged strains: I tagged the *LDB18* ORF with a 3HA epitope using the same strategy, described for creation of the *LDB18-3HA* single tagged strain. However, PCR products were transformed into competent TAP-tagged strains (*ARP1-TAP*, *NIP100-TAP*, and *DYN3-TAP*). Correct tagging of 3HA epitope was confirmed by genomic PCR and western blots as well (Fig. 2.7).

Construction of the *LDB18-GFP* strain: The *GFP* module followed by *KanMX6* marker was amplified from pFA6a-GFP (S65T)-kanMX6 plasmid DNA through PCR (Longtine *et al.*, 1998). PCR products were transformed into competent cells (BY4742). Homologous recombination was confirmed by genomic PCR using primer LDB18.TAGTEST and KAN.RTEST.

Construction of the *LDB18-3CFP* strain: A plasmid p1523 containing three *CFP* modules in tandem followed by a *URA3* selectable marker was kindly provided by John Cooper's lab (Lee *et al.*, 2003; Lee *et al.*, 2005). The *LDB18* ORF (without the start codon) was amplified from BY4742 genomic DNA, using primer LDB18-3CFP.F and LDB18-3CFP.R. Both the amplified DNA and the plasmid p1523 were digested with *BamHI* restriction enzyme. The two digested products were purified by phenol:chloroform, ligated at 16°C for two hours, and transformed into competent DH5α *E.coli* cells. Plasmids were extracted from several individual colonies and digested with restriction enzymes to ensure correct direction of insertion. After confirmation of the right orientation, several plasmids were sequenced to ensure that no mutation had occured. One plasmid with correct insertion (p1523-ldb18) was then linearized with *Bgl II* and transformed into competent BY4742 cells. Transformants were selected on SC-ura, and the integration of 3CFP into the genome was confirmed by genomic PCR using primer LDB18.TAGTEST and GFP.RTEST. The plasmid p1523-ldb18 was used as a positive control for PCR.

## 4.3 PCR Protocols to amplify the desired DNA sequence for homologous recombination

The Expand Long Template PCR System (Roche, Mannheim Germany) was used to amplify the desired DNA sequence for homologous recombination. For a 50 μL PCR reaction, 200-500 ng genomic DNA (or ~50 ng plasmid DNA) was used as template. Final concentration of 350 μM dNTP, 300 nM of both primers, and 0.75 μL of 5 U/μL expand enzyme mix were added. 1× Expand Long Template Buffer 2 (200 mM Tris-HCl pH 8.4, 500 mM KCl, and 2.75 mM $MgCl_{2)}$ was used.

The PCR reactions were set as following:

| | | |
|---|---|---|
| 94 °C | 2 min | |
| 94 °C | 10 s | ] 35 cycles |
| 50~55 °C | 1 min | |
| 68 °C | 3 min | |
| 68 °C | 10 min | |
| 4° C | hold | |

## 4.4 Concentration of PCR products

The amplified DNA was concentrated for transformation into yeast by ethanol precipitation. 0.1 volumes of 3M NaOAc and 2 volumes of 95% ethanol was added, followed by 20 min incubation on ice. The pellets were then washed by 70% ethanol, dried at 37 °C for 20 min, and dissolved in 10μL sterile distilled water or TE buffer (10 mM Tris-Cl pH 7.5, 1 mM EDTA/NaOH pH 8.0)

## 4.5 Transformation of *S. cerevisiae*

Transformation of *S. cerevisiae* was based on the lithium-acetate method previously described (Schiestl and Gietz, 1989; Gietz andWoods, 2002; Wach *et al.*, 1994).

Preparation of competent cells: A small loop of yeast cells was inoculated from 2-3 day old colonies on YPAD plates into 5mL YPAD liquid and grown overnight at 30 °C with agitaton (250 rpm). The overnight culture was inoculated into 50 mL YPAD liquid medium to give an $OD_{600}$ of 0.1-0.2. The 50 mL culture was grown for 4-6 hrs until the final $OD_{600}$ reached 0.5-0.7 (approximately $1.2\times10^7$ cells/mL). The cells were harvested by centrifugation (4000×g, 5min, room temperature), washed once with 0.1-0.5 volumes of sterile distilled water, and once with 0.1-0.2 volumes of SORB (100 mM lithium acetate, 10 mM Tris-HCl pH 8, 1 mM EDTA/NaOH pH 8, 1 M Sorbitol, adjusted with dilute HAc to pH 8 and sterile filtered). SORB was removed and the cells were finally resuspended in a total volume of 360 μL SORB (per 50mL of cell culture). 40 μL ice-cold carrier DNA (Salmon Sperm sheared single stranded DNA) was added. The cells were aliquoted and stored at -80 °C.

Transformation of DNA into competent cells: 50 μL thawed competent cells and 10 μL concentrated PCR product (or 10 μL competent cells with 2 μL plasmid DNA) were mixed well before 6 volumes of PEG (100mM lithium acetate, 10mM Tris-HCl pH 8, 1mM EDTA/NaOH pH 8, 40% polyethylene glycol 3350, sterile filtered) was added. The suspension was mixed well, and incubated at room temperature for approximately 30 minutes. Dimethyl sulfoxide (DMSO) was added to a final concentration of 5%. The mixture was placed in a 42 °C water bath for 5-20 min. The cells were spun down (4000×g for 2 min), resuspended in 100-200 μL of sterile water, and plated onto synthetic drop-out medium lacking the amino acid corresponding to the auxotophy marker (i.e., SD-his plates for *HIS3MX6* marker). An exception is *KanR* marker, for which the cells were resuspended in 3 mL YPAD liquid medium after being spun down, to recover from

42 °C heat shock. The cells were incubated in a shaker at 30 °C for 2-3 hrs, collected and spread on YPAD+G418 plates (200 mg/L G418). Transformants were usually visible after 2-3 days. For KanR selection, the transformation often resulted in many transient transformants, which could be eliminated by replica-plating onto fresh G418 plates. Stable transformants were visible after 1 day of incubation.

## 4.6 Genomic DNA extraction

Preparation of cells: A single colony was inoculated into 5 mL YPAD liquid and grown at 30 °C overnight with agitation (~250 rpm). 1.5 mL of the overnight culture was pelleted in a 1.5 mL centrifuge tube (13,200×g, 30s). Cells were washed with 0.5 mL sterile distilled water, and resuspended in 300μL lysis buffer (2% Triton X-100, 1% SDS, 0.1M NaCl, 10 mM Tris-HCl pH 8, 1 mM EDTA/NaOH pH 8).

Lysing the cells: 200-300 uL acid washed 0.5mm glass beads (BioSpec, Bartlesvill OK) and 200uL phenol/chlorophorm/isoamyl alcohol (25:24:1, Sigma) were added to the cell suspension. The mixture was vortexed at maximum speed in a fridge for 6 min followed by 5 min centrifugation at 13,200×g.

DNA extracting: 200 μL of the top aqueous layer was removed. 450 μL of 95% ethanol was added and mixed with this layer. DNA was precipitated by centrifugation (13,200×g, 5 min), followed by addition of 500 μL 70% ethanol to wash the pellet (13,200×g, 5 min). Ethanol was removed, the DNA pellet was dried at 37°C then re-suspended in 50μL TE buffer or sterile distilled water.

## 4.7 Genomic PCR confirmation of transformants

To determine whether PCR products were correctly integrated into yeast chromosomal DNA, a 25 μL PCR reaction was set, using recombinant Taq DNA Polymerase (Invitrogen). The final mix contained 200-500 ng genomic DNA, 50.2 mM dNTP, 0.5 μM of both primers, 1× PCR buffer (200 mM Tris-HCl pH 8.4, 500 mM KCl ), 1.5mM $MgCl_2$ and 1U Taq DNA Polymerase.

The PCR reactions were set as following:

| | | |
|---|---|---|
| 94 °C | 3 min | |
| 94 °C | 45 s | ⎫ |
| 55~60 °C | 30 s | ⎬ 35 cycles |
| 72 °C | 1-2 min | ⎭ |
| 72 °C | 10 min | |
| 4 °C | hold | |

## 4.8 Synthetic lethality assay

Crossing of two strains: The *MATa ldb18Δ::URA3* strain was crossed with each *xxxΔ::KanMX4* deletion strains to test for synthetic lethality or synthetic growth defects. A loop-ful of cells of both strains were obtained from fresh colonies, mixed well on a

new YPAD plate, and incubated at 30 °C overnight.

Selecting diploids: Cells from the mixed mass were then streaked onto fresh SD-ura+G418 plates, and incubated for 2-3 days to select for diploids.

Sporulation of diploids: Fresh cells from the double selective plates were transferred to sporulation plates (1% potassium acetate, 2% agar) to sporulate for at least 3 days. Cells could be checked under the microscope to determine if sporulation had occurred.

Tetrad dissection: After around 50% of the cells had sporulated, the asci were digested with 0.275 U/mL (or ~6,000 Fishman units/mL) ß–Glucuronidase /Arysulfatase (Roche) for 10 min, then streaked to YPAD plates. The tetrads were dissected with a micromanipulator. The dissected spores were incubated on the original YPAD plates for 2-3 days.

Determining genotype of each progeny: Colonies from the original YPAD plates were then replica-plated to SC-ura and YPAD+G418 plates, to test for the *ldb18Δ::URA3* and *xxxΔ::KanMX4* alleles. Mating type of a colony was determined by replica-plating the colony to YPAD plates with lawns of Y2081 (*MATa*) or Y2082 (*MATα*) cells. After 1-2 days, a halo would be seen around a colony if mating occurred between the colony and Y2081 or Y2082 cells. A halo therefore indicated that the mating type of the colony was opposite to the lawns.

## 4.9 Use DAPI-staining to determine nuclear positioning defects

Growth of cells: A single colony from a fresh plate was inoculated into 5 mL YPAD liquid medium and grown at 30°C overnight with agitation (~250 rpm) to a final $OD_{600}$ 2~3. The overnight culture was inoculated into 5 mL fresh YPAD liquid to give an $OD_{600}$ of 0.05-0.1. The new culture was allowed to grow at 30 °C for 6-7 hrs or at 15 °C for ~2 days until their $OD_{600}$ reached 0.8-1.0.

Fixation of cells: Cell suspensions were collected in a 1.5 mL microfuge tube, fixed by adding 2 volumes of 95% ethanol and incubating at 4 °C for at least 10 minutes.

DAPI staining: The ethanol-fixed cells were pelleted down, washed in 0.1 M potassium phosphate buffer (pH 7.0), and incubated with 1 μg/mL DAPI (4',6-diamidino-2-phenylindole, Sigma) for 5 min. 100 μL DAPI was usually needed for 0.5 mL cell culture from above. The DAPI-stained cells were washed with 0.1 M potassium phosphate buffer (Tarnowski *et al.*, 1991).

Couting cell numbers of each morphology under microscope: Cells were observed under microscope with a DAPI filter (exciter: D360/40, emitter: D460/50, Olympus). Cell numbers were counted and placed into one of the following categories: a) unbudded cell with a single nuclear mass; b) budded cell with a single nuclear mass in the mother; c) budded cell two nuclear masses, one in the mother and one in the bud; d) budded cell with two nuclear masses in the mother but none in the bud; and e) unbudded cell with two or more nuclear masses. At least 300 cells were counted for each strain.

Experiments were performed in triplicate. Average percentage of cell numbers for each category and standard errors were calculated.

## 4.10 Time-lapse movies of spindle movements

Growth of cells: 2-3 colonies from a fresh plate were inoculated into 5 mL YPAD liquid and grown at 30 °C overnight with agitation (~250 rpm). The cells were inoculated into new SC complete liquid medium at a 1:1000 dilution. The diluted cultures were then grown at 30 °C overnight until the $OD_{600}$ reached 0.7-0.9.

Induction of GFP-tubulin: Cells were pelleted from SC complete medium and washed in sterile water. Cells were then resuspended in SC-met liquid medium and grown for ~3 hrs (30°C) or 5~6 hrs (15°C).

Making agarose-padded slides: After induction, 1 mL cells were pelleted down and resuspended in ~50 uL SC-met liquid medium. An agarose pad in simplified non-fluorescent media (1 mM potassium phosphate buffer pH 7.0, 4mM $MgSO_4$, 20mM $(NH4)_2SO_4$, 0.84g/L CSM mixture, 2% glucose, and 1-2% agarose added) was made on a pre-cleaned slide ( size 3×1", Thickness 0.93-1.05mm, Becton, Dickinson and Company, Portsmouth NH). A cover slip (22×22mm, Fisher Scientific, Ottawa Ontario) was used to cover the cells on the pad. The cover slip was sealed with Vaseline.

Taking images under microscope: The cells were visualized and images were taken under GFP filter (emitter: 470/40, exciation 525/50, Olympus). The Image-pro program was set in such way that images were taken on multiple focus layers with one field of view every 5 min lasting for a period of time (i.e. 2 hrs).

## 4.11 Western blot

Growth of cells: A single colony from a fresh plate was inoculated into 5 mL YPAD liquid medium and grown at 30 °C overnight with agitation (~250 rpm) to $OD_{600}$ 2~3. The overnight culture was inoculated into 5 mL fresh YPAD liquid medium to give an $OD_{600}$ 0.1-0.2. The diluted cultures were then grown at 30°C for 4-5 hrs until the $OD6_{00}$ reached 1.0-1.2.

Lysis of cells: 2.5-3.0 OD of the cells were pelleted (13,200×g, 2min), and washed by sterile water. Cells were resuspended in 200 µL 0.1M NaOH, incubated at room temperature for 5 min, pelleted, and resuspended in 50 µL 1×SDS sample buffer (60 mM Tris-HCl pH 6.8, 5% glycerol, 2% SDS, 4% ß-mercaptoethanol, 0.0025% bromophenol blue). The cell suspension was then boiled at 100 °C for 5 min and pelleted again (Kushnirov, 2000).

SDS-PAGE electrophoresis: 7 µL of the supernatant from above was added to a mini SDS-PAGE gel (Mini-Protean 3 Cell system, Bio-Rad, Hercules CA). Electrophoresis was conducted at 100 volts for 4 hrs.

Western Transfer: The proteins were transferred to a PVDF membrane (Amersham, Buckinghamshire UK) using a mini transfer system (Mini Trans-Blot Electrophoretic

Transfer Cell, Bio-Rad) at 30V in 4 °C fridge overnight, following the manufacturer's instructions.

Membrane blocking and probing: The membrane was blocked with 1xTBST buffer (20 mM Tris-HCl pH 7.6, 125 mM NaCl, and 0.1% Tween 20) mixed with 5% non-fat milk for at least 2 hrs at room temperature (or 4 °C overnight). The primary anti-body was added to the blocking solution, and incubated at room temperature for at least 2 hrs. The membrane was then washed 3 times in 1xTBST buffer, each time for 10 min. The secondary HRP conjugated antibody was subsequently added in blocking solution, and the membrane was incubated in it for 1 hr at room temperature. The membrane was then washed in 1xTBST (2 brief washes, 15 min washes in large volume, followed by 3 washes, each for 5 min).

ECL Detection: The antigen was detected using ECL Plus Western Blotting Detection Reagents (Amersham) following the manufacturer's instructions. Chemiluminescence BioMax Light Film (Kodark, Rochester NY) was exposed to the membrane for 0.5-3 min and developed in a dark room.

Antibodies used in this study:

Goat Anti-HA (Bethyl, Montgomery Texas): 1:3000-1:1000 dilution.

Rabbit PAP (Peroxidase-Anti-Peroxidase Soluble Complex, Sigma): this antiserum is developed in rabbit using Horseradish Peroxidase as the immunogen. Because protein A domain in the TAP epitope will bind to antibodies raised in rabbit, this PAP antibody will increases sensitivity of the detection. Used in 1:4000-1:10000 dilution for this study.

Rabbit Anti-Jnm1 (a generous gift from Dr. Kelly Tatchell, Louisiana State University Medical Center, Shreveport LA): 1:5000 dilution.

Secondary antibodies (HRP conjugated goat anti-rabbit, Sigma or donkey anti-goat, Bethyl): 1:10000 dilution.

## 4.12 Affinity chromatography

Growth of cells: A single colony from a fresh plate was inoculated into 5 mL YPAD liquid medium, and grown at 30 °C overnight with agitation (~250 rpm) until $OD_{600}$ 2-3. The culture was inoculated into 50 mL fresh YPAD liquid to give an $OD_{600}$ 0.1-0.2. The diluted cultures were then growing at 30 °C for 5-6 hrs until the $OD_{600}$ reached 1.0-1.2.

Lysis of cells: 50 mL cell culture were harvested by centrifugation (4000×g, 10 min) and washed by sterile water. Cells were then re-suspended in 200 µL NP-40 lysis buffer (pH 7.2, 15 mM $Na_2HPO_4$, 10 mM $NaH_2PO_4$, 1% NP-40, 150 mM NaCl, 2 mM EDTA, 50 mM NaF, 0.1 mM $Na_3VO_4$) with protease inhibitor added (Complete mini protease inhibitor tablets, Roche). About 200 µL 0.5 mm acid-treated glass beads (Bio Specs) were added to the suspension. The mixture was vortexed at maximum speed for 1 min, followed by a 1 min break, 10 rounds. The cells were observed under microscope after 10 rounds of bead beating. If less than 90% of the cells were lysed, a few additional rounds were performed.

Obtaining cell lysates: All the beads were removed from the suspension. The suspension was then diluted by adding 2 mL of NP-40 lysis buffer with protease inhibitor. The diluted suspension was cleared by 10 min centrifugation at 4000×g, 4°C.

Loading cell lysates to IgG column: A column (Bio-Rad) was packed with 0.5 mL IgG sepharose 6 Fast Flow (Amersham). The gel was washed with at least 5 bed volumes TST (50 mM Tris pH7.6, 150 mM NaCl and 0.05% Tween 20) to remove ethanol. The column was equilibrated by 0.5 M HAc (pH 3.4) and TST washes, alternatively for 2 rounds. Half of the cleared lysate was applied to the sepharose column (the other half worked as a control for the "input"). The column was rocked at 4 °C for 2 hrs (or overnight).

Washing and elution of IgG column: The flow through from the gel by gravity feed was collected. The gel was washed with at least 10 bed volumes of TST until $A_{280}$ was around 0.0, followed by a wash with2 bed volumes 5 mM $NH_4Ac$ (pH 5.0). The bound protein was then eluted with 3-4 bed volumes of 0.5 M HAc (pH 3.4).

Concentrating proteins:

The eluted proteins were concentrated by adding TCA to a final concentration of 15%. The suspension was incubated on ice for 2 hrs (or overnight) after TCA addition. The proteins were pelleted by centrifugation (13,200×g, 4°C, 15 min). The protein pellets were washed with 500 µL ice-cold acetone twice, then re-suspended in 10 µL 1×SDS sample buffer. The suspension was boiled for 5 min then pelleted.

The other half of the cleared lysate (that was not applied to the column) worked as a control for the "input". Proteins in the input and the flow-through (the suspension collected after binding) were concentrated by adding 4 volumes of ice-cold acetone and incubating at -20 °C for at least 2 hrs). The proteins were pelleted by centrifugation (4000×g, 4 °C, 15min), and re-suspended in 1×SDS sample buffer.

Gel electrophoresis: Samples of input, flow through, washes, and elutions were then loaded to a SDS-PAGE gel. Electrophoresis was conducted at 100 volts for 4 hrs.

Membrane probing: The western blot procedure was described in Section 2.11. If a membrane needed multiple detections, it was stripped for 30 min in stripping buffer (62.5 mM Tris pH 6.7, 100 mm ß-mercaptoethanol, 2% SDS) at room temperature, then washed 3 times (each time 10 min) with 1×TBST buffer before re-blocking and probing.

## 4.13 Primers used in this study

Table 4.2 provides a complete list of all primers used in this study.

For deletion of the *LDB18* ORF: The LDB18.F1 primer is an 80mer that contains (5'-->3'): 60 bases directly upstream of the *LDB18* ORF (not including the start condon), followed by 20 bases homologous to the 5' sequence on the *URA3* (or *KanMX4/6*) module. The 80mer LDB18.R1 primer contains 60 bases directly downstream of the *LDB18* ORF (not including the stop codon), followed by 20 bases homologous to the 3' sequence on the *URA3* (or *KanMX4/6*) module (Longtine *et al.*, 1998).

For testing correct deletion of an ORF: The ORF.FTEST primers contain 20 bases upstream of the open reading frame. The ORF.RTEST primers are 20mer homologous to the sequence on the ORF. Primer KAN.RTEST and URA3.RTEST are homologous to the sequence on the *KanMX4/6* and *URA3* module, respectively.

For epitope tagging of Ldb18: The LDB18.F2 primer is an 80mer that contain (5'-->3'): 60 bases directly at the 3' end of the *LDB18* ORF (right before but not including the stop codon), followed by 20 bases homologous to the 5' sequence of the *3HA-KanMX6* module on the pFA6a-3HA-kanMX6 plasmid (Longtine *et al.*, 1998). The 80mer LDB18.R1 primer contains 60 bases directly downstream of the *LDB18* ORF (right after but not including the stop codon), followed by 20 bases homologous to the 3' sequence of the *3HA-KanMX6* module.

For testing whether an ORF is epitope-tagged: The ORF.TAGTEST primers (forward primers) are 20mer homologous to the sequence on the ORF. The reverse primers are homologous to sequences on the epitope module (3HA, TAP, or GFP).

For tagging Ldb18 with three CFP modules in tandem: The LDB18-3CFP.F primer contains (from 5' to 3'): a few random bases, *BamH I* restriction sequence, and 21 bases from the 5' end of the *LDB18* ORF (right after but not including the start codon). The LDB18-3CFP.R primer contains the following: a few random bases, *BamH I* restriction site, sequence for a $(Gly\text{-}Ala)_3$ linker, and 24 bases homologous to the 3' end of the *LDB18* ORF (right before but not including the stop codon).

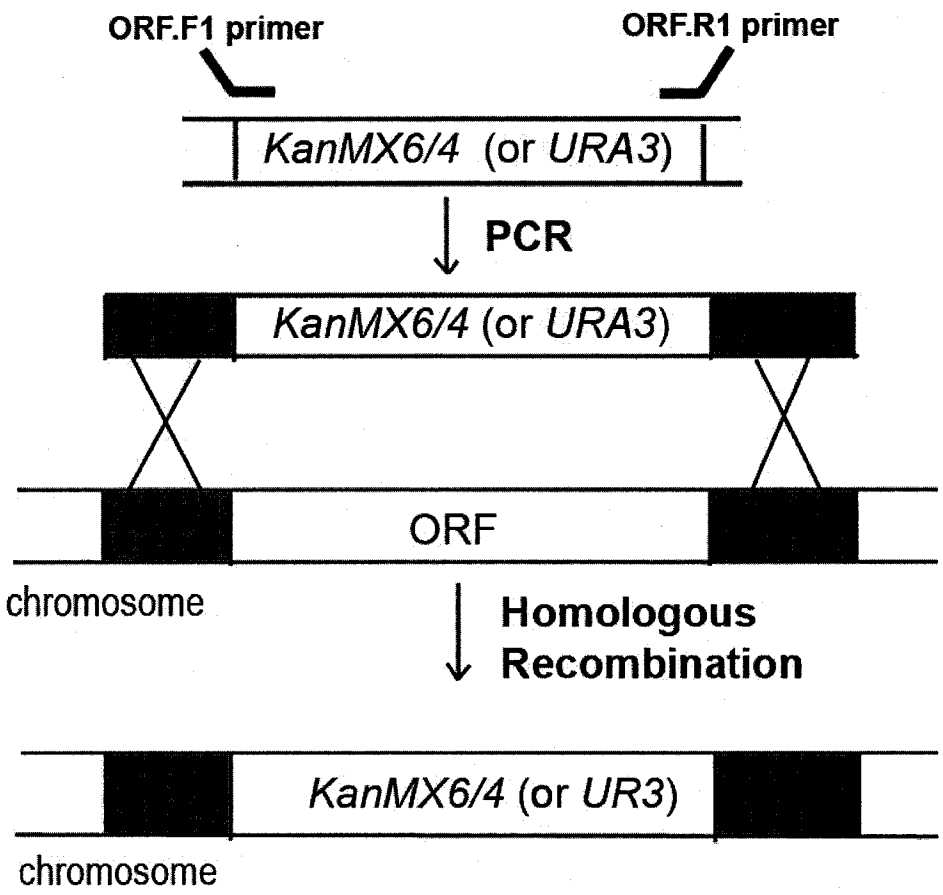


**Figure 4.1. The PCR-based strategy for making deletion strains.** The ORF. F1 80mer primer contains 60 bases directly upstream of the *LDB18* open reading frame (not including the ATG), followed by 20 bases homologous to the 5' sequence on the *KanMX4/6* (or *URA3*) module. The 80mer LDB18.R1 primer contains 60 bases directly downstream of the *LDB18* open reading frame (not including the stop codon) followed by 20 bases homologous to the 3' sequence on the *KanMX4/6* (or *URA3*) module. The template is the DNA of a plasmid. PCR protocol is described in Section 2.3. Amplified DNA is concentrated (Section 2.4) and transformed (Section 2.5) into competent host cells. The ORF is therefore replaced by *KanMX4/6* (or *URA3*) through homologous recombination. The transformants are selected on YPAD+G418 (or SC-Ura) plates.

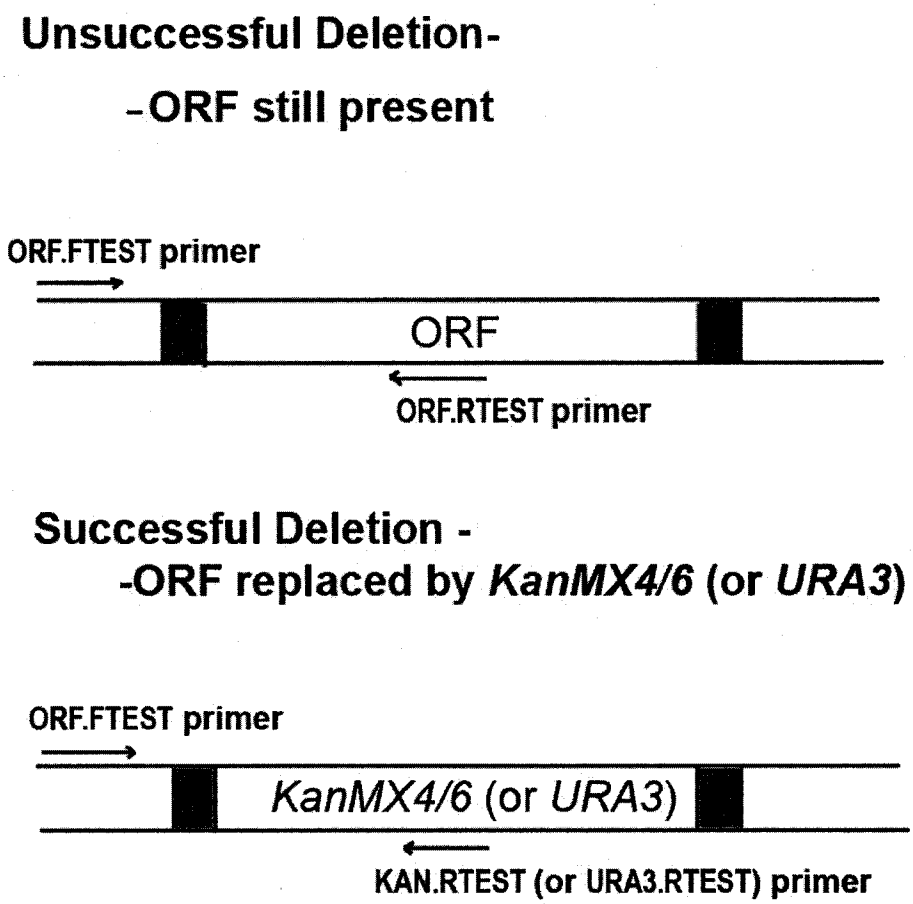


**Figure 4.2. Genomic PCR confirmation to determine whether the ORF is still present.** The ORF.FTEST primers contain 20 bases upstream of the open reading frame. The ORF.RTEST primers are 20mer homologous to the sequence on the open reading frame. Primers KAN.RTEST and URA3.RTEST contain sequence homologous to the sequence on *KanMX4/6* and *URA3* module, respectively. Genomic DNA from the transformants are extracted (Section 2.6) and used as template for PCR (Section 2.7). If the ORF is still present, PCR with ORF.FTEST and ORF.RTEST (but not KAN.RTEST/URA3.RTEST) primers will produce a specific band, vice versa for the case when ORF has been replaced by *KanMX4/6* (or *URA3*).

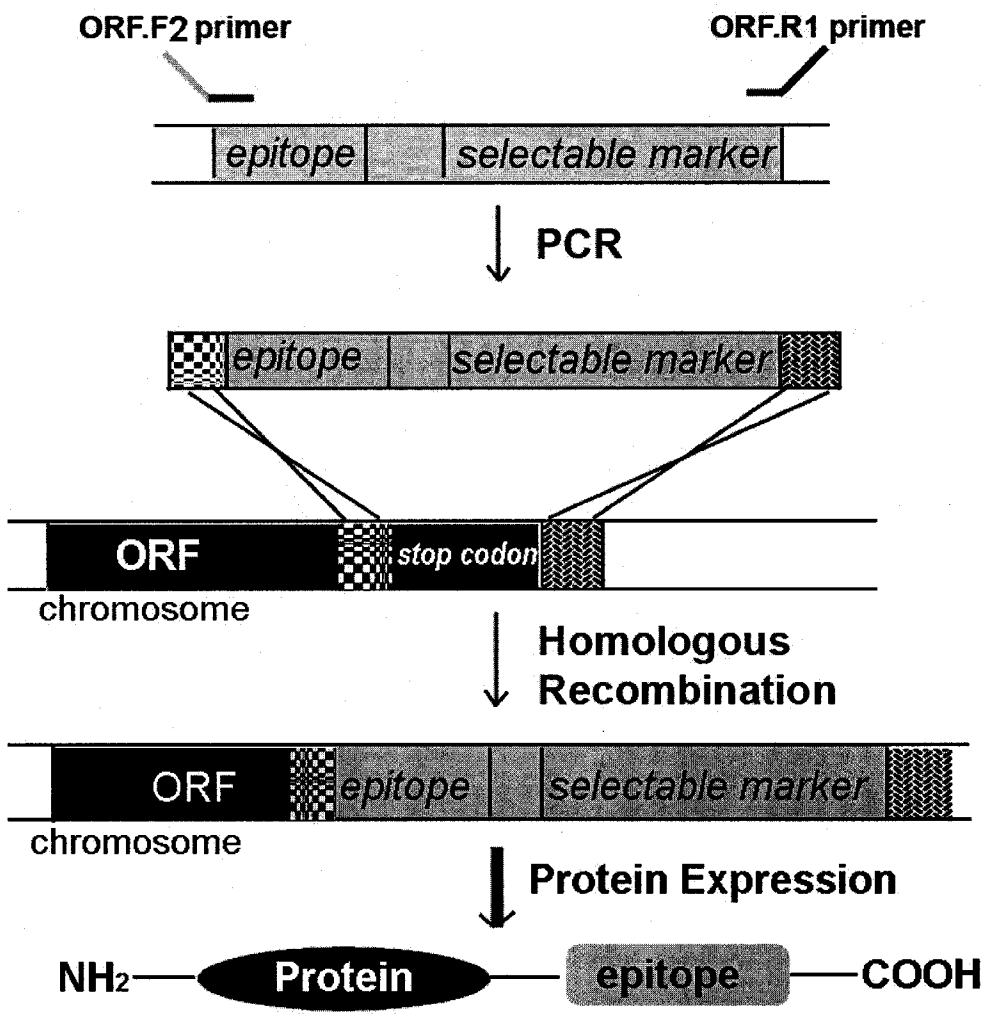


**Figure 4.3. The PCR-based strategy for tagging the ORF with an epitope.** The ORF. F2 80mer primer contains 60 bases homologous to the 3' sequence of the ORF (right before the stop codon), followed by 20 bases homologous to the 5' sequence on the epitope-selectable marker module. The 80mer LDB18.R1 primer contains 60 bases directly downstream of the ORF (right after the stop codon) followed by 20 bases homologous to the 3' sequence on the epitope-selectable marker module. The template is the DNA of a plasmid (Longtine *et al.*, 1998). PCR protocol is described in Section 2.3. Amplified DNA is concentrated and transformed into competent host cells. The ORF is therefore tagged with the epitope through homologous recombination. The transformants are selected according to the selectable marker.

Table 4.1 Strains used in this study

| Strain Name | Genotype | Origin or Source |
|---|---|---|
| BY4742 | *MATα his3Δ1 leu2Δ0 lys2Δ0 ura3Δ0* | Open Biosystems, Huntsville, AL |
| BY4741 | *MATa his3Δ1 leu2Δ0 met15Δ0 ura3Δ0* | Open Biosystems |
| Y2295 | *MATa ura3-52 lys2-801 leu2-Δ1 his3-Δ200 trp1-Δ63* | John Cooper, Washington Univesity, St Louis, MO |
| Y2296 | *MATα ura3-52 lys2-801 leu2-Δ1 his3-Δ200 trp1-Δ63* | John Cooper |
| *ldb18Δ::KanMX4* | *MATα his3Δ1 leu2Δ0 lys2Δ0 ura3Δ0 ldb18Δ::KanMX4* | Open Biosystems Yeast Knockout Strains |
| *ldb18Δ::URA3* | *MATa ura3-52 lys2-801 leu2-Δ1 his3-Δ200 trp1-Δ63 ldb18Δ::URA3* | This study (from Y2295) |
| *arp1Δ::KanMX4* | Same as BY4742 except *ARP1* deletion | Open Biosystems |
| *bik1Δ::KanMX4* | Same as BY4742 except *BIK1* deletion | Open Biosystems |
| *bim1Δ::KanMX4* | Same as BY4742 except *BIM1* deletion | Open Biosystems |
| *bni1Δ::KanMX4* | Same as BY4742 except *BNI1* deletion | Open Biosystems |
| *boi2Δ::KanMX4* | Same as BY4742 except *BOI2* deletion | Open Biosystems |
| *clb4Δ::KanMX4* | Same as BY4742 except *CLB4* deletion | Open Biosystems |
| *cpr6Δ::KanMX4* | Same as BY4742 except *CPR6* deletion | Open Biosystems |
| *dyn1Δ::KanMX4* | Same as BY4742 except *DYN1* deletion | Open Biosystems |
| *dyn2Δ::KanMX4* | Same as BY4742 except *DYN2* deletion | Open Biosystems |
| *dyn3Δ::KanMX4* | Same as BY4742 except *DYN3* deletion | Open Biosystems |
| *fab1Δ::KanMX4* | Same as BY4742 except *FAB1* deletion | Open Biosystems |
| *hcm1Δ::KanMX4* | Same as BY4742 except *HCM1* deletion | Open Biosystems |
| *mon1Δ::KanMX4* | Same as BY4742 except *MON1* deletion | Open Biosystems |
| *nbp2Δ::KanMX4* | Same as BY4742 except *NBP2* deletion | Open Biosystems |
| *smi1Δ::KanMX4* | Same as BY4742 except *SMI1* deletion | Open Biosystems |
| *vam7Δ::KanMX4* | Same as BY4742 except *VAM7* deletion | Open Biosystems |
| *vid22Δ::KanMX4* | Same as BY4742 except *VID22* deletion | Open Biosystems |
| *vps29Δ::KanMX4* | Same as BY4742 except *VPS29* deletion | Open Biosystems |
| *vps35Δ::KanMX4* | Same as BY4742 except *VPS35* deletion | Open Biosystems |
| *ARP1-TAP* | *MATa HIS3 leu2Δ0 met15Δ0 ura3Δ0 ARP1-TAP* | Open Biosystems |

| | | |
|---|---|---|
| *DYN3-TAP* | *MATa HIS3 leu2Δ0 met15Δ0 ura3Δ0 DYN3-TAP* | Open Biosystems |
| *NIP100-TAP* | *MATa HIS3 leu2Δ0 met15Δ0 ura3Δ0 NIP100-TAP* | Open Biosystems |
| *LDB18-3HA* | *MATα his3Δ1 leu2Δ0 lys2Δ0 ura3Δ0 LDB18-3HA KanMX6* | This study (from BY4742) |
| *GFP-TUB1* | *MATa ade2 ade3 ura3::GFP-TUB1 leu2 trp1 LYS2* | John Cooper |
| *ldb18Δ::KanMX6 GFP-TUB1* | *MATa ade2 ade3 ura3::GFP-TUB1 leu2 trp1 LYS2 ldb18Δ::KanMX* | This study (from *GFP-TUB1*) |
| *ARP1-TAP LDB18-3HA* | *MATa HIS3 leu2Δ0 met15Δ0 ura3Δ0 ARP1-TAP LDB18-3HA KanMX6* | This study (from *ARP1-TAP*) |
| *DYN3-TAP LDB18-3HA* | *MATa HIS3 leu2Δ0 met15Δ0 ura3Δ0 DYN3-TAP LDB18-3HA KanMX6* | This study (from *DYN3-TAP*) |
| *NIP100-TAP LDB18-3HA* | *MATa HIS3 leu2Δ0 met15Δ0 ura3Δ0 NIP100-TAP LDB18-3HA KanMX6* | This study (from *NIP100-TAP*) |
| *LDB18-GFP* | *MATa ura3-52 lys2-801 leu2-Δ1 his3-Δ200 trp1-Δ63 KanMX6 LDB18-GFP* | This study (from 2295) |
| Y2081 | *MATα sst2Δ ste3Δ* | John Cooper |
| Y2082 | *MATa bar1Δ* | John Cooper |
| *BUB2-CFP* | Same as Y2295 except *BUB2-CFP KanR* | This study |
| *BFA1-YFP* | Same as Y2296 except *BFA1-YFP HIS5* | This study |
| *CSE4-YFP* | Same as Y2296 except *CSE4-YFP HIS5* | This study |
| *BUB2-CFP BFA1-YFP* | Cross of *BUB2-CFP* and *BFA1-YFP* | This study |
| *BFA1-YFP-CFP* | Same as Y2296 except *BFA1-YFP-CFP HIS5* | This study |
| *BUB2-YFP-CFP* | Same as Y2296 except *BUB2-YFP-CFP HIS5* | This study |
| *BUB2-CFP CSE4-YFP* | Cross of *BUB2-CFP* and *CSE4-YFP* | This study |

Table 4.2 Oligos used in this study.

| Primer Name | Sequence | Comments |
|---|---|---|
| LDB18.F1 | GAACTTATAGAATGTTCT CTCGAGCTTCCAAGGCC ATTAGCCTCTACCAAAG GAAGTTTGCGGATCCCC GGGTTAATTAAG | Forward primer for *LDB18* deletion |
| LDB18.R1 | AAGTATATATATATATAT ATATATATATATATATA TATATATGTATATACGC ACACATGTGATGAATTC GAGCTCGTTTAAAC | Reverse primer for *LDB18* deletion or C-terminal epitope tagging |
| LDB18.F2 | CGGATTCTTCCAGTTCCA GAAAAAGAGGCTGTTG AATTTACAAAAGGTAA TTTATAGTACGCGGATC CCCGGGTTAATTAAG | Forward primer for *LDB18* C-terminal epitope tagging |
| LDB18.FTEST | TGTCTGGAGACCAAGTGA AG | Forward primer for testing *LDB18* deletion (704 bps upstream of Ldb18) |
| LDB18.RTEST | TCTGGAACTGGAAGAATC CG | Reverse primer for testing *LDB18* deletion (492bps after start codon on Ldb18 sequence) |
| KAN.RTEST | CGATTGTATGGGAAGCCC G | Reverse primer for testing *KanMX* module (600bps after start codon) |
| LDB18.TAGTE ST | ATGGCTGAAGACATCGAG A | Forward primer for testing C-terminal epitope tag of *LDB18* (348bps before stop codon) |
| LDB18-3CFP.F | CCAGggatccCCTGGTCTTA AGCTTGTTGAA | Forward primer for integration of *LDB18* sequence onto the 3CFP vector plasmid (adding a *BamH* I restriction site) |
| LDB18-3CFP.R | CCAGggatccAGCACCAGCA CCAGCACCCGTACTATA AATTACCTTTTGTAA | Reverse primer for integration of *LDB18* sequence onto the 3CFP vector plasmid (adding a *BamH* I restriction site) |

| | | |
|---|---|---|
| GFP.RTEST | CATCACCATCTAATTCAAC | Reverse primer for testing C-terminal GFP (or CFP, YFP) tagging |
| URA3.RTEST | 5'CGCAATGTCAACAGTACCCTT-3' | Reverse primer for testing *URA3* module (495bps after start codon) |
| ARP1.TAGTEST | TTGTTCGCACGATGAAAGAG | Forward primer for testing C-terminal epitope tag of Arp1 (503bps before stop codon) |
| DYN3.TAGTEST | CCAAAAGTTGTGGCTGAATG | Forward primer for testing C-terminal epitope tag of Dyn3 (592bps before stop codon) |
| NIP100.TAGTEST | TGAGGAAAATTGTGGCAAAAC | Forward primer for testing C-terminal epitope tag of Nip100 (493bps before stop codon) |
| F2CHK | AACCCGGGGATCCGTCGACC | Reverse primer for testing C-terminal TAP tagging |
| ARP1.FTEST | CATCAGGAATTAGCAAGGGC | Forward primer for testing *ARP1* deletion |
| ARP1.RTEST | CTGCTCTGTGATATCTGCTC | Reverse primer for testing *ARP1* deletion |
| BIK1.FTEST | GCAGTAAAAGAACCTTGACC | Forward primer for testing *BIK1* deletion |
| BIK1.RTEST | TCATTCATGTGGCCATTGTC | Reverse primer for testing *BIK1* deletion |
| BIM1.FTEST | TACCGGTCAATCTGCTGATG | Forward primer for testing *BIM1* deletion |
| BIM1.RTEST | GCTTGTATCGCTACCAACTG | Reverse primer for testing *BIM1* deletion |
| BNI1.FTEST | ACTCCATACCACACACACAC | Forward primer for testing *BNI1* deletion |
| BNI1.RTEST | GAGGCAGTGGAAGAAGATGT | Reverse primer for testing *BNI1* deletion |
| DYN1.FTEST | GCGAATGGAGTAGGCAATCT | Forward primer for testing *DYN1* deletion |
| DYN1.RTEST | GACGATACGCCATGTGTGAT | Reverse primer for testing *DYN1* deletion |
| DYN2.FTEST | GAGAAGAGAATGCTTGGATGG | Forward primer for testing *DYN2* deletion |
| DYN2.RTEST | ATCCTCTTTCAGCTTGTCGGTC | Reverse primer for testing *DYN2* deletion |
| DYN3.FTEST | CCAGCCATTCGTTACAACCAT | Forward primer for testing *DYN3* deletion |

| | | |
|---|---|---|
| DYN3.RTEST | ACTGCCATACTGTAGTGT GTC | Reverse primer for testing *DYN3* deletion |
| JNM1.FTEST | ATCTTGACAACCGTCCAT AGG | Forward primer for testing *JNM1* deletion |
| JNM1.RTEST | GTTTCGAGAAGCTTCTTC CTC | Reverse primer for testing *JNM1* deletion |
| KAR9.FTEST | GTAAGGAGCATGATGACC AG | Forward primer for testing *KAR9* deletion |
| KAR9.RTEST | CAGTTGTCTCCGTATGCG TT | Reverse primer for testing *KAR9* deletion |
| NIP100.FTEST | CATTACTACTACTCTGTC GCC | Forward primer for testing *NIP100* deletion |
| NIP100.RTEST | TGTTTCTTGCGCTGCATTA CC | Reverse primer for testing *NIP100* deletion |
| NUM1.FTEST | TAAGGATTTGGCAGCTGC AGT | Forward primer for testing *NUM1* deletion |
| NUM1.RTEST | AGTGAGCTCCTCAATCTT GTC | Reverse primer for testing *NUM1* deletion |
| PAC1.FTEST | AAACCATTCAGGTCTTGC GTG | Forward primer for testing *PAC1* deletion |
| PAC1.RTEST | GTAGTTTGACGGAAGTGA CAG | Reverse primer for testing *PAC1* deletion |
| PAC11.FTEST | GCATATCGAGGAATCCCA TTG | Forward primer for testing *PAC11* deletion |
| PAC11.RTEST | ATCCTGTTGCATGTTCGA TGG | Reverse primer for testing *PAC11* deletion |
| BOI2.FTEST | AGATTTGAGAGGTACCAG GTG | Forward primer for testing *BOI2* deletion |
| BOI2.RTEST | CAGTAGTGCATTGTCTAT GTC | Reverse primer for testing *BOI2* deletion |
| CLB4.FTEST | TCGCAGGCTTGATATTTC GC | Forward primer for testing *CLB4* deletion |
| CLB4.RTEST | CATCACAACATCATGGGT ATC | Reverse primer for testing *CLB4* deletion |
| CPR6.FTEST | AAGGTAGTGAAAGGCACT TC | Forward primer for testing *CPR6* deletion |
| CPR6.RTEST | ATAGCTTTCAAGACGGTG TCG | Reverse primer for testing *CPR6* deletion |
| FAB1.FTEST | GTCATTGTACTCTTTCGTG C | Forward primer for testing *FAB1* deletion |
| FAB1.RTEST | ATCGAAGACACTTCATCG CC | Reverse primer for testing *FAB1* deletion |
| HCM1.FTEST | CATCTCCAAAGACCTTTA CG | Forward primer for testing *HCM1* deletion |

| | | |
|---|---|---|
| HCM1.RTEST | AGATCATCATTGCCTTCT CC | Reverse primer for testing *HCM1* deletion |
| MON1.FTEST | GGTATCAAGCAGTAAGGA AG | Forward primer for testing *MON1* deletion |
| MON1.RTEST | TTGCCGTGCATGCAATAG ATC | Reverse primer for testing *MON1* deletion |
| NBP2.FTEST | ATCGCCTAGACGAATTTC CTC | Forward primer for testing *NBP2* deletion |
| NBP2.RTEST | ATTCTCCACCTCGTTCTCA C | Reverse primer for testing *NBP2* deletion |
| SMI1.FTEST | TAACATGCATTGCACCAC CG | Forward primer for testing *SMI1* deletion |
| SMI1.RTEST | AGGAATCCAAGCAGGAT GTG | Reverse primer for testing *SMI1* deletion |
| VAM7.FTEST | TTGACTTGGAGTCATAGG CG | Forward primer for testing *VAM7* deletion |
| VAM7.RTEST | ATCCTGTTCTAGTCGCTCT C | Reverse primer for testing *VAM7* deletion |
| VID22.FTEST | GTGAAATGGAACGTGAA GGTG | Forward primer for testing *VID22* deletion |
| VID22.RTEST | GTGAGTTGGCGTTCTGAT TG | Reverse primer for testing *VID22* deletion |
| VPS29.FTEST | GTTGAGGAATTAGGAATA CCG | Forward primer for testing *VPS29* deletion |
| VPS29.RTEST | GTACAGCTACCTGGATTA AC | Reverse primer for testing *VPS29* deletion |
| VPS35.FTEST | TGGACGAGTATTACAGTG AG | Forward primer for testing *VPS35* deletion |
| VPS35.RTEST | AGACGTACTAGTTGAGAC C | Reverse primer for testing *VPS35* deletion |
| BUB2.F2 | CCTGCTCAAATTTATGAC CTATTGGTAGACCACTT GACCGACCCAGACATA TATATACCGCGGATCCC CGGGTTAATTAA | Forward primer for *BUB2* C-terminal epitope tagging |
| BUB2.R1 | ATACAGACATATAAACGT TGTAGAATTAAACGAT AAAATATAATATTTCTT CACATAGTGATGAATTC GAGCTCGTTTAAAC | Reverse primer for *BUB2* deletion or C-terminal epitope tagging |
| BFA1.F2 | AGCAAGAGAAAATCCTAT ATGTATGAAATCAGGA ACATGGTAATCAATTCG ACAAAAGATCGGATCC CCGGGTTAATTAA | Forward primer for *BFA1* C-terminal epitope tagging |

| | | |
|---|---|---|
| BFA1.R1 | TTCTATCTAATTTTGGAATGTAAGAGAAATGAATGTACTCAAGATAACGGTAAAGAAACAGAATTCGAGCTCGTTTAAAC | Reverse primer for *BFA1* deletion or C-terminal epitope tagging |
| CSE4.F2 | AGAATTACTATAATGAAGAAAGACATGCAACTAGCAAGAAGAATCAGGGGACAGTTTATTGGTCGACGGATCCCCGGG | Forward primer for *CSE4*-terminal epitope tagging |
| CSE4.R1 | TATGCTAATATGACCTTATAATAACCTTATTTAAAACATTTAAAGTACCTTAAGTCAATAATCGATGAATTCGAGCTCG | Reverse primer for *CSE4* deletion or C-terminal epitope tagging |
| BUB2.TAGTEST | TCCTCACTCTCTCAACTTCGCTACC | Forward primer for testing C-terminal epitope tag of Bub2 |
| BFA1.TAGTEST | ACGCAGGACACAATTTTGGCG | Forward primer for testing C-terminal epitope tag of Bfa1 |
| CSE4.TAGTEST | GTGCGAACTCATTCATATGCC | Forward primer for testing C-terminal epitope tag of Cse4 |
| HIS5.RTEST | CGCTTCTAGAAAGAGCTTCGT | Reverse primer for testing *HIS5* module |

Table 4.3 Plasmids used in this study

| Name | Comments | Origin or Source |
|---|---|---|
| 4339 | *URA3* module for making deletion strains | Charles Boone, University of Toronto, ON |
| pFA6a-kanMX6 | for making deletion strains | Mark Longtine, University of North Carolina, NC (Longtine *et al.*, 1998) |
| pFA6a-3HA-KanMX6 | for 3HA tagging | Mark Longtine |
| pFA6a-GFP(S65T)-KanMX6 | for GFP tagging | Mark Longtine |
| p1523 | *3CFP-URA* module | John Cooper, Washington Univerisy, St Louis, MO |
| p1523-LDB18 | Truncated *LDB18* sequenc inserted onto p1523, to make LDB18-3CFP fusion | This study |
| pDH3 | *CFP-KANR* module | Yeast Resource Center, University of Washington, Seattle, WA |
| pDH5 | *YFP-HIS5* module | Yeast Resource Center |
| pDH18 | *YFP-CFP-HIS5* module | Yeast Resource Center |

# 5. References


Adames, N.R., and J.A. Cooper. 2000. Microtubule interactions with the cell cortex causing nuclear movements in *Saccharomyces cerevisiae*. *J Cell Biol.* 149:863-74.

Adames, N.R., J.R. Oberle, and J.A. Cooper. 2001. The surveillance mechanism of the spindle position checkpoint in yeast. *J Cell Biol.* 153:159-68.

Ahmad, F.J., C.J. Echeverri, R.B. Vallee, and P.W. Baas. 1998. Cytoplasmic dynein and dynactin are required for the transport of microtubules into the axon. *J Cell Biol.* 140:391-401.

Amberg, D.C., J.E. Zahner, J.W. Mulholland, J.R. Pringle, and D. Botstein. 1997. Aip3p/Bud6p, a yeast actin-interacting protein that is involved in morphogenesis and the selection of bipolar budding sites. *Mol Biol Cell.* 8:729-53.

Andrews, B., and V. Measday. 1998. The cyclin family of budding yeast: abundant use of a good idea. *Trends Genet.* 14:66-72.

Asakawa, K., S. Yoshida, F. Otake, and A. Toh-e. 2001. A novel functional domain of Cdc15 kinase is required for its interaction with Tem1 GTPase in *Saccharomyces cerevisiae*. *Genetics.* 157:1437-50.

Askham, J.M., K.T. Vaughan, H.V. Goodson, and E.E. Morrison. 2002. Evidence that an interaction between EB1 and p150(*Glued*) is required for the formation and maintenance of a radial microtubule array anchored at the centrosome. *Mol Biol Cell.* 13:3627-45.

Ayscough, K.R., J. Stryker, N. Pokala, M. Sanders, P. Crews, and D.G. Drubin. 1997. High rates of actin filament turnover in budding yeast and roles for actin in establishment and maintenance of cell polarity revealed using the actin inhibitor latrunculin-A. *J Cell Biol.* 137:399-416.

Baker, D.J., J. Chen, and J.M. van Deursen. 2005. The mitotic checkpoint in cancer and aging: what have mice taught us? *Curr Opin Cell Biol.* 17:583-9.

Bardin, A.J., and A. Amon. 2001. Men and sin: what's the difference? *Nat Rev Mol Cell Biol.* 2:815-26.

Bardin, A.J., R. Visintin, and A. Amon. 2000. A mechanism for coupling exit from mitosis to partitioning of the nucleus. *Cell.* 102:21-31.

Barton, N.R., and L.S. Goldstein. 1996. Going mobile: microtubule motors and chromosome segregation. *Proc Natl Acad Sci U S A.* 93:1735-42.

Beach, D.L., J. Thibodeaux, P. Maddox, E. Yeh, and K. Bloom. 2000. The role of the proteins Kar9 and Myo2 in orienting the mitotic spindle of budding yeast. *Curr Biol.* 10:1497-506.

Beaudouin, J., D. Gerlich, N. Daigle, R. Eils, and J. Ellenberg. 2002. Nuclear envelope breakdown proceeds by microtubule-induced tearing of the lamina. *Cell.* 108:83-96.

Berlin, V., C.A. Styles, and G.R. Fink. 1990. BIK1, a protein required for microtubule function during mating and mitosis in *Saccharomyces cerevisiae*, colocalizes with tubulin. *J Cell Biol.* 111:2573-86.

Berrueta, L., J.S. Tirnauer, S.C. Schuyler, D. Pellman, and B.E. Bierer. 1999. The APC-associated protein EB1 associates with components of the dynactin complex and cytoplasmic dynein intermediate chain. *Curr Biol.* 9:425-8.

Bingham, J.B., S.J. King, and T.A. Schroer. 1998. Purification of dynactin and dynein from brain tissue. *Methods Enzymol.* 298:171-84.

Bingham, J.B., and T.A. Schroer. 1999. Self-regulated polymerization of the actin-related protein Arp1. *Curr Biol.* 9:223-6.

Bloom, G.S., T.A. Schoenfeld, and R.B. Vallee. 1984. Widespread distribution of the major polypeptide component of MAP 1 (microtubule-associated protein 1) in the nervous system. *J Cell Biol.* 98:320-30.

Bloom, K. 2000. It's a kar9ochore to capture microtubules. *Nat Cell Biol.* 2:E96-8.

Bloom, K. 2001. Nuclear migration: cortical anchors for cytoplasmic dynein. *Curr Biol.* 11:R326-9.

Bosl, W.J., and R. Li. 2005. Mitotic-exit control as an evolved complex system. *Cell.* 121:325-33.

Brandon, N.J., E.J. Handford, I. Schurov, J.C. Rain, M. Pelling, B. Duran-Jimeniz, L.M. Camargo, K.R. Oliver, D. Beher, M.S. Shearman, and P.J. Whiting. 2004. Disrupted in Schizophrenia 1 and Nudel form a neurodevelopmentally regulated protein complex: implications for schizophrenia and other major neurological disorders. *Mol Cell Neurosci.* 25:42-55.

Brodsky L.I., A.V. Vasiliev, L. Kalaidzidis Ya., S. Osipov Yu., R.L.Tatuzov, S. I. Feranchuk 1992. GeneBee: the program package for biopolymer structure analysis *Dimacs* 8:127-139.

Brodsky L.I., V.V. Ivanov, L. Kalai dzidis Ya., A.M. Leontovich, V.K. Nikolaev, S. I. Feranchuk, V.A.Drachev 1995. GeneBee-NET:Internet-based server for analyzing biopolymers structure. *Biochemistry* 60: 923-928.

Bu, W., and L.K. Su. 2003. Characterization of functional domains of human EB1 family proteins. *J Biol Chem.* 278:49721-31.

Burkhardt, J.K., C.J. Echeverri, T. Nilsson, and R.B. Vallee. 1997. Overexpression of the dynamitin (p50) subunit of the dynactin complex disrupts dynein-dependent maintenance of membrane organelle distribution. *J Cell Biol.* 139:469-84.

Campbell, K.S., S. Cooper, M. Dessing, S. Yates, and A. Buder. 1998. Interaction of p59fyn kinase with the dynein light chain, Tctex-1, and colocalization during cytokinesis. *J Immunol.* 161:1728-37.

Carminati, J.L., and T. Stearns. 1997. Microtubules orient the mitotic spindle in yeast through dynein-dependent interactions with the cell cortex. *J Cell Biol.* 138:629-41.

Carminati, J.L., and T. Stearns. 1999. Cytoskeletal dynamics in yeast. *Methods Cell Biol.* 58:87-105.

Carvalho, P., M.L. Gupta, Jr., M.A. Hoyt, and D. Pellman. 2004. Cell cycle control of kinesin-mediated transport of Bik1 (CLIP-170) regulates microtubule stability and dynein activation. *Dev Cell.* 6:815-29.

Casamayor, A., and M. Snyder. 2002. Bud-site selection and cell polarity in budding yeast. *Curr Opin Microbiol.* 5:179-86.

Castillon, G.A., N.R. Adames, C.H. Rosello, H.S. Seidel, M.S. Longtine, J.A. Cooper, and R.A. Heil-Chapdelaine. 2003. Septins have a dual role in controlling mitotic exit in budding yeast. *Curr Biol.* 13:654-8.

Cau, J., and A. Hall. 2005. Cdc42 controls the polarity of the actin and microtubule cytoskeletons through two distinct signal transduction pathways. *J Cell Sci.* 118:2579-87.

Chumakov K.M. and S.V. Yushmanov 1998. The maximum topological similarity principle in molecular systematics, *Mol. Genet. Microbiol. Virusol.* 3: 3-9, Russian.

Cid, V.J., L. Adamikova, M. Sanchez, M. Molina, and C. Nombela. 2001. Cell cycle control of septin ring dynamics in the budding yeast. *Microbiology.* 147:1437-50.

Clamp, M., J. Cuff, S.M. Searle, and G.J. Barton. 2004. The Jalview Java alignment editor. *Bioinformatics.* 20:426-7.

Clark, S.W., and D.I. Meyer. 1992. Centractin is an actin homologue associated with the centrosome. *Nature.* 359:246-50.

Clark, S.W., and D.I. Meyer. 1994. ACT3: a putative centractin homologue in *S. cerevisiae* is required for proper orientation of the mitotic spindle. *J Cell Biol.* 127:129-38.

Collins, C.A., and R.B. Vallee. 1989. Preparation of microtubules from rat liver and testis: cytoplasmic dynein is a major microtubule associated protein. *Cell Motil Cytoskeleton.* 14:491-500.

Corbacho, I., I. Olivero, and L.M. Hernandez. 2005. A genome-wide screen for *Saccharomyces cerevisiae* nonessential genes involved in mannosyl phosphate transfer to mannoprotein-linked oligosaccharides. *Fungal Genet Biol.* 42:773-90.

Cottingham, F.R., and M.A. Hoyt. 1997. Mitotic spindle positioning in *Saccharomyces cerevisiae* is accomplished by antagonistically acting microtubule motor proteins. *J Cell Biol.* 138:1041-53.

Cuff, J.A., and G.J. Barton. 1999. Evaluation and improvement of multiple sequence methods for protein secondary structure prediction. *Proteins.* 34:508-19.

D'Amours, D., and A. Amon. 2004. At the interface between signaling and executing anaphase--Cdc14 and the FEAR network. *Genes Dev.* 18:2581-95.

Damelin, M., and T.H. Bestor. 2007. The decatenation checkpoint. *Br J Cancer.* 96:201-5.

De Clercq, A., and D. Inze. 2006. Cyclin-dependent kinase inhibitors in yeast, animals, and plants: a functional comparison. *Crit Rev Biochem Mol Biol.* 41:293-313.

den Hollander, P., and R. Kumar. 2006. Dynein light chain 1 contributes to cell cycle progression by increasing cyclin-dependent kinase 2 activity in estrogen-stimulated cells. *Cancer Res.* 66:5941-9.

DeZwaan, T.M., E. Ellingson, D. Pellman, and D.M. Roof. 1997. Kinesin-related KIP3 of *Saccharomyces cerevisiae* is required for a distinct step in nuclear migration. *J Cell Biol.* 138:1023-40.

Dick, T., U. Surana, and W. Chia. 1996. Molecular and genetic characterization of SLC1, a putative *Saccharomyces cerevisiae* homolog of the metazoan cytoplasmic dynein light chain 1. *Mol Gen Genet.* 251:38-43.

Dillman, J.F., 3rd, and K.K. Pfister. 1994. Differential phosphorylation in vivo of cytoplasmic dynein associated with anterogradely moving organelles. *J Cell Biol.* 127:1671-81.

Dohner, K., A. Wolfstein, U. Prank, C. Echeverri, D. Dujardin, R. Vallee, and B. Sodeik. 2002. Function of dynein and dynactin in herpes simplex virus capsid transport. *Mol Biol Cell.* 13:2795-809.

Dujardin, D.L., and R.B. Vallee. 2002. Dynein at the cortex. *Curr Opin Cell Biol.* 14:44-9.

Dunphy, W.G. 1994. The decision to enter mitosis. *Trends Cell Biol.* 4:202-7.

Echeverri, C.J., B.M. Paschal, K.T. Vaughan, and R.B. Vallee. 1996. Molecular characterization of the 50-kD subunit of dynactin reveals function for the complex in chromosome alignment and spindle organization during mitosis. *J Cell Biol.* 132:617-33.

Eckley, D.M., S.R. Gill, K.A. Melkonian, J.B. Bingham, H.V. Goodson, J.E. Heuser, and T.A. Schroer. 1999. Analysis of dynactin subcomplexes reveals a novel actin-related protein associated with the Arp1 minifilament pointed end. *J Cell Biol.* 147:307-20.

Engelender, S., A.H. Sharp, V. Colomer, M.K. Tokito, A. Lanahan, P. Worley, E.L. Holzbaur, and C.A. Ross. 1997. Huntingtin-associated protein 1 (HAP1) interacts with the p150Glued subunit of dynactin. *Hum Mol Genet.* 6:2205-12.

Eshel, D., L.A. Urrestarazu, S. Vissers, J.C. Jauniaux, J.C. van Vliet-Reedijk, R.J. Planta, and I.R. Gibbons. 1993. Cytoplasmic dynein is required for normal nuclear segregation in yeast. *Proc Natl Acad Sci U S A.* 90:11172-6.

Evangelista, M., K. Blundell, M.S. Longtine, C.J. Chow, N. Adames, J.R. Pringle, M. Peter, and C. Boone. 1997. Bni1p, a yeast formin linking Cdc42p and the actin cytoskeleton during polarized morphogenesis. *Science.* 276:118-22.

Farkasovsky, M., and H. Kuntzel. 1995. Yeast Num1p associates with the mother cell cortex during S/G2 phase and affects microtubular functions. *J Cell Biol.* 131:1003-14.

Fink, G., I. Schuchardt, J. Colombelli, E. Stelzer, and G. Steinberg. 2006. Dynein-mediated pulling forces drive rapid mitotic spindle elongation in *Ustilago maydis*. *Embo J.* 25:4897-908.

Fisk, H.A., and M.P. Yaffe. 1997. Mutational analysis of Mdm1p function in nuclear and mitochondrial inheritance. *J Cell Biol.* 138:485-94.

Frenz, L.M., S.E. Lee, D. Fesquet, and L.H. Johnston. 2000. The budding yeast Dbf2 protein kinase localises to the centrosome and moves to the bud neck in late mitosis. *J Cell Sci.* 113 Pt 19:3399-408.

Fujiwara, T., K. Tanaka, E. Inoue, M. Kikyo, and Y. Takai. 1999. Bni1p regulates microtubule-dependent nuclear migration through the actin cytoskeleton in *Saccharomyces cerevisiae*. *Mol Cell Biol.* 19:8016-27.

Gadde, S., and R. Heald. 2004. Mechanisms and molecules of the mitotic spindle. *Curr Biol.* 14:R797-805.

Galigniana, M.D., J.M. Harrell, H.M. O'Hagen, M. Ljungman, and W.B. Pratt. 2004. Hsp90-binding immunophilins link p53 to dynein during p53 transport to the nucleus. *J Biol Chem.* 279:22483-9.

Garces, J.A., I.B. Clark, D.I. Meyer, and R.B. Vallee. 1999. Interaction of the p62 subunit of dynactin with Arp1 and the cortical actin cytoskeleton. *Curr Biol.* 9:1497-500.

Garnjobst, L., and E.L. Tatum. 1967. A survey of new morphological mutants in *Neurospora crassa*. *Genetics.* 57:579-604.

Gee, M.A., J.E. Heuser, and R.B. Vallee. 1997. An extended microtubule-binding structure within the dynein motor domain. *Nature*. 390:636-9.

Geiser, J.R., E.J. Schott, T.J. Kingsbury, N.B. Cole, L.J. Totis, G. Bhattacharyya, L. He, and M.A. Hoyt. 1997. *Saccharomyces cerevisiae* genes required in the absence of the CIN8-encoded spindle motor act in functionally diverse mitotic pathways. *Mol Biol Cell*. 8:1035-50.

Gepner, J., M. Li, S. Ludmann, C. Kortas, K. Boylan, S.J. Iyadurai, M. McGrail, and T.S. Hays. 1996. Cytoplasmic dynein function is essential in *Drosophila melanogaster*. *Genetics*. 142:865-78.

Geymonat, M., A. Spanos, S.J. Smith, E. Wheatley, K. Rittinger, L.H. Johnston, and S.G. Sedgwick. 2002. Control of mitotic exit in budding yeast. *In vitro* regulation of Tem1 GTPase by Bub2 and Bfa1. *J Biol Chem*. 277:28439-45.

Ghaemmaghami, S., W.K. Huh, K. Bower, R.W. Howson, A. Belle, N. Dephoure, E.K. O'Shea, and J.S. Weissman. 2003. Global analysis of protein expression in yeast. *Nature*. 425:737-41.

Giansanti, M.G., S. Bonaccorsi, B. Williams, E.V. Williams, C. Santolamazza, M.L. Goldberg, and M. Gatti. 1998. Cooperative interactions between the central spindle and the contractile ring during *Drosophila* cytokinesis. *Genes Dev*. 12:396-410.

Gibbons, B.H., and I.R. Gibbons. 1987. Vanadate-sensitized cleavage of dynein heavy chains by 365-nm irradiation of demembranated sperm flagella and its effect on the flagellar motility. *J Biol Chem*. 262:8354-9.

Gibbons, I.R., and A. Rowe. 1965. Dynein: a protein with adenosine triphosphatase activity from cilia. *Science* 149: 424-426

Gietz, R.D., and R.A. Woods. 2002. Transformation of yeast by lithium acetate/single-stranded carrier DNA/polyethylene glycol method. *Methods Enzymol*. 350:87-96.

Gill, S.R., T.A. Schroer, I. Szilak, E.R. Steuer, M.P. Sheetz, and D.W. Cleveland. 1991. Dynactin, a conserved, ubiquitously expressed component of an activator of vesicle motility mediated by cytoplasmic dynein. *J Cell Biol*. 115:1639-50.

Gladfelter, A.S., L. Kozubowski, T.R. Zyla, and D.J. Lew. 2005. Interplay between septin organization, cell cycle and cell shape in yeast. *J Cell Sci*. 118:1617-28.

Gladfelter, A.S., J.R. Pringle, and D.J. Lew. 2001. The septin cortex at the yeast mother-bud neck. *Curr Opin Microbiol*. 4:681-9.

Gonczy, P. 2002. Nuclear envelope: torn apart at mitosis. *Curr Biol*. 12:R242-4.

Goodenough, U.W., and J.E. Heuser. 1985. Substructure of inner dynein arms, radial spokes, and the central pair/projection complex of cilia and flagella. *J Cell Biol*. 100:2008-18.

Goshima, G., and M. Yanagida. 2000. Establishing biorientation occurs with precocious separation of the sister kinetochores, but not the arms, in the early spindle of budding yeast. *Cell*. 100:619-33.

Grava, S., F. Schaerer, M. Faty, P. Philippsen, and Y. Barral. 2006. Asymmetric recruitment of dynein to spindle poles and microtubules promotes proper spindle orientation in yeast. *Dev Cell*. 10:425-39.

Gruneberg, U., K. Campbell, C. Simpson, J. Grindlay, and E. Schiebel. 2000. Nud1p links astral microtubule organization and the control of exit from mitosis. *Embo J*. 19:6475-88.

Guignot, J., E. Caron, C. Beuzon, C. Bucci, J. Kagan, C. Roy, and D.W. Holden. 2004. Microtubule motors control membrane dynamics of *Salmonella*-containing vacuoles. *J Cell Sci.* 117:1033-45.

Gulli, M.P., M. Jaquenoud, Y. Shimada, G. Niederhauser, P. Wiget, and M. Peter. 2000. Phosphorylation of the Cdc42 exchange factor Cdc24 by the PAK-like kinase Cla4 may regulate polarized growth in yeast. *Mol Cell.* 6:1155-67.

Gupta, M.L., Jr., P. Carvalho, D.M. Roof, and D. Pellman. 2006. Plus end-specific depolymerase activity of Kip3, a kinesin-8 protein, explains its role in positioning the yeast mitotic spindle. *Nat Cell Biol.* 8:913-23.

Harada, A., Y. Takei, Y. Kanai, Y. Tanaka, S. Nonaka, and N. Hirokawa. 1998. Golgi vesiculation and lysosome dispersion in cells lacking cytoplasmic dynein. *J Cell Biol.* 141:51-9.

Harte, P.J., and D.R. Kankel. 1982. Genetic analysis of mutations at the *Glued* locus and interacting loci in *Drosophila melanogaster. Genetics.* 101:477-501.

He, X., S. Asthana, and P.K. Sorger. 2000. Transient sister chromatid separation and elastic deformation of chromosomes during mitosis in budding yeast. *Cell.* 101:763-75.

Heald, R., R. Tournebize, A. Habermann, E. Karsenti, and A. Hyman. 1997. Spindle assembly in *Xenopus* egg extracts: respective roles of centrosomes and microtubule self-organization. *J Cell Biol.* 138:615-28.

Heil-Chapdelaine, R.A., J.R. Oberle, and J.A. Cooper. 2000. The cortical protein Num1p is essential for dynein-dependent interactions of microtubules with the cortex. *J Cell Biol.* 151:1337-44.

Heil-Chapdelaine, R.A., N.K. Tran, and J.A. Cooper. 2000. Dynein-dependent movements of the mitotic spindle in *Saccharomyces cerevisiae* Do not require filamentous actin. *Mol Biol Cell.* 11:863-72.

Hirokawa, N., Y. Noda, and Y. Okada. 1998. Kinesin and dynein superfamily proteins in organelle transport and cell division. *Curr Opin Cell Biol.* 10:60-73.

Ho, Y., A. Gruhler, A. Heilbut, G.D. Bader, L. Moore, S.L. Adams, A. Millar, P. Taylor, K. Bennett, K. Boutilier, L. Yang, C. Wolting, I. Donaldson, S. Schandorff, J. Shewnarane, M. Vo, J. Taggart, M. Goudreault, B. Muskat, C. Alfarano, D. Dewar, Z. Lin, K. Michalickova, A.R. Willems, H. Sassi, P.A. Nielsen, K.J. Rasmussen, J.R. Andersen, L.E. Johansen, L.H. Hansen, H. Jespersen, A. Podtelejnikov, E. Nielsen, J. Crawford, V. Poulsen, B.D. Sorensen, J. Matthiesen, R.C. Hendrickson, F. Gleeson, T. Pawson, M.F. Moran, D. Durocher, M. Mann, C.W. Hogue, D. Figeys, and M. Tyers. 2002. Systematic identification of protein complexes in *Saccharomyces cerevisiae* by mass spectrometry. *Nature.* 415:180-3.

Holleran, E.A., L.A. Ligon, M. Tokito, M.C. Stankewich, J.S. Morrow, and E.L. Holzbaur. 2001. beta III spectrin binds to the Arp1 subunit of dynactin. *J Biol Chem.* 276:36598-605.

Holleran, E.A., M.K. Tokito, S. Karki, and E.L. Holzbaur. 1996. Centractin (ARP1) associates with spectrin revealing a potential mechanism to link dynactin to intracellular organelles. *J Cell Biol.* 135:1815-29.

Holy, T.E., and S. Leibler. 1994. Dynamic instability of microtubules as an efficient way to search in space. *Proc Natl Acad Sci U S A.* 91:5682-5.

Holzbaur, E.L., J.A. Hammarback, B.M. Paschal, N.G. Kravit, K.K. Pfister, and R.B. Vallee. 1991. Homology of a 150K cytoplasmic dynein-associated polypeptide with the *Drosophila* gene *Glued*. *Nature*. 351:579-83.

Holzbaur, E.L., and R.B. Vallee. 1994. DYNEINS: molecular structure and cellular function. *Annu Rev Cell Biol*. 10:339-72.

Hoogenraad, C.C., A. Akhmanova, S.A. Howell, B.R. Dortland, C.I. De Zeeuw, R. Willemsen, P. Visser, F. Grosveld, and N. Galjart. 2001. Mammalian Golgi-associated Bicaudal-D2 functions in the dynein-dynactin pathway by interacting with these complexes. *Embo J*. 20:4041-54.

Hoyt, M.A., L. He, K.K. Loo, and W.S. Saunders. 1992. Two *Saccharomyces cerevisiae* kinesin-related gene products required for mitotic spindle assembly. *J Cell Biol*. 118:109-20.

Hoyt, M.A., L. He, L. Totis, and W.S. Saunders. 1993. Loss of function of *Saccharomyces cerevisiae* kinesin-related *CIN8* and *KIP1* is suppressed by *KAR3* motor domain mutations. *Genetics*. 135:35-44.

Huffaker, T.C., J.H. Thomas, and D. Botstein. 1988. Diverse effects of beta-tubulin mutations on microtubule formation and function. *J Cell Biol*. 106:1997-2010.

Hughes, S.M., K.T. Vaughan, J.S. Herskovits, and R.B. Vallee. 1995. Molecular analysis of a cytoplasmic dynein light intermediate chain reveals homology to a family of ATPases. *J Cell Sci*. 108 ( Pt 1):17-24.

Huisman, S.M., and M. Segal. 2005. Cortical capture of microtubules and spindle polarity in budding yeast - where's the catch? *J Cell Sci*. 118:463-71.

Hwa Lim, H., F.M. Yeong, and U. Surana. 2003. Inactivation of mitotic kinase triggers translocation of MEN components to mother-daughter neck in yeast. *Mol Biol Cell*. 14:4734-43.

Hwang, E., J. Kusch, Y. Barral, and T.C. Huffaker. 2003. Spindle orientation in *Saccharomyces cerevisiae* depends on the transport of microtubule ends along polarized actin cables. *J Cell Biol*. 161:483-8.

Inoue, S., and E.D. Salmon. 1995. Force generation by microtubule assembly/disassembly in mitosis and related movements. *Mol Biol Cell*. 6:1619-40.

Ito, T., T. Chiba, and M. Yoshida. 2001. Exploring the protein interactome using comprehensive two-hybrid projects. *Trends Biotechnol*.19:S23-7.

Iushmanov, S.V., and K.M. Chumakov. 1988. [Algorithms for constructing phylogenetic trees of maximum topological similarity]. *Mol Gen Mikrobiol Virusol*:9-15.

Jacobs, C.W., A.E. Adams, P.J. Szaniszlo, and J.R. Pringle. 1988. Functions of microtubules in the *Saccharomyces cerevisiae* cell cycle. *J Cell Biol*. 107:1409-26.

Jensen, S., M. Geymonat, A.L. Johnson, M. Segal, and L.H. Johnston. 2002. Spatial regulation of the guanine nucleotide exchange factor Lte1 in *Saccharomyces cerevisiae*. *J Cell Sci*. 115:4977-91.

Jin, T., L. Yue, and J. Li. 2001. In vivo interaction between dynamitin and MacMARCKS detected by the fluorescent resonance energy transfer method. *J Biol Chem*. 276:12879-84.

Johnson, K.A., and J.S. Wall. 1983. Structure and molecular weight of the dynein ATPase. *J Cell Biol*. 96:669-78.

Kahana, J.A., G. Schlenstedt, D.M. Evanchuk, J.R. Geiser, M.A. Hoyt, and P.A. Silver. 1998. The yeast dynactin complex is involved in partitioning the mitotic spindle between mother and daughter cells during anaphase B. *Mol Biol Cell.* 9:1741-56.

Kahana, J.A., B.J. Schnapp, and P.A. Silver. 1995. Kinetics of spindle pole body separation in budding yeast. *Proc Natl Acad Sci U S A.* 92:9707-11.

Kaldis, P. 1999. The cdk-activating kinase (CAK): from yeast to mammals. *Cell Mol Life Sci.* 55:284-96.

Karki, S., and E.L. Holzbaur. 1995. Affinity chromatography demonstrates a direct binding between cytoplasmic dynein and the dynactin complex. *J Biol Chem.* 270:28806-11.

Karki, S., and E.L. Holzbaur. 1999. Cytoplasmic dynein and dynactin in cell division and intracellular transport. *Curr Opin Cell Biol.* 11:45-53.

Karki, S., B. LaMonte, and E.L. Holzbaur. 1998. Characterization of the p22 subunit of dynactin reveals the localization of cytoplasmic dynein and dynactin to the midbody of dividing cells. *J Cell Biol.* 142:1023-34.

Karki, S., M.K. Tokito, and E.L. Holzbaur. 2000. A dynactin subunit with a highly conserved cysteine-rich motif interacts directly with Arp1. *J Biol Chem.* 275:4834-9.

Karpova, T.S., K. Tatchell, and J.A. Cooper. 1995. Actin filaments in yeast are unstable in the absence of capping protein or fimbrin. *J Cell Biol.* 131:1483-93.

Keaton, M.A., and D.J. Lew. 2006. Eavesdropping on the cytoskeleton: progress and controversy in the yeast morphogenesis checkpoint. *Curr Opin Microbiol.* 9:540-6.

Kim, H., S.C. Ling, G.C. Rogers, C. Kural, P.R. Selvin, S.L. Rogers, and V.I. Gelfand. 2007. Microtubule binding by dynactin is required for microtubule organization but not cargo transport. *J Cell Biol.* 176:641-51.

King, R.W., R.J. Deshaies, J.M. Peters, and M.W. Kirschner. 1996. How proteolysis drives the cell cycle. *Science.* 274:1652-9.

King, R.W., J.M. Peters, S. Tugendreich, M. Rolfe, P. Hieter, and M.W. Kirschner. 1995. A 20S complex containing CDC27 and CDC16 catalyzes the mitosis-specific conjugation of ubiquitin to cyclin B. *Cell.* 81:279-88.

King, S.J., M. Bonilla, M.E. Rodgers, and T.A. Schroer. 2002. Subunit organization in cytoplasmic dynein subcomplexes. *Protein Sci.* 11:1239-50.

King, S.J., C.L. Brown, K.C. Maier, N.J. Quintyne, and T.A. Schroer. 2003. Analysis of the dynein-dynactin interaction *in vitro* and *in vivo*. *Mol Biol Cell.* 14:5089-97.

King, S.J., and T.A. Schroer. 2000. Dynactin increases the processivity of the cytoplasmic dynein motor. *Nat Cell Biol.* 2:20-4.

King, S.M. 2000. The dynein microtubule motor. *Biochim Biophys Acta.* 1496:60-75.

King, S.M., E. Barbarese, J.F. Dillman, III, R.S. Patel-King, J.H. Carson, and K.K. Pfister. 1996. Brain cytoplasmic and flagellar outer arm dyneins share a highly conserved Mr 8,000 light chain. *J Biol Chem.* 271:19358-66.

King, S.M., J.F. Dillman, 3rd, S.E. Benashski, R.J. Lye, R.S. Patel-King, and K.K. Pfister. 1996. The mouse t-complex-encoded protein Tctex-1 is a light chain of brain cytoplasmic dynein. *J Biol Chem.* 271:32281-7.

King, S.M., C.G. Wilkerson, and G.B. Witman. 1991. The Mr 78,000 intermediate chain of *Chlamydomonas* outer arm dynein interacts with alpha-tubulin *in situ*. *J Biol Chem.* 266:8401-7.

King, S.M., and G.B. Witman. 1990. Localization of an intermediate chain of outer arm dynein by immunoelectron microscopy. *J Biol Chem.* 265:19807-11.

Kini, A.R., and C.A. Collins. 2001. Modulation of cytoplasmic dynein ATPase activity by the accessory subunits. *Cell Motil Cytoskeleton.* 48:52-60.

Kirschner. 1995. A 20S complex containing CDC27 and CDC16 catalyzes the mitosis-specific conjugation of ubiquitin to cyclin B. *Cell.* 81:279-88.

Kloc, M., N.R. Zearfoss, and L.D. Etkin. 2002. Mechanisms of subcellular mRNA localization. *Cell.* 108:533-44.

Kohno, H., K. Tanaka, A. Mino, M. Umikawa, H. Imamura, T. Fujiwara, Y. Fujita, K. Hotta, H. Qadota, T. Watanabe, Y. Ohya, and Y. Takai. 1996. Bni1p implicated in cytoskeletal control is a putative target of Rho1p small GTP binding protein in *Saccharomyces cerevisiae*. *Embo J.* 15:6060-8.

Komarnitsky, S.I., Y.C. Chiang, F.C. Luca, J. Chen, J.H. Toyn, M. Winey, L.H. Johnston, and C.L. Denis. 1998. DBF2 protein kinase binds to and acts through the cell cycle-regulated MOB1 protein. *Mol Cell Biol.* 18:2100-7.

Kon, T., M. Nishiura, R. Ohkura, Y.Y. Toyoshima, and K. Sutoh. 2004. Distinct functions of nucleotide-binding/hydrolysis sites in the four AAA modules of cytoplasmic dynein. *Biochemistry.* 43:11266-74.

Kopec, K., and J.P. Chambers. 1997. Effect of Alzheimer's brain extracts on dynein immunoreactivity in PC12 cells. *Proc Soc Exp Biol Med.* 216:429-37.

Kops, G.J., B.A. Weaver, and D.W. Cleveland. 2005. On the road to cancer: aneuploidy and the mitotic checkpoint. *Nat Rev Cancer.* 5:773-85.

Kormanec, J., I. Schaaff-Gerstenschlager, F.K. Zimmermann, D. Perecko, and H. Kuntzel. 1991. Nuclear migration in *Saccharomyces cerevisiae* is controlled by the highly repetitive 313 kDa NUM1 protein. *Mol Gen Genet.* 230:277-87.

Kozubowski, L., J.R. Larson, and K. Tatchell. 2005. Role of the septin ring in the asymmetric localization of proteins at the mother-bud neck in *Saccharomyces cerevisiae*. *Mol Biol Cell.* 16:3455-66.

Kuhle, V., D. Jackel, and M. Hensel. 2004. Effector proteins encoded by *Salmonella* pathogenicity island 2 interfere with the microtubule cytoskeleton after translocation into host cells. *Traffic.* 5:356-70.

Kumar, S., I.H. Lee, and M. Plamann. 2000. Cytoplasmic dynein ATPase activity is regulated by dynactin-dependent phosphorylation. *J Biol Chem.* 275:31798-804.

Kurihara, L.J., C.T. Beh, M. Latterich, R. Schekman, and M.D. Rose. 1994. Nuclear congression and membrane fusion: two distinct events in the yeast karyogamy pathway. *J Cell Biol.* 126:911-23.

Lee, L., S.K. Klee, M. Evangelista, C. Boone, and D. Pellman. 1999. Control of mitotic spindle position by the *Saccharomyces cerevisiae* formin Bni1p. *J Cell Biol.* 144:947-61.

Lee, S.E., L.M. Frenz, N.J. Wells, A.L. Johnson, and L.H. Johnston. 2001. Order of function of the budding-yeast mitotic exit-network proteins Tem1, Cdc15, Mob1, Dbf2, and Cdc5. *Curr Biol.* 11:784-8.

Lee, W.L., M.A. Kaiser, and J.A. Cooper. 2005. The offloading model for dynein function: differential function of motor subunits. *J Cell Biol.* 168:201-7.

Lee, W.L., J.R. Oberle, and J.A. Cooper. 2003. The role of the lissencephaly protein Pac1 during nuclear migration in budding yeast. *J Cell Biol.* 160:355-64.

Lees-Miller, J.P., D.M. Helfman, and T.A. Schroer. 1992. A vertebrate actin-related protein is a component of a multisubunit complex involved in microtubule-based vesicle motility. *Nature.* 359:244-6.

Lew, D.J., and D.J. Burke. 2003. The spindle assembly and spindle position checkpoints. *Annu Rev Genet.* 37:251-82.

Li, J., W.L. Lee, and J.A. Cooper. 2005. NudEL targets dynein to microtubule ends through LIS1. *Nat Cell Biol.* 7:686-90.

Li, J.J., and S.A. Li. 2006. Mitotic kinases: the key to duplication, segregation, and cytokinesis errors, chromosomal instability, and oncogenesis. *Pharmacol Ther.* 111:974-84.

Li, S., J. Finley, Z.J. Liu, S.H. Qiu, H. Chen, C.H. Luan, M. Carson, J. Tsao, D. Johnson, G. Lin, J. Zhao, W. Thomas, L.A. Nagy, B. Sha, L.J. DeLucas, B.C. Wang, and M. Luo. 2002. Crystal structure of the cytoskeleton-associated protein glycine-rich (CAP-Gly) domain. *J Biol Chem.* 277:48596-601.

Li, S.H., and X.J. Li. 1998. Aggregation of N-terminal huntingtin is dependent on the length of its glutamine repeats. *Hum Mol Genet.* 7:777-82.

Li, Y.Y., E. Yeh, T. Hays, and K. Bloom. 1993. Disruption of mitotic spindle orientation in a yeast dynein mutant. *Proc Natl Acad Sci U S A.* 90:10096-100.

Liakopoulos, D., J. Kusch, S. Grava, J. Vogel, and Y. Barral. 2003. Asymmetric loading of Kar9 onto spindle poles and microtubules ensures proper spindle alignment. *Cell.* 112:561-74.

Liang, Y., W. Yu, Y. Li, Z. Yang, X. Yan, Q. Huang, and X. Zhu. 2004. Nudel functions in membrane traffic mainly through association with Lis1 and cytoplasmic dynein. *J Cell Biol.* 164:557-66.

Ligon, L.A., S.S. Shelly, M. Tokito, and E.L. Holzbaur. 2003. The microtubule plus-end proteins EB1 and dynactin have differential effects on microtubule polymerization. *Mol Biol Cell.* 14:1405-17.

Lim, H.H., P.Y. Goh, and U. Surana. 1996. Spindle pole body separation in *Saccharomyces cerevisiae* requires dephosphorylation of the tyrosine 19 residue of Cdc28. *Mol Cell Biol.* 16:6385-97.

Lippincott, J., K.B. Shannon, W. Shou, R.J. Deshaies, and R. Li. 2001. The Tem1 small GTPase controls actomyosin and septin dynamics during cytokinesis. *J Cell Sci.* 114:1379-86.

Lippincott-Schwartz, J. 1998. Cytoskeletal proteins and Golgi dynamics. *Curr Opin Cell Biol.* 10:52-9.

Longtine, M.S., and E. Bi. 2003. Regulation of septin organization and function in yeast. *Trends Cell Biol.* 13:403-9.

Longtine, M.S., A. McKenzie, 3rd, D.J. Demarini, N.G. Shah, A. Wach, A. Brachat, P. Philippsen, and J.R. Pringle. 1998. Additional modules for versatile and economical PCR-based gene deletion and modification in *Saccharomyces cerevisiae*. *Yeast.* 14:953-61.

Luca, F.C., M. Mody, C. Kurischko, D.M. Roof, T.H. Giddings, and M. Winey. 2001. *Saccharomyces cerevisiae* Mob1p is required for cytokinesis and mitotic exit. *Mol Cell Biol.* 21:6972-83.

Lupas, A., M. Van Dyke, and J. Stock. 1991. Predicting coiled coils from protein sequences. *Science.* 252:1162-4.

Maddox, P.S., K.S. Bloom, and E.D. Salmon. 2000. The polarity and dynamics of microtubule assembly in the budding yeast *Saccharomyces cerevisiae. Nat Cell Biol.* 2:36-41.

Mah, A.S., J. Jang, and R.J. Deshaies. 2001. Protein kinase Cdc15 activates the Dbf2-Mob1 kinase complex. *Proc Natl Acad Sci U S A.* 98:7325-30.

Malumbres, M., and M. Barbacid. 2007. Cell cycle kinases in cancer. *Curr Opin Genet Dev.* 17:60-5.

Marchler-Bauer, A., and S.H. Bryant. 2004. CD-Search: protein domain annotations on the fly. *Nucleic Acids Res.* 32:W327-31.

McAinsh, A.D., J.D. Tytell, and P.K. Sorger. 2003. Structure, function, and regulation of budding yeast kinetochores. *Annu Rev Cell Dev Biol.* 19:519-39.

McDonald, D., M.A. Vodicka, G. Lucero, T.M. Svitkina, G.G. Borisy, M. Emerman, and T.J. Hope. 2002. Visualization of the intracellular behavior of HIV in living cells. *J Cell Biol.* 159:441-52.

McGrail, M., J. Gepner, A. Silvanovich, S. Ludmann, M. Serr, and T.S. Hays. 1995. Regulation of cytoplasmic dynein function *in vivo* by the *Drosophila Glued* complex. *J Cell Biol.* 131:411-25.

McMillan, J.N., and K. Tatchell. 1994. The JNM1 gene in the yeast *Saccharomyces cerevisiae* is required for nuclear migration and spindle orientation during the mitotic cell cycle. *J Cell Biol.* 125:143-58.

Mendenhall, M.D., and A.E. Hodge. 1998. Regulation of Cdc28 cyclin-dependent protein kinase activity during the cell cycle of the yeast *Saccharomyces cerevisiae. Microbiol Mol Biol Rev.* 62:1191-243.

Merdes, A., K. Ramyar, J.D. Vechio, and D.W. Cleveland. 1996. A complex of NuMA and cytoplasmic dynein is essential for mitotic spindle assembly. *Cell.* 87:447-58.

Mikami, A., B.M. Paschal, M. Mazumdar, and R.B. Vallee. 1993. Molecular cloning of the retrograde transport motor cytoplasmic dynein (MAP 1C). *Neuron.* 10:787-96.

Miller, R.K., S.C. Cheng, and M.D. Rose. 2000. Bim1p/Yeb1p mediates the Kar9p-dependent cortical attachment of cytoplasmic microtubules. *Mol Biol Cell.* 11:2949-59.

Miller, R.K., S. D'Silva, J.K. Moore, and H.V. Goodson. 2006. The CLIP-170 orthologue Bik1p and positioning the mitotic spindle in yeast. *Curr Top Dev Biol.* 76:49-87.

Miller, R.K., K.K. Heller, L. Frisen, D.L. Wallack, D. Loayza, A.E. Gammie, and M.D. Rose. 1998. The kinesin-related proteins, Kip2p and Kip3p, function differently in nuclear migration in yeast. *Mol Biol Cell.* 9:2051-68.

Miller, R.K., D. Matheos, and M.D. Rose. 1999. The cortical localization of the microtubule orientation protein, Kar9p, is dependent upon actin and proteins required for polarization. *J Cell Biol.* 144:963-75.

Miller, R.K., and M.D. Rose. 1998. Kar9p is a novel cortical protein required for cytoplasmic microtubule orientation in yeast. *J Cell Biol.* 140:377-90.

Modig, C., E. Stromberg, and M. Wallin. 1994. Different stability of posttranslationally modified brain microtubules isolated from cold-temperate fish. *Mol Cell Biochem.* 130:137-47.

Moore, J.K., S. D'Silva, and R.K. Miller. 2006. The CLIP-170 homologue Bik1p promotes the phosphorylation and asymmetric localization of Kar9p. *Mol Biol Cell.* 17:178-91.

Morgan, D.O. 1997. Cyclin-dependent kinases: engines, clocks, and microprocessors. *Annu Rev Cell Dev Biol.* 13:261-91.

Morris, N.R. 2003. Nuclear positioning: the means is at the ends. *Curr Opin Cell Biol.* 15:54-9.

Muhua, L., N.R. Adames, M.D. Murphy, C.R. Shields, and J.A. Cooper. 1998. A cytokinesis checkpoint requiring the yeast homologue of an APC-binding protein. *Nature.* 393:487-91.

Muhua, L., T.S. Karpova, and J.A. Cooper. 1994. A yeast actin-related protein homologous to that in vertebrate dynactin complex is important for spindle orientation and nuclear migration. *Cell.* 78:669-79.

Mullins, R.D., J.F. Kelleher, and T.D. Pollard. 1996. Actin' like actin? *Trends Cell Biol.* 6:208-12.

Nakamura, M., X.Z. Zhou, and K.P. Lu. 2001. Critical role for the EB1 and APC interaction in the regulation of microtubule polymerization. *Curr Biol.* 11:1062-7.

Nasmyth, K. 1996. At the heart of the budding yeast cell cycle. *Trends Genet.* 12:405-12.

Nasmyth, K. 2002. Segregating sister genomes: the molecular biology of chromosome separation. *Science.* 297:559-65.

Nasmyth, K. 2005. How do so few control so many? *Cell.* 120:739-46.

Neff, N.F., J.H. Thomas, P. Grisafi, and D. Botstein. 1983. Isolation of the beta-tubulin gene from yeast and demonstration of its essential function in vivo. *Cell.* 33:211-9.

O'Toole, E.T., M. Winey, and J.R. McIntosh. 1999. High-voltage electron tomography of spindle pole bodies and early mitotic spindles in the yeast *Saccharomyces cerevisiae*. *Mol Biol Cell.* 10:2017-31.

Ogawa, K. 1991. Four ATP-binding sites in the midregion of the beta heavy chain of dynein. *Nature.* 352:643-5.

Ohi, R., and K.L. Gould. 1999. Regulating the onset of mitosis. *Curr Opin Cell Biol.* 11:267-73.

Oiwa, K., and H. Sakakibara. 2005. Recent progress in dynein structure and mechanism. *Curr Opin Cell Biol.* 17:98-103.

Ozeki, Y., T. Tomoda, J. Kleiderlein, A. Kamiya, L. Bord, K. Fujii, M. Okawa, N. Yamada, M.E. Hatten, S.H. Snyder, C.A. Ross, and A. Sawa. 2003. Disrupted-in-Schizophrenia-1 (DISC-1): mutant truncation prevents binding to NudE-like (NUDEL) and inhibits neurite outgrowth. *Proc Natl Acad Sci U S A.* 100:289-94.

Palmer, R.E., D.S. Sullivan, T. Huffaker, and D. Koshland. 1992. Role of astral microtubules and actin in spindle orientation and migration in the budding yeast, *Saccharomyces cerevisiae*. *J Cell Biol.* 119:583-93.

Pan, X., D.S. Yuan, D. Xiang, X. Wang, S. Sookhai-Mahadeo, J.S. Bader, P. Hieter, F. Spencer, and J.D. Boeke. 2004. A robust toolkit for functional profiling of the yeast genome. *Mol Cell.* 16:487-96.

Paschal, B.M., E.L. Holzbaur, K.K. Pfister, S. Clark, D.I. Meyer, and R.B. Vallee. 1993. Characterization of a 50-kDa polypeptide in cytoplasmic dynein preparations reveals a complex with p150*GLUED* and a novel actin. *J Biol Chem.* 268:15318-23.

Paschal, B.M., and R.B. Vallee. 1987. Retrograde transport by the microtubule-associated protein MAP 1C. *Nature.* 330:181-3.

Payne, C., V. Rawe, J. Ramalho-Santos, C. Simerly, and G. Schatten. 2003. Preferentially localized dynein and perinuclear dynactin associate with nuclear pore complex proteins to mediate genomic union during mammalian fertilization. *J Cell Sci.* 116:4727-38.

Pazour, G.J., and J.L. Rosenbaum. 2002. Intraflagellar transport and cilia-dependent diseases. *Trends Cell Biol.* 12:551-5.

Pearson, C.G., and K. Bloom. 2004. Dynamic microtubules lead the way for spindle positioning. *Nat Rev Mol Cell Biol.* 5:481-92.

Pereira, G., T. Hofken, J. Grindlay, C. Manson, and E. Schiebel. 2000. The Bub2p spindle checkpoint links nuclear migration with mitotic exit. *Mol Cell.* 6:1-10.

Pereira, G., T.U. Tanaka, K. Nasmyth, and E. Schiebel. 2001. Modes of spindle pole body inheritance and segregation of the Bfa1p-Bub2p checkpoint protein complex. *Embo J.* 20:6359-70.

Peters, J.M. 1998. SCF and APC: the Yin and Yang of cell cycle regulated proteolysis. *Curr Opin Cell Biol.* 10:759-68.

Peterson, J.B., and H. Ris. 1976. Electron-microscopic study of the spindle and chromosome movement in the yeast *Saccharomyces cerevisiae*. *J Cell Sci.* 22:219-42.

Pfarr, C.M., M. Coue, P.M. Grissom, T.S. Hays, M.E. Porter, and J.R. McIntosh. 1990. Cytoplasmic dynein is localized to kinetochores during mitosis. *Nature.* 345:263-5.

Pfister, K.K., S.E. Benashski, J.F. Dillman, 3rd, R.S. Patel-King, and S.M. King. 1998. Identification and molecular characterization of the p24 dynactin light chain. *Cell Motil Cytoskeleton.* 41:154-67.

Pines, J. 1999. Four-dimensional control of the cell cycle. *Nat Cell Biol.* 1:E73-9.

Plamann, M., P.F. Minke, J.H. Tinsley, and K.S. Bruno. 1994. Cytoplasmic dynein and actin-related protein Arp1 are required for normal nuclear distribution in filamentous fungi. *J Cell Biol.* 127:139-149.

Plough, H.H., and P.T. Ives. 1935. Induction of mutations by high temperature in *Drosophila*. *Genetics.* 20:42-69.

Presley, J.F., N.B. Cole, T.A. Schroer, K. Hirschberg, K.J. Zaal, and J. Lippincott-Schwartz. 1997. ER-to-Golgi transport visualized in living cells. *Nature.* 389:81-5.

Pringle, J.R., and L.H. Hartwell. 1981. The *Saccharomyces cerevisiae* cell cycle. The Molecular Biology of the Yeast *Saccharomyces*: Life Cycle and Inheritance. J.N. Strathern, E.W. Jones, and J.R. Broach, editors. Cold Spring Harbor Laboratory, Cold Spring Harbor, NY. 97-142

Pringle, J.R., Broach, J.R., and Jones, E.W. 1997. The molecular and cellular biology of the yeast *Saccharomyces*: Cell cycle and cell biology. Cold Spring Harbor Laboratory, New York. 2-90

Pruyne, D., M. Evangelista, C. Yang, E. Bi, S. Zigmond, A. Bretscher, and C. Boone. 2002. Role of formins in actin assembly: nucleation and barbed-end association. *Science*. 297:612-5.

Puls, I., C. Jonnakuty, B.H. LaMonte, E.L. Holzbaur, M. Tokito, E. Mann, M.K. Floeter, K. Bidus, D. Drayna, S.J. Oh, R.H. Brown, Jr., C.L. Ludlow, and K.H. Fischbeck. 2003. Mutant dynactin in motor neuron disease. *Nat Genet*. 33:455-6.

Quintyne, N.J., and T.A. Schroer. 2002. Distinct cell cycle-dependent roles for dynactin and dynein at centrosomes. *J Cell Biol*. 159:245-54.

Raich, W.B., A.N. Moran, J.H. Rothman, and J. Hardin. 1998. Cytokinesis and midzone microtubule organization in *Caenorhabditis elegans* require the kinesin-like protein ZEN-4. *Mol Biol Cell*. 9:2037-49.

Read, E.B., H.H. Okamura, and D.G. Drubin. 1992. Actin- and tubulin-dependent functions during *Saccharomyces cerevisiae* mating projection formation. *Mol Biol Cell*. 3:429-44.

Rose, M.D. 1996. Nuclear fusion in the yeast *Saccharomyces cerevisiae*. *Annu Rev Cell Dev Biol*. 12:663-95.

Rosenbaum, J.L., and G.B. Witman. 2002. Intraflagellar transport. *Nat Rev Mol Cell Biol*. 3:813-25.

Rusan, N.M., U.S. Tulu, C. Fagerstrom, and P. Wadsworth. 2002. Reorganization of the microtubule array in prophase/prometaphase requires cytoplasmic dynein-dependent microtubule transport. *J Cell Biol*. 158:997-1003.

Sakato, M., and S.M. King. 2003. Calcium regulates ATP-sensitive microtubule binding by *Chlamydomonas* outer arm dynein. *J Biol Chem*. 278:43571-9.

Sakchaisri, K., S. Asano, L.R. Yu, M.J. Shulewitz, C.J. Park, J.E. Park, Y.W. Cho, T.D. Veenstra, J. Thorner, and K.S. Lee. 2004. Coupling morphogenesis to mitotic entry. *Proc Natl Acad Sci U S A*. 101:4124-9.

Salina, D., K. Bodoor, D.M. Eckley, T.A. Schroer, J.B. Rattner, and B. Burke. 2002. Cytoplasmic dynein as a facilitator of nuclear envelope breakdown. *Cell*. 108:97-107.

Saunders, W.S. 2002. The FEAR factor. *Mol Cell*. 9:207-9.

Saunders, W.S., and M.A. Hoyt. 1992. Kinesin-related proteins required for structural integrity of the mitotic spindle. *Cell*. 70:451-8.

Saunders, W.S., D. Koshland, D. Eshel, I.R. Gibbons, and M.A. Hoyt. 1995. *Saccharomyces cerevisiae* kinesin- and dynein-related proteins required for anaphase chromosome segregation. *J Cell Biol*. 128:617-24.

Schafer, D.A., S.R. Gill, J.A. Cooper, J.E. Heuser, and T.A. Schroer. 1994. Ultrastructural analysis of the dynactin complex: an actin-related protein is a component of a filament that resembles F-actin. *J Cell Biol*. 126:403-12.

Schafer, D.A., Y.O. Korshunova, T.A. Schroer, and J.A. Cooper. 1994. Differential localization and sequence analysis of capping protein beta-subunit isoforms of vertebrates. *J Cell Biol*. 127:453-65.

Schatz, P.J., L. Pillus, P. Grisafi, F. Solomon, and D. Botstein. 1986. Two functional alpha-tubulin genes of the yeast *Saccharomyces cerevisiae* encode divergent proteins. *Mol Cell Biol*. 6:3711-21.

Schiestl, R.H., and R.D. Gietz. 1989. High efficiency transformation of intact yeast cells using single stranded nucleic acids as a carrier. *Curr Genet*. 16:339-46.

Schott, D., T. Huffaker, and A. Bretscher. 2002. Microfilaments and microtubules: the news from yeast. *Curr Opin Microbiol.* 5:564-74.

Schroer, T.A. 1994. New insights into the interaction of cytoplasmic dynein with the actin-related protein, Arp1. *J Cell Biol.* 127:1-4.

Schroer, T.A. 2004. Dynactin. *Annu Rev Cell Dev Biol.* 20:759-79.

Schroer, T.A., and M.P. Sheetz. 1991. Two activators of microtubule-based vesicle transport. *J Cell Biol.* 115:1309-18.

Schroer, T.A., E.R. Steuer, and M.P. Sheetz. 1989. Cytoplasmic dynein is a minus end-directed motor for membranous organelles. *Cell.* 56:937-46.

Schuyler, S.C., J.Y. Liu, and D. Pellman. 2003. The molecular function of Ase1p: evidence for a MAP-dependent midzone-specific spindle matrix. Microtubule-associated proteins. *J Cell Biol.* 160:517-28.

Schwartz, K., K. Richards, and D. Botstein. 1997. *BIM1* encodes a microtubule-binding protein in yeast. *Mol Biol Cell.* 8:2677-91.

Segal, M., K. Bloom, and S.I. Reed. 2002. Kar9p-independent microtubule capture at Bud6p cortical sites primes spindle polarity before bud emergence in *Saccharomyces cerevisiae*. *Mol Biol Cell.* 13:4141-55.

Sharp, D.J., and G.C. Rogers. 2004. A Kin I-dependent Pacman-flux mechanism for anaphase A. *Cell Cycle.* 3:707-10.

Sharp, D.J., G.C. Rogers, and J.M. Scholey. 2000. Cytoplasmic dynein is required for poleward chromosome movement during mitosis in *Drosophila* embryos. *Nat Cell Biol.* 2:922-30.

Sheeman, B., P. Carvalho, I. Sagot, J. Geiser, D. Kho, M.A. Hoyt, and D. Pellman. 2003. Determinants of *S. cerevisiae* dynein localization and activation: implications for the mechanism of spindle positioning. *Curr Biol.* 13:364-72.

Sherr, C.J., and J.M. Roberts. 1999. CDK inhibitors: positive and negative regulators of G1-phase progression. *Genes Dev.* 13:1501-12.

Shirayama, M., Y. Matsui, K. Tanaka, and A. Toh-e. 1994. Isolation of a CDC25 family gene, MSI2/LTE1, as a multicopy suppressor of *ira1*. *Yeast.* 10:451-61.

Shirayama, M., Y. Matsui, and E.A. Toh. 1994. The yeast *TEM1* gene, which encodes a GTP-binding protein, is involved in termination of M phase. *Mol Cell Biol.* 14:7476-82.

Shou, W., J.H. Seol, A. Shevchenko, C. Baskerville, D. Moazed, Z.W. Chen, J. Jang, A. Shevchenko, H. Charbonneau, and R.J. Deshaies. 1999. Exit from mitosis is triggered by Tem1-dependent release of the protein phosphatase Cdc14 from nucleolar RENT complex. *Cell.* 97:233-44.

Silvanovich, A., M.G. Li, M. Serr, S. Mische, and T.S. Hays. 2003. The third P-loop domain in cytoplasmic dynein heavy chain is essential for dynein motor function and ATP-sensitive microtubule binding. *Mol Biol Cell.* 14:1355-65.

Simanis, V. 2003. Events at the end of mitosis in the budding and fission yeasts. *J Cell Sci.* 116:4263-75.

Sodeik, B., M.W. Ebersold, and A. Helenius. 1997. Microtubule-mediated transport of incoming herpes simplex virus 1 capsids to the nucleus. *J Cell Biol.* 136:1007-21.

Song, S., and K.S. Lee. 2001. A novel function of *Saccharomyces cerevisiae* CDC5 in cytokinesis. *J Cell Biol.* 152:451-69.

Soto, A.M., and C. Sonnenschein. 2004. The somatic mutation theory of cancer: growing problems with the paradigm? *Bioessays*. 26:1097-107.

Spiliotis, E.T., and W.J. Nelson. 2006. Here come the septins: novel polymers that coordinate intracellular functions and organization. *J Cell Sci*. 119:4-10.

Starr, D.A., B.C. Williams, T.S. Hays, and M.L. Goldberg. 1998. ZW10 helps recruit dynactin and dynein to the kinetochore. *J Cell Biol*. 142:763-74.

Stearns, T., M.A. Hoyt, and D. Botstein. 1990. Yeast mutants sensitive to antimicrotubule drugs define three genes that affect microtubule function. *Genetics*. 124:251-62.

Stegmeier, F., R. Visintin, and A. Amon. 2002. Separase, polo kinase, the kinetochore protein Slk19, and Spo12 function in a network that controls Cdc14 localization during early anaphase. *Cell*. 108:207-20.

Steuer, E.R., L. Wordeman, T.A. Schroer, and M.P. Sheetz. 1990. Localization of cytoplasmic dynein to mitotic spindles and kinetochores. *Nature*. 345:266-8.

Straight, A.F., W.F. Marshall, J.W. Sedat, and A.W. Murray. 1997. Mitosis in living budding yeast: anaphase A but no metaphase plate. *Science*. 277:574-8.

Straight, A.F., J.W. Sedat, and A.W. Murray. 1998. Time-lapse microscopy reveals unique roles for kinesins during anaphase in budding yeast. *J Cell Biol*. 143:687-94.

Sullivan, D.S., and T.C. Huffaker. 1992. Astral microtubules are not required for anaphase B in *Saccharomyces cerevisiae*. *J Cell Biol*. 119:379-88.

Suzuki, M., R. Igarashi, M. Sekiya, T. Utsugi, S. Morishita, M. Yukawa, and Y. Ohya. 2004. Dynactin is involved in a checkpoint to monitor cell wall synthesis in *Saccharomyces cerevisiae*. *Nat Cell Biol*. 6:861-71.

Tai, A.W., J.Z. Chuang, and C.H. Sung. 1998. Localization of Tctex-1, a cytoplasmic dynein light chain, to the Golgi apparatus and evidence for dynein complex heterogeneity. *J Biol Chem*. 273:19639-49.

Tarnowski, B.I., F.G. Spinale, and J.H. Nicholson. 1991. DAPI as a useful stain for nuclear quantitation. *Biotech Histochem*. 66:297-302.

Tatusova, T.A., and T.L. Madden. 1999. BLAST 2 Sequences, a new tool for comparing protein and nucleotide sequences. *FEMS Microbiol Lett*. 174:247-50.

Thompson, J.D., D.G. Higgins, and T.J. Gibson. 1994. CLUSTAL W: improving the sensitivity of progressive multiple sequence alignment through sequence weighting, position-specific gap penalties and weight matrix choice. *Nucleic Acids Res*. 22:4673-80.

Tirnauer, J.S., E. O'Toole, L. Berrueta, B.E. Bierer, and D. Pellman. 1999. Yeast Bim1p promotes the G1-specific dynamics of microtubules. *J Cell Biol*. 145:993-1007.

Tokito, M.K., and E.L. Holzbaur. 1998. The genomic structure of DCTN1, a candidate gene for limb-girdle muscular dystrophy (LGMD2B). *Biochim Biophys Acta*. 1442:432-6.

Tokito, M.K., D.S. Howland, V.M. Lee, and E.L. Holzbaur. 1996. Functionally distinct isoforms of dynactin are expressed in human neurons. *Mol Biol Cell*. 7:1167-80.

Tolliday, N., N. Bouquin, and R. Li. 2001. Assembly and regulation of the cytokinetic apparatus in budding yeast. *Curr Opin Microbiol*. 4:690-5.

Tong, A.H., G. Lesage, G.D. Bader, H. Ding, H. Xu, X. Xin, J. Young, G.F. Berriz, R.L. Brost, M. Chang, Y. Chen, X. Cheng, G. Chua, H. Friesen, D.S. Goldberg, J. Haynes, C. Humphries, G. He, S. Hussein, L. Ke, N. Krogan, Z. Li, J.N. Levinson, H. Lu, P. Menard, C. Munyana, A.B. Parsons, O. Ryan, R. Tonikian, T. Roberts, A.M. Sdicu, J. Shapiro, B. Sheikh, B. Suter, S.L. Wong, L.V. Zhang, H. Zhu, C.G. Burd, S. Munro, C. Sander, J. Rine, J. Greenblatt, M. Peter, A. Bretscher, G. Bell, F.P. Roth, G.W. Brown, B. Andrews, H. Bussey, and C. Boone. 2004. Global mapping of the yeast genetic interaction network. *Science*. 303:808-13.

Tulu, U.S., N.M. Rusan, and P. Wadsworth. 2003. Peripheral, non-centrosome-associated microtubules contribute to spindle formation in centrosome-containing cells. *Curr Biol*. 13:1894-9.

Tytell, J.D., and P.K. Sorger. 2006. Analysis of kinesin motor function at budding yeast kinetochores. *J Cell Biol*. 172:861-74.

Vaisberg, E.A., M.P. Koonce, and J.R. McIntosh. 1993. Cytoplasmic dynein plays a role in mammalian mitotic spindle formation. *J Cell Biol*. 123:849-58.

Vale, R.D. 2003. The molecular motor toolbox for intracellular transport. *Cell*. 112:467-80.

Valetti, C., D.M. Wetzel, M. Schrader, M.J. Hasbani, S.R. Gill, T.E. Kreis, and T.A. Schroer. 1999. Role of dynactin in endocytic traffic: effects of dynamitin overexpression and colocalization with CLIP-170. *Mol Biol Cell*. 10:4107-20.

Vallee, R.B., and M.A. Gee. 1998. Make room for dynein. *Trends Cell Biol*. 8:490-4.

Vallee, R.B., J.C. Williams, D. Varma, and L.E. Barnhart. 2004. Dynein: An ancient motor protein involved in multiple modes of transport. *J Neurobiol*. 58:189-200.

van Hemert, M.J., G.E. Lamers, D.C. Klein, T.H. Oosterkamp, H.Y. Steensma, and G.P. van Heusden. 2002. The *Saccharomyces cerevisiae* Fin1 protein forms cell cycle-specific filaments between spindle pole bodies. *Proc Natl Acad Sci U S A*. 99:5390-3.

Vaughan, K.T., S.H. Tynan, N.E. Faulkner, C.J. Echeverri, and R.B. Vallee. 1999. Colocalization of cytoplasmic dynein with dynactin and CLIP-170 at microtubule distal ends. *J Cell Sci*. 112 ( Pt 10):1437-47.

Vaughan, K.T., and R.B. Vallee. 1995. Cytoplasmic dynein binds dynactin through a direct interaction between the intermediate chains and p150*Glued*. *J Cell Biol*. 131:1507-16.

Vaughan, P.S., P. Miura, M. Henderson, B. Byrne, and K.T. Vaughan. 2002. A role for regulated binding of p150(*Glued*) to microtubule plus ends in organelle transport. *J Cell Biol*. 158:305-19.

Vierula, P.J., and J.M. Mais. 1997. A gene required for nuclear migration in *Neurospora crassa* codes for a protein with cysteine-rich, LIM/RING-like domains. *Mol Microbiol*. 24:331-40.

Visintin, R., K. Craig, E.S. Hwang, S. Prinz, M. Tyers, and A. Amon. 1998. The phosphatase Cdc14 triggers mitotic exit by reversal of Cdk-dependent phosphorylation. *Mol Cell*. 2:709-18.

Visintin, R., E.S. Hwang, and A. Amon. 1999. Cfi1 prevents premature exit from mitosis by anchoring Cdc14 phosphatase in the nucleolus. *Nature*. 398:818-23.

Visintin, R., F. Stegmeier, and A. Amon. 2003. The role of the polo kinase Cdc5 in controlling Cdc14 localization. *Mol Biol Cell.* 14:4486-98.

Wach, A., A. Brachat, R. Pohlmann, and P. Philippsen. 1994. New heterologous modules for classical or PCR-based gene disruptions in *Saccharomyces cerevisiae. Yeast.* 10:1793-808.

Walker, J.E., M. Saraste, M.J. Runswick, and N.J. Gay. 1982. Distantly related sequences in the alpha- and beta-subunits of ATP synthase, myosin, kinases and other ATP-requiring enzymes and a common nucleotide binding fold. *Embo J.* 1:945-51.

Wang, Y., F. Hu, and S.J. Elledge. 2000. The Bfa1/Bub2 GAP complex comprises a universal checkpoint required to prevent mitotic exit. *Curr Biol.* 10:1379-82.

Wang, Y., F. Hu, and S.J. Elledge. 2000. The Bfa1/Bub2 GAP complex comprises a universal checkpoint required to prevent mitotic exit. *Curr Biol.* 10:1379-82.

Waterman-Storer, C.M., and E.L. Holzbaur. 1996. The product of the *Drosophila* gene, *Glued*, is the functional homologue of the *p150Glued* component of the vertebrate dynactin complex. *J Biol Chem.* 271:1153-9.

Waterman-Storer, C.M., S. Karki, and E.L. Holzbaur. 1995. The p150*Glued* component of the dynactin complex binds to both microtubules and the actin-related protein centractin (Arp-1). *Proc Natl Acad Sci U S A.* 92:1634-8.

Waterman-Storer, C.M., S.B. Karki, S.A. Kuznetsov, J.S. Tabb, D.G. Weiss, G.M. Langford, and E.L. Holzbaur. 1997. The interaction between cytoplasmic dynein and dynactin is required for fast axonal transport. *Proc Natl Acad Sci U S A.* 94:12180-5.

Wheatley, S.P., and Y. Wang. 1996. Midzone microtubule bundles are continuously required for cytokinesis in cultured epithelial cells. *J Cell Biol.* 135:981-9.

Williams, B.C., M.F. Riedy, E.V. Williams, M. Gatti, and M.L. Goldberg. 1995. The *Drosophila* kinesin-like protein KLP3A is a midbody component required for central spindle assembly and initiation of cytokinesis. *J Cell Biol.* 129:709-23.

Winey, M., L. Goetsch, P. Baum, and B. Byers. 1991. MPS1 and MPS2: novel yeast genes defining distinct steps of spindle pole body duplication. *J Cell Biol.* 114:745-54.

Winsor, B., and E. Schiebel. 1997. Review: an overview of the *Saccharomyces cerevisiae* microtubule and microfilament cytoskeleton. *Yeast.* 13:399-434.

Winzeler, E.A., D.D. Shoemaker, A. Astromoff, H. Liang, K. Anderson, B. Andre, R. Bangham, R. Benito, J.D. Boeke, H. Bussey, A.M. Chu, C. Connelly, K. Davis, F. Dietrich, S.W. Dow, M. El Bakkoury, F. Foury, S.H. Friend, E. Gentalen, G. Giaever, J.H. Hegemann, T. Jones, M. Laub, H. Liao, N. Liebundguth, D.J. Lockhart, A. Lucau-Danila, M. Lussier, N. M'Rabet, P. Menard, M. Mittmann, C. Pai, C. Rebischung, J.L. Revuelta, L. Riles, C.J. Roberts, P. Ross-MacDonald, B. Scherens, M. Snyder, S. Sookhai-Mahadeo, R.K. Storms, S. Veronneau, M. Voet, G. Volckaert, T.R. Ward, R. Wysocki, G.S. Yen, K. Yu, K. Zimmermann, P. Philippsen, M. Johnston, and R.W. Davis. 1999. Functional characterization of the *S. cerevisiae* genome by gene deletion and parallel analysis. *Science.* 285:901-6.

Xiang, X., S.M. Beckwith, and N.R. Morris. 1994. Cytoplasmic dynein is involved in nuclear migration in *Aspergillus nidulans. Proc Natl Acad Sci U S A.* 91:2100-4.

Yeh, E., R.V. Skibbens, J.W. Cheng, E.D. Salmon, and K. Bloom. 1995. Spindle dynamics and cell cycle regulation of dynein in the budding yeast, *Saccharomyces cerevisiae*. *J Cell Biol.* 130:687-700.

Yin, H., D. Pruyne, T.C. Huffaker, and A. Bretscher. 2000. Myosin V orientates the mitotic spindle in yeast. *Nature*. 406:1013-5.

Yoshida, S., and A. Toh-e. 2001. Regulation of the localization of Dbf2 and mob1 during cell division of *Saccharomyces cerevisiae*. *Genes Genet Syst.* 76:141-7.

Yoshida, S., and A. Toh-e. 2002. Budding yeast Cdc5 phosphorylates Net1 and assists Cdc14 release from the nucleolus. *Biochem Biophys Res Commun.* 294:687-91.

Yue, L., S. Lu, J. Garces, T. Jin, and J. Li. 2000. Protein kinase C-regulated dynamitin-macrophage-enriched myristoylated alanine-rice C kinase substrate interaction is involved in macrophage cell spreading. *J Biol Chem.* 275:23948-56.

Zachariae, W., and K. Nasmyth. 1999. Whose end is destruction: cell division and the anaphase-promoting complex. *Genes Dev.* 13:2039-58.

Zahner, J.E., H.A. Harkins, and J.R. Pringle. 1996. Genetic analysis of the bipolar pattern of bud site selection in the yeast *Saccharomyces cerevisiae*. *Mol Cell Biol.* 16:1857-70.

Ziman, M., D. Preuss, J. Mulholland, J.M. O'Brien, D. Botstein, and D.I. Johnson. 1993. Subcellular localization of Cdc42p, a *Saccharomyces cerevisiae* GTP-binding protein involved in the control of cell polarity. *Mol Biol Cell.* 4:1307-16.

# APPENDIX:

# Using FRET to study protein interactions

## I. Background

### a. Mitotic exit is controlled by the MEN proteins

Nuclear migration, mitotic exit, and cytokinesis in *S. cerevisiae* are precisely regulated, and are coupled to one another such that cytokinesis cannot be performed until the nucleus is properly positioned. The spindle position checkpoint ensures the cell does not exit from mitosis before nuclear migration into the neck.

As described previously, the activity of the phosphatase Cdc14 is crucial for mitotic exit (Visintin *et al.*, 1999; Visintin *et al.*, 1998). During most of the cell cycle, Cdc14 is sequestered in the nucleolus by the anchor protein Net1. When released into the cytoplasm, Cdc14 contributes to both Clb2 degradation and accumulation of the Cdk inhibitor Sic1 (Visintin *et al.*, 1998). Inactivation of the mitotic Cdks leads to spindle disassembly, chromosomal decondensation and cytokinesis.

At the point of the metaphase-to-anaphase transition, Cdc14 is partially released into the nucleoplasm by the FEAR pathway (Stegmeier *et al.*, 2002). However, the partial release of Cdc14 is not enough to trigger mitotic exit. In order for the cell to exit mitosis, Cdc14 needs to be fully released into the cytoplasm (during late anaphase), which requires the activity of a signal transduction cascade called the mitotic exit network (MEN) (Lee *et al.*, 2001). The MEN proteins include the GTPase Tem1, Cdc14, Cdc5 (the yeast homologue of *Drosophila* polo kinase), Cdc15 (a MAP-kinase-like kinase), Dbf2 (Ser/Thr kinase), and Mob1, a proposed activator of Dbf2. All the MEN proteins are required to maintain the full release Cdc14, thus are all crucial for mitotic exit. In mutants lacking MEN activity, Cdc14 released during early anaphase returns to the nucleolus later, without triggering mitotic exit (Lee *et al.*, 2001).

Although genetic evidence suggests that all the MEN components work in a common pathway, little is known about their specific functions. Cdc14 is thought to be at the bottom of this pathway; Cdc14 liberation by *net1* (Net1 sequesters Cdc14 in the nucleolus) mutations bypasses the essential role of the other MEN proteins for mitotic

exit. Overexpression of Cdc14 leads to ectopic Clb2 degradation and Sic1 accumulation; and this effect does not require Dbf2 or Cdc15 (although it is a bit delayed in *cdc5* conditional mutants). Cdc14 overexpression also suppresses the temperature-sensitive lethality of *tem1*, *cdc5* and *dbf2* conditional mutants (Visintin *et al.*, 1998). Furthermore, in conditional mutants of the other MEN proteins, Cdc14 remains sequestered in the nucleolus. All these observations suggest that the other MEN proteins act upstream of Cdc14 to promote its release from the nucleolus.

The Ras-like GTPase Tem1 functions at the top of the MEN (Shirayama *et al.*, 1994b). Overexpression of Cdc15, Cdc5, Cdc14 suppresses the temperature sensitivity and growth defect of *tem1* conditional mutants. Cdc15, a homologue to mitogen-activated protein kinases, acts downstream of Tem1 (Lee *et al.*, 2001). Cdc15 interacts with Tem1 in a yeast two-hybrid essay and co-immunoprecipitates with Tem1 (Asakawa *et al.*, 2001; Bardin *et al.*, 2000). It is also suggested that the direct interaction between Cdc15 and Tem1 occurs only when Tem1 is active (in its GTP-binding state) (Asakawa *et al.*, 2001).

The protein kinase Dbf2 is presumably downstream of Cdc15. Dbf2 is believed to form a heterodimer with Mob1 (Komarnitsky *et al.*, 1998). *In vitro* studies show that Cdc15 activates Dbf2 by phosphorylating it on two sites and this activation requires the presence of Mob1 (Mah *et al.*, 2001). Overexpression of Cdc15 fails to activate Dbf2 in the absence of Mob1, suggesting Mob1 is required for Dbf2 activation.

Cdc5, the polo-like kinase, seems to be multifunctional during mitosis, and its role within the MEN is complex. It may act at more than one point and regulates the activities of several MEN components, one of its roles being to promote the kinase activity of Dbf2 (Lee *et al.*, 2001). Cdc5 is also a component of the FEAR network, which triggers the partial release of Cdc14 during early anaphase (Vinsintin *et al.*, 2003).

How the MEN proteins promote the full release of Cdc14 remains to be understood. It is suggested that Cdc5 phosphorylates Net1 and assists release of Cdc14 from the nucleolus. However, timing of Cdc14 release is independent of Cdc5, suggesting there must be other mechanisms for Cdc14 release (Yoshida and Toh-e, 2002).

### b. Regulation of the MEN activity

Tem1 activity is regulated by the Bub2-Bfa1 complex (GTPase activating protein, or GAP) and Lte1 (a putative guanine exchange factor, or GEF). Tem1 localizes preferentially to the cytoplasmic face of the old SPB, which is destined to move into the bud (Pereira *et al.*, 2000). The Bub2/Bfa1 complex colocalizes with Tem1 on the outer plaque of SPB, keeping Tem1 in its inactive form (GDP bound) (Pereira *et al.*, 2000; Geymonat *et al.*, 2002). The GEF protein Lte1 becomes sequestered in the bud concomitant with bud formation (Shirayama *et al.*, 1994b). It is thought that when the spindle moves into the neck, bringing Tem1 into contact with Lte1, Tem1 is activated (GTP bound), which in turn activates other components of the MEN. The nuclear position thus controls the activation of Tem1 and mitotic exit (refer to section 1.1.4 for more details).

Cdc5 may phosphorylate Bfa1, which inhibits the GAP activity of Bub2/Bfa1 (Lee *et al.*, 2001). However, the timing and regulation of this phosphorylation by Cdc5 remains to be understood. Alternatively, Bub2/Bfa1 activity may be controlled by the presence of cytoplasmic microtubules in the bud neck (Adames *et al.*, 2001). How the cell sensers the existence of cytoplasmic microtubules in the neck and sends a signal to Bub2/Bfa1 is not clear. It is also possible that there are regulators of Tem1 that have not been discovered yet, or different MEN components other than Tem1 may count for the Cdc14 release from the nucleolus.

### c. The links between mitotic exit and cytokinesis

Cytokineis is a process that largely involves the cytoskeleton proteins. At the onset of the cell cycle, septins form a cluster of filaments that assembles a ring at the destined bud site. Myosin II, the actin-based motor, also forms a ring structure at this site. As the bud emerges and enlarges, septin filaments broadens onto both the mother and bud sides of the neck. At the end of the cell cycle, a septum made of chitin and other cell wall components is deposited at the neck. The actomysoin ring provides contractile force for ingression of the plasma membrane. Cell separation is then accomplished by separation between the mother and bud, and subsequent degradation of part of the chitin layer joining the two cells.

The MEN pathway is essential for cytokinesis (Bardin and Amon, 2001). MEN mutants are deficient both in mitotic exit and cytokinesis, and it has to be noted here that the requirement of the MEN for cytokinesis is more than an indirect consequence of cells requiring the MEN to exit mitosis. Most of MEN mutants, when grown at the semi-permissive temperature, are capable of exiting from mitosis but display a severe cytokinesis deficiency (Lim *et al.*, 2003). Overexpression of *SIC1* in the *mob1-77* mutant (this mutant arrests before mitotic exit at non-permissive temperature) enables inactivation of mitotic Cdks (Luca *et al.*, 2001). However, these cells cannot undergo proper cytokinesis, suggesting a direct role for Mob1 in cytokinesis. A *cdc5* mutant demonstrates the same pattern as *mob1-77* (Song and Lee, 2001). In addition, in *net1-1* cells, the mitotic exit function of Tem1 is bypassed; however, *tem1 net1-1* double mutants have cytokinesis deficiency, suggesting Tem1 is directly required for cytokinesis (Shou *et al.*, 1999).

The MEN proteins are often translocated to the mother-bud neck after Cdc14 full release and Cdk inactivation (Frenz *et al.*, 2000). Evidence shows that actomyosin and septin dynamics require Tem1, and Tem1 also interacts with actomyosin ring regulators *in vitro* (Lippincott *et al.*, 2001). Therefore, it can be speculated that the MEN proteins regulate the assembly of actomyosin ring and its contraction during cytokinesis.

Although the MEN functions in cytokinesis independently of their roles in mitotic exit, mitotic Cdk inactivation is still necessary for cytokinesis. So far there has been no report about any mutant that undergoes cytokinesis when the mitotic kinase activity is at high level. Furthermore, the translocation of Dbf2 to the bud neck requires the inactivation of mitotic Cdks.

In summary, it is postulated that at late anaphase, the MEN proteins trigger full relase of Cdc14, which inactivates mitotic Cdk and allows cytokinesis to occur; subsequently, Cdk inactivation leads to the translocation of the MEN proteins to the mother-bud neck, where they regulate cytokinesis.

## II. Objectives of this study

Most MEN proteins have been shown to localize at the SPBs, at least during some cell cycle stages (Bardin and Amon, 2001). Cdc15 and Dbf2 localize to both SPBs during anaphase, whereas Cdc5 localizes to both SPBs during metaphase and anaphase. The SPB localization of MEN proteins is very important for their roles in promoting mitotic exit. For example, localization of Dbf2 to the SPBs is required for the activation of this protein. Nud1, a SPB component, functions as a scaffold for Bub2/Bfa1 complex and other MEN components. Cells carrying a temperature-sensitive allele of *NUD1* arrest at the end of mitosis, with Tem1, Cdc15, and Dbf2 mislocalized (Gruneberg *et al.*, 2000).

Localization of the MEN proteins is also important for their functions in cytokinesis. Some of them are indeed translocated to the mother-bud neck during cytokinesis. Therefore, localization of the MEN proteins changes, depending on the cell cycle progression. Tem1 localizes preferentially to the cytoplasmic face of the old SPB during anaphase, whereas during late telophase, the asymmetry of Tem1 localization is lost and it is found on both SPBs (Pereira *et al.*, 2000). The Tem1 regulator Bub2/Bfa1, whose localization is similar to Tem1, is required for the asymmetric localization of Tem1 during an earlier stage, but not for the symmetric localization of Tem1 to SPBs during telophase.

Although numerous genetic or biochemical experiments have been done to identify the interactions among the MEN components and their regulators, a clear picture illustrating the interactions between them and their relative order of function is lacking. It also has to be noted that these protein interactions change as the cell cycle proceeds. Therefore, it would be interesting to study protein interactions at a particular point during the cell cycle.

There are various ways to study protein interactions, the yeast two-hybrid essay and protein co-immunoprecipitation (Co-IP) are possibly the most commonly-used methods. However, neither of them can simultaneously demonstrate when and where a protein interaction is occurring. In addition, previous studies on these MEN proteins often used overexpressed proteins. These studies can be misleading, as over-production of a protein may affect its localization and activity, especially in these tightly coordinated, and cell cycle-regulated events.

I decided to use the fluorescence resonance energy transfer (FRET) method to study these protein interactions (between the MEN proteins as well as their regulators) during mitosis. FRET has been an appealing approach for examining physiologically relevant protein-protein interactions. This method involves a donor and an acceptor fluorophore attached to the proteins of interest (Fig.A1). The incident light is set such that it excites the donor but not the acceptor fluorophore. When the donor is excited, its energy is transferred to the acceptor, which then emits light at a longer wavelength (corresponding to the excitation spectrum of the acceptor). For the energy transfer to take place, the two fluorophores must be in close proximity (usually <10nm or 100Å). If one protein of interest is fused to the donor fluorophor, and the other protein to be tested is fused with the acceptor, energy transfer between the two fluorophores will reflect that these proteins are possibly in close proximity and interacting.

The FRET method would have these following benefits: 1) since both proteins are fused to a fluorophore, protein localizations can be investigated; 2) the method can help determine at what particular time or spatial point a protein interaction is taking place; 3) when used on live cells, FRET could provide a dynamic picture of protein interactions as a cell is progressing through the cell cycle. In addition, since I attempted to study these protein interactions closely resembling the physiological processes in a real cell, the fluorophores I used were green fluorescent variants encoded in PCR products integrated into the chromosomes in frame with the genes of interest, still under control of their natural promoters.

Nevertheless, this method has drawbacks. For example, it will not identify interactions between unknown proteins. In addition, previous FRET studies have largely been done *in vitro* or with overexpressed proteins, and there have been few reports on FRET done with proteins at their endogenous level *in vivo*. My trial thus is fairly new and can be risky. It is also expensive as a fluorescence microscope with the right filters for both donor and acceptor fluorophores is required. A sensitive camera with low background is necessary to take fluorescent images, and corresponding software on the computer is needed for calculations to determine whether energy transfer has occurred. Despite all these shortcomings, if this new method is actually successful, information can

be obtained about the temporal and spatial coordination of the mitotic events, which will be exciting

# III. Methods and materials

## a. Constructing the strains

As the FRET method is fairly new, it needs to be tested first whether or not the system actually works. My first attempt was to determine the interaction between Bub2 and Bfa1, as they are known to interact with each other and form a complex. A strain containing both Bub2-CFP fusion and Bfa1-YFP fusion thus served as a tester strain. Cse4, a kinetochore component, does not interact with either Bub2 or Bfa1, so a *BUB2-CFP CSE4-YFP* strain was used as a negative control. The *BUB2-YFP-CFP* (Bub2 fused to YFP-CFP in tandem) and *BUB2-YFP-CFP* strains were also constructed as positive controls.

The strategy for constructing these strains is illustrated in Fig. A3. CFP integration was made in *MAT*a and YFP integration in an isogenic *MAT*α strain. These two strains were then mated, and diploids were selected based double selective markers (*KanR* for CFP and *HIS5* for YFP). The diploids were sporulated and tetrad dissection was performed on the asci to obtain haploid progeny containing both *CFP* and *YFP* integration. The primers, strains, and plasmids are included in Table 4.1, 4.2, and Table 4.3. For the PCR strategy, genome integration, and tetrad dissection, refer to the methods described for the Ldb18 project.

## b. FRET measurements and calculations

Detection of FRET signal —YFP emission (545nm) when the incident light is for CFP excitation (440nm) — will indicate that energy transfer occurs between the two fluorophores. However, because the broad emission spectrum of CFP extends beyond 545nm, CFP emission spectrum spills over into the spectrum of YFP emission, which means some of the CFP emission can be detected as the FRET signal even when energy transfer has not taken place. In addition, the incident light at 440nm also directly excites YFP, although at a minimal extent. This direct excitation will be mistakenly detected as FRET signal as well. These two spill-overs are called "overlap factors", and have to be considered for FRET measurements (Fig. A2).

To take into account the spill-overs, strains containing a single integration of CFP or YFP were also constructed. Light emission signals were measured at three "channels": the "FRET channel", the "CFP channel", and the "YFP channel" (Table A1). The overlap factors were calculated by dividing the "FRET channel" signal by the "CFP channel"/"YFP channel" signal in strains with a single integration of CFP/YFP. A "FRET ratio" was calculated to determine whether the signal seen in the "FRET channel" was due to spill-overs or was a consequence of energy transfer between two fluorophores. The calculations are shown below:

CFP overlap factor = FRET channel / CFP channel (in a CFP fusion strain)

YFP overlap factor = FRET channel / YFP channel (in a YFP fusion strain)

FRET ratio = FRET channel / (CFP channel×CFP overlap factor + YFP channel × YFP overlap factor) (in the double-fusion strain)

Table A1. The excitation/ emission wavelength for all channels

| | YFP channel | FRET channel | CFP channel |
|---|---|---|---|
| Excitation | 500nm | 440nm | 440nm |
| Emission | 545nm | 545nm | 480nm |

Cells were grown to log phase and an agarose-pad slide was made (refer to the method described in "making a slide for GFP-tubulin movies" for the Ldb18 project in the text).

Cells on a slide were visualized and images were taken with different "channels" (Table A1). As CFP tends to photo bleach rapidly, images were taken at "YFP channel" first, followed by "FRET channel", and lastly "CFP channel". The exposure time for each channel was 2s. The Image-Pro program was used for specific settings of each channel, and images were saved on a computer (Fig. A5).

Fluorescence measurements were done on images using the Image-Pro program (Fig. A6). For each bright spot of fluorescence, the intensity ($I_1$) (of pixels) was measured. The background intensity ($I_0$) was determined by averaging the intensities of 3 spots adjacent to the fluorescent spot (shown in Fig. A6). The corrected ($I_C$) intensity of each fluorescent spot was obtained by subtracting the background from the overall intensity ($I_C$

$= I_1 - I_0$). For each strain, fluorescence intensities with every channel were measured for at least 300 spots.

CFP overlap factor was calculated for each spot in a strain with single CFP integration, and the average was taken. YFP overlap factor was determined in a similar way, except in a strain with single YFP integration. FRET ratio was then calculated for each single spot in the double fusion strain using the CFP and YFP overlap factors. Because these protein interactions may be cell cycle regulated, cells were grouped together according to their stages during the cell cycle proceeding. The overall FRET ratio for a particular strain was the mean value of all spots that were measured for this strain.

## IV. Results and discussions

Construction of the tester strain (*BUB2-CFP BFA1-YFP*), the positive control strain (*BUB2-YFP-CFP*), and the negative control strain (*BUB2-CFP CSE4-YFP*) strains were all successful (Fig. A4).

If FRET worked, the FRET ratio in the tester strain (*BUB2-CFP BFA1-YFP*) should be larger than the negative control strain (*BUB2-CFP CSE4-YFP*). However, the FRET ratio determined for the test strain was 1.50 (standard deviation 0.32), and 1.68 (standard deviation 0.29) for the negative control strain, each with approximately 400 samples. The positive control strain (*BUB2-YFP-CFP*) showed a FRET ratio of 1.53 (standard deviation 0.26). Statistical analysis revealed no significant differences for these ratios.

Since cell-cycle progression may make a difference, for the tester strain, I then divided the 400 samples into different groups according to their cell-cycle stages. However, no significant differences were observed for the FRET ratios of cells in G1/S, G2/M, metaphase, anaphase, or telophase.

It was unfortunate that the method was not successful to examine protein interactions in this study. The failure may be attributed to two aspects. Firstly, during the experiment, it came to my notice that the CFP overlap factor was relatively high (approximately 0.45) comparing to the YFP overlap factor (approximately 0.05). In fact, a bright spot can be detected under the "FRET channel" even in a straining containing only the CFP fusion, indicating high noise posed by the CFP spillover. Secondly, this

study was conducted at endogenous level, instead of overexpressing the proteins. As the fluorescent signal starts at relatively low intensity (as compared to *in vitro* studies or overexpression of the proteins), the background will have a large impact on the measurements. It is noteworthy that in this study, the exposure time was set at two seconds, because any shorter exposure time did not provide significant signals under these channels. In contrast, *in vitro* studies have reported exposure time as short as 0.2 seconds (Hailey *et al.*, manuscript from Yeast Resource Center). Increase of the exposure time may not only correspondingly increase the background noise, but also leads to photo bleach problem, which then results in deviations of the fluorescence intensity measurements.

In summary, this study used FRET to examine the protein interactions at endogenous level as a new trial. Yet, protein abundance, spectrum overlap, and camera sensitivity are the problems that remain to be addressed for future improvements.

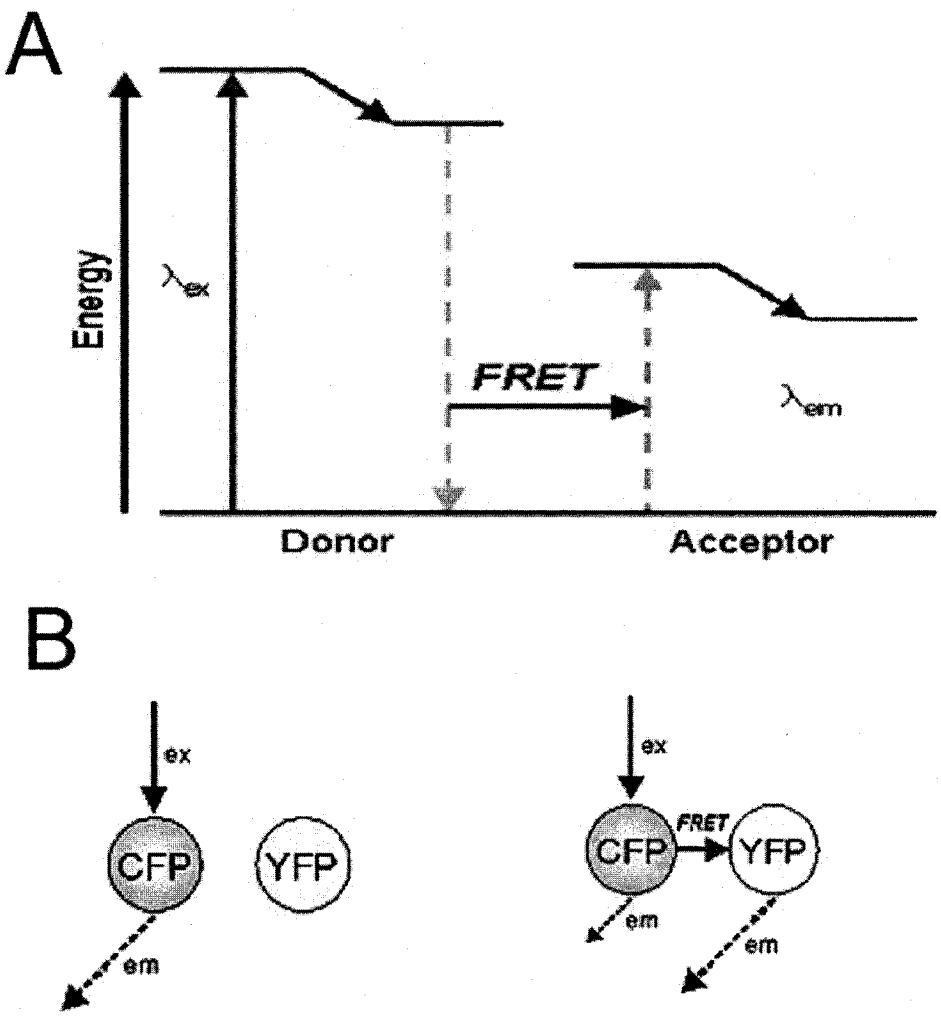


**Figure A1. The principle of FRET (fluorescence resonance energy transfer).** (A) Once the donor fluorophore is excited, during the lifetime of its excited state, an energy field is created by the oscillation of the excited electron. If an acceptor fluorophore is in proximity, it can be excited through resonance within this energy field. This is called fluorescence resonance energy transfer. The transfer efficiency highly depends on the distance between the two fluorophores. (B) CFP and YFP can work in combination, with CFP as the donor and YFP as the acceptor.

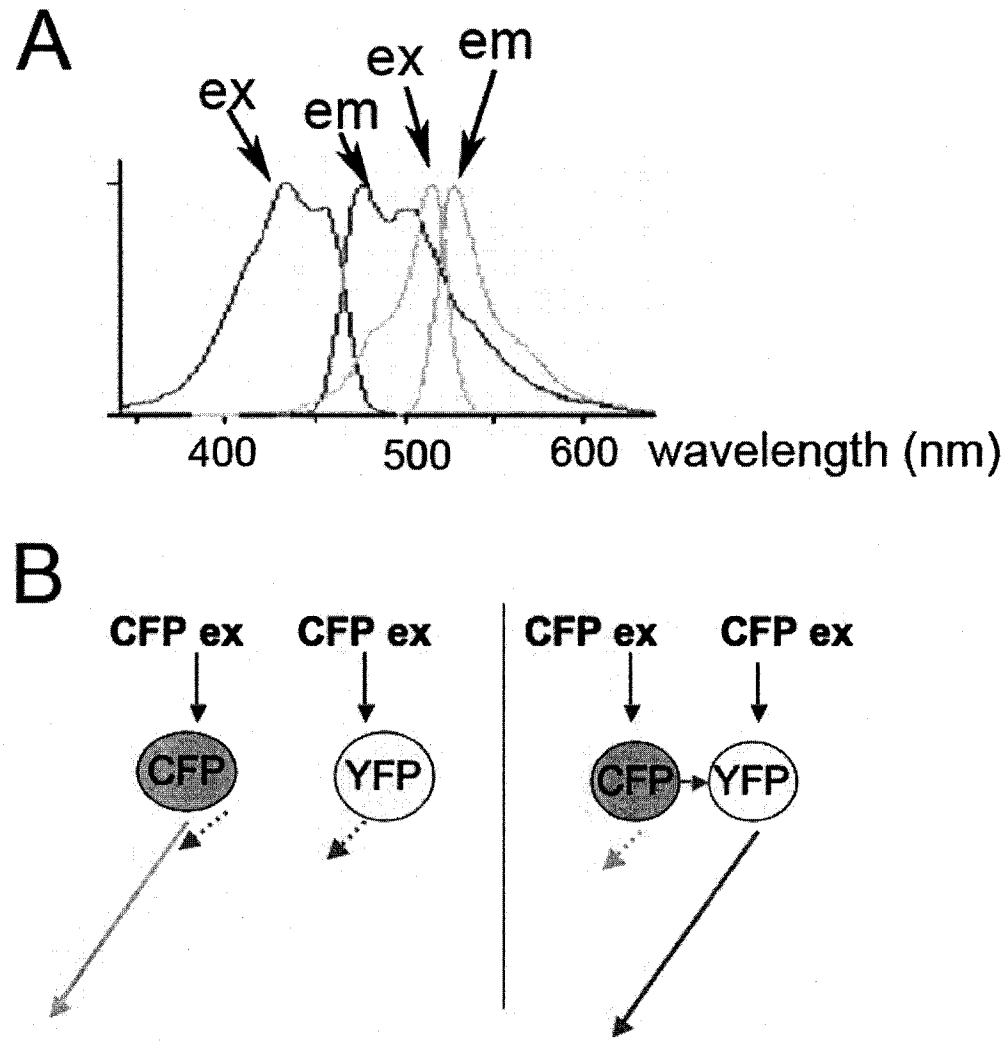


**Figure A2. Spectrum overlap of CFP and YFP leads to "overlap factors".** (A) The broad emission spectrum of CFP extends into the YFP emission spectrum, so some of the CFP emission will be detected as the FRET signal even when FRET is not occuring. In addition, the incident light at 440nm also directly excites YFP, because the YFP excitation spectrum spills into the CFP excitation spectrum. The blue lines are spectrums for CFP, and the green lines for YFP. "ex" represents "exciation" and "em" represents "emission". (B) When conducting measurements of the "FRET channel", both "spillovers" will be mistakenly detected as FRET signal.

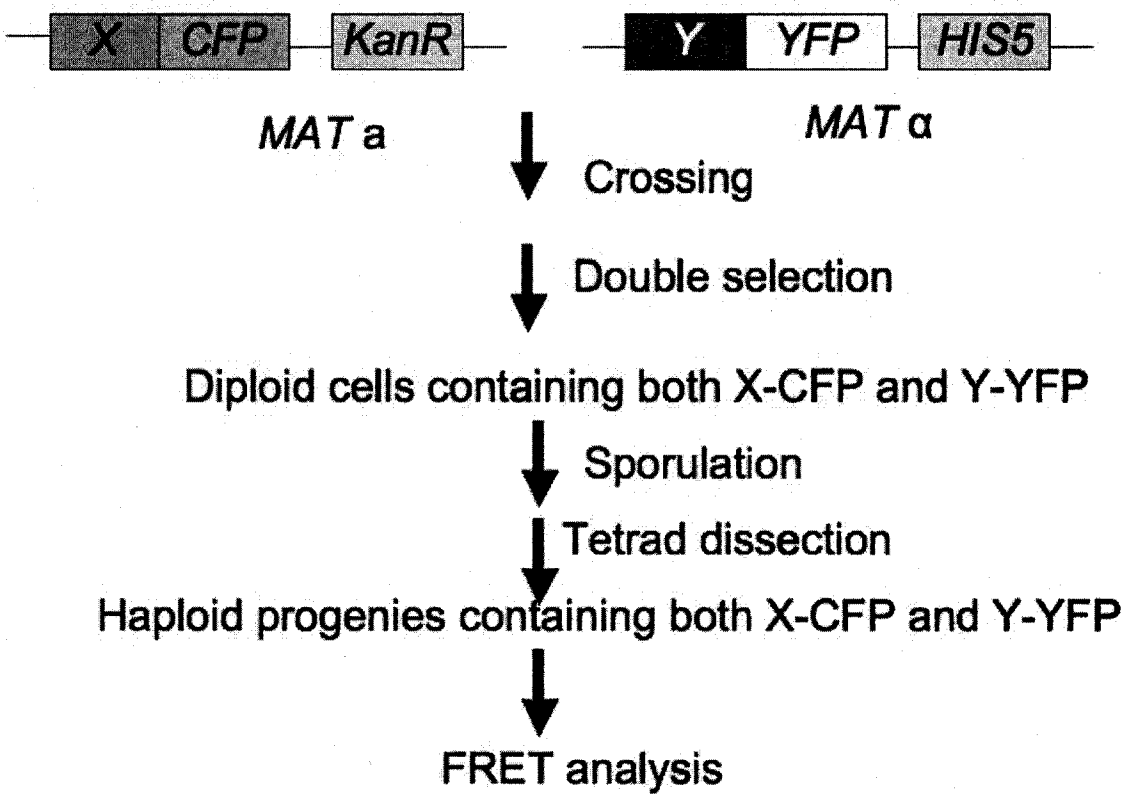


**Figure A3. Construction of the strains for FRET analysis.** CFP integration was made in *MAT*a and YFP integration in an isogenic *MAT*α strain. These two strains were then mated, and diploids were selected based on double selective markers (*KanR* for CFP and *HIS5* for YFP). The diploids were sporulated and tetrad dissection was performed on the asci to obtain haploid progeny containing both CFP and YFP integration.

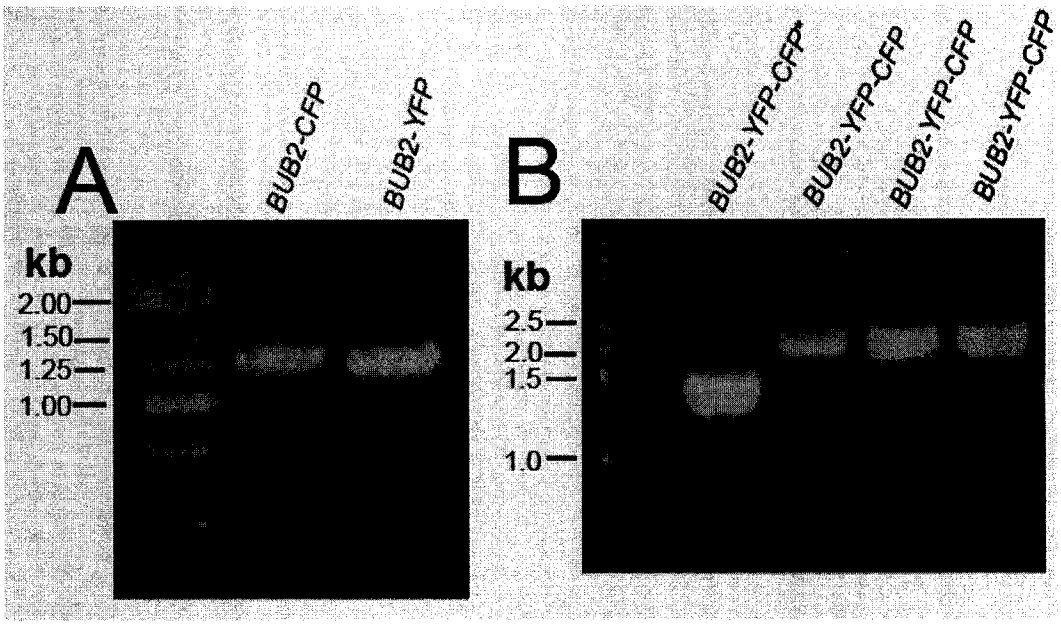


**Figure A4. Confirmation of CFP/YFP integration into the genome.** The PCR strategy can be referred to the method part of the Ldb18 project in the text. The *CFP-KanR* module was amplified using pDH3 as the template, and pDH5 used for *YFP-HIS5*, pDH18 used for *YFP-CFP-HIS5* (Yeast Resource center, University of Washington, Seattle, WA). The amplified modules were integrated into the genome right before the stop codon of the ORF of interest. Transformants were selected on YPAD+G418 (or SC-ura) plates, and genomic PCR was performed using the BUB2.TAGTEST and KAN.RTEST (or HIS5.RTEST) primers. " * " indicates a truncated fusion of Bub2-YFP-CFP (when observed under microscope, only YFP can be seen for this strain).

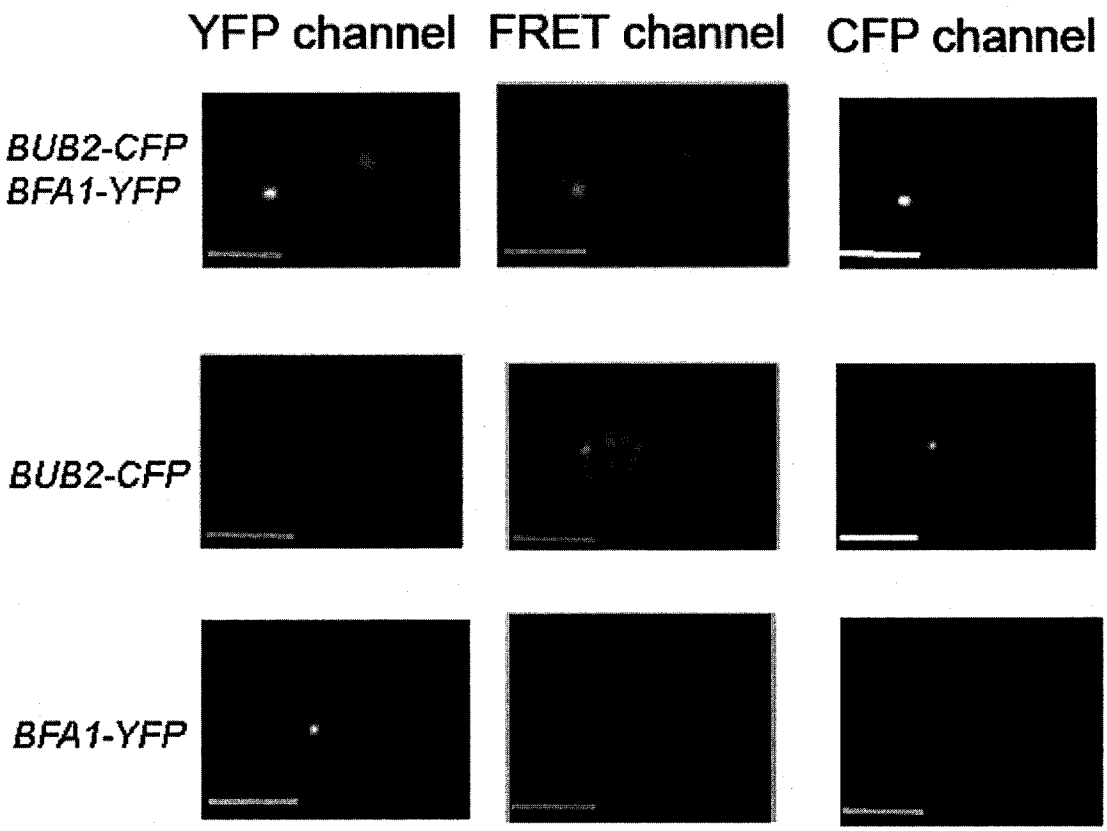


**Figure A5. An example of images taken under three different channels.** For growth of the cells and the method of making an agrose-pad slide, refer to the method used for "making GFP-tublin movies" (the method described for the Ldb18 project in the text), except that the strains used here were as indicated. Images were taken under YFP channel first, followed by the FRET channel, and the CFP channel. For wavelength settings for each channel, refer to Table A1. Exposure time for each channel was 2 seconds. Bar represents 4 μm.

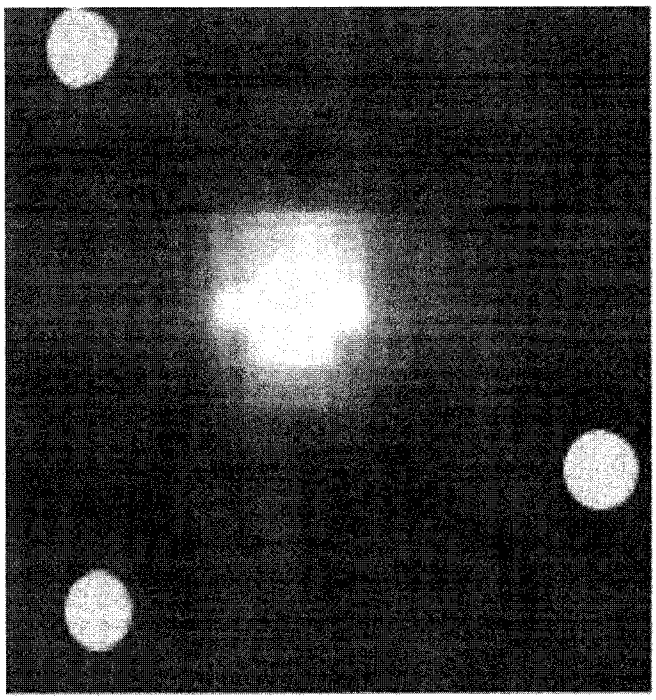

**Figure A6. An example for measuring the fluorescence intensity.** Fluorescence measurements were done on images using the Image-Pro program. For each bright spot of fluorescence, the intensity ($I_1$) (of pixels) was measured. The background intensity ($I_0$) was determined by averaging the intensities of 3 spots adjacent to the fluorescent spot. The corrected ($I_C$) intensity of each fluorescent spot was obtained by subtracting the background from the overall intensity ($I_C = I_1 - I_0$). Yellow spots on the picture indicate the three spots that were measured for background intensity.